



universität  
wien

# DIPLOMARBEIT

Titel der Diplomarbeit

**Potential mechanisms behind blood pressure modulation by  
melatonin: expression analysis of melatonin receptors  
MT<sub>1</sub> and MT<sub>2</sub> in the rat aorta**

angestrebter akademischer Grad

Magister der Pharmazie (Mag. pharm.)

Verfasser

Martin Schepelmann

Matrikelnummer:

0404524

Studienkennzahl lt. Studienblatt:

A449 (Pharmazie)

Betreuer:

Ao. Univ.-Prof. Mag. Dr. Walter Jäger

Wien, am 22. Juni 2010



## ACKNOWLEDGEMENT

First, I wish to thank my supervisor at the University of Vienna, Ao. Univ.-Prof. Dr. Walter Jäger, for making this diploma thesis possible and valuable insight and support during the completion of the project.

I also want to thank Prof. RNDr. Michal Zeman from the Comenius University of Bratislava and his student Lubos Molcan for their hospitality, the provision of the samples, and the successful cooperation in general.

Moreover, I am grateful to my lab colleague Vivienne Pohl for her help in introducing me to all the methods and for her patience with me during the months of our common work.

I also really want to express my gratitude to all members of the Department of Pathophysiology and Allergy Research, especially to Hana Uhrova, Mag. Martin Svoboda, Mag. Katrin Wlcek, Mag. Juliane Riha and Dr. Giovanna Bises, for their continuous assistance and readiness to answer all the questions of a newcomer, and for being such nice people to work and have fun with.

A big thank you goes to my friends, who accepted that my spare time was very limited in the past seven months.

Very special thanks go to family – my parents, Enna and Wolfgang Schepelmann, who have supported and encouraged me throughout the whole course of my studies, and my sister Alexandra, who helped me at very short notice during the proofreading stage of my thesis.

And finally, I want to thank my supervisor at the Medical University Vienna, Ao. Univ.-Prof. Dr. Isabella "Bella" Ellinger, who *a/ways* looks on the bright side of life! I am immensely grateful for the opportunity to work in her lab as well as for her permanent encouragement and help – but most of all, I am honored to have won her as a friend.

My grandmother, Maria Wandl, was the kindest and nicest person I have ever known. Sadly, she died much too soon this spring. I like to think that she was always proud of our family and me, and I wish to dedicate this work to her.

*Edel sei der Mensch,  
Hilfreich und gut!  
Denn das allein  
Unterscheidet ihn  
Von allen Wesen,  
Die wir kennen.*

*J. W. v. Goethe*



# TABLE OF CONTENTS

<b>1 ABSTRACT / KURZFASSUNG</b>	<b>1</b>
<b>2 INTRODUCTION</b>	<b>5</b>
<b>2.1 General information about melatonin</b>	<b>5</b>
<b>2.2 Melatonin biosynthesis</b>	<b>6</b>
2.2.1 Adrenergic control of melatonin biosynthesis	7
2.2.2 Melatonin metabolism	8
<b>2.3 Melatonin receptors and other melatonin binding proteins</b>	<b>8</b>
2.3.1 MT <sub>1</sub> and MT <sub>2</sub> – G-protein coupled receptors	8
2.3.2 Other melatonin binding sites	13
<b>2.4 Antioxidative effects of melatonin</b>	<b>14</b>
<b>2.5 Pharmacological aspects of melatonin</b>	<b>15</b>
<b>2.6 Melatonin and blood pressure regulation</b>	<b>16</b>
2.6.1 General overview on blood pressure regulation	16
2.6.2 The aorta	17
2.6.3 Reduced melatonin levels lead to hypertension	18
2.6.4 Influence of melatonin on animal models of hypertension	19
2.6.5 Influence of melatonin on the BP of humans	20
2.6.6 Contribution of MT <sub>1</sub> and MT <sub>2</sub> to BP regulation	22
<b>3 AIMS</b>	<b>25</b>
<b>4 MATERIALS AND METHODS</b>	<b>27</b>
<b>4.1 Samples</b>	<b>27</b>
4.1.1 Various rat organs for PCR method establishment	27
4.1.2 Rat aortas from two different time points	27
4.1.3 Rat aortas from SHR and control rats	27
4.1.4 Additional rat aortas for IF experiments	28
4.1.5 Mouse organs for IF experiments	28
<b>4.2 RNA isolation from frozen tissues</b>	<b>28</b>
4.2.1 Background	28
4.2.2 Materials	29
4.2.3 Method	30
<b>4.3 Quantification and purity assessment of RNA and DNA</b>	<b>31</b>
4.3.1 Background	31
4.3.2 Materials	31

4.3.3 Method	32
<b>4.4 Agarose gel-electrophoresis (GE)</b>	<b>33</b>
4.4.1 Background	33
4.4.2 Buffers and solutions	33
4.4.3 Preparation of agarose gels	35
4.4.4 Electrophoresis	36
<b>4.5 Reverse Transcription</b>	<b>38</b>
4.5.1 Background	38
4.5.2 Materials	38
4.5.3 Method	39
<b>4.6 PCR – Polymerase chain reaction</b>	<b>40</b>
4.6.1 Background	40
4.6.2 General procedure	42
4.6.3 Primers, mastermixes and temperature programs	43
<b>4.7 DNase treatment of RNA samples</b>	<b>49</b>
4.7.1 Background	49
4.7.2 Materials	49
4.7.3 Method	49
<b>4.8 DNA extraction and purification from agarose gels</b>	<b>50</b>
4.8.1 Background	50
4.8.2 Materials	50
4.8.3 Method	51
<b>4.9 DNA Sequencing and sequence comparison</b>	<b>52</b>
<b>4.10 Real time PCR (qPCR)</b>	<b>52</b>
4.10.1 Background	52
4.10.2 Materials	53
4.10.3 Method	54
4.10.4 Analysis of results	56
<b>4.11 Immunofluorescence</b>	<b>57</b>
4.11.1 Background	57
4.11.2 Tissue sectioning	59
4.11.3 Buffers, solutions and reagents	61
4.11.4 Staining procedures for cryo-sections	63
4.11.5 Staining procedures for HOPE®-fixated paraffin sections	68
4.11.6 Antibodies and blocking buffers	69
4.11.7 Photography of IF-stained sections	71
4.11.8 Experiment parameters	72

<b>5 RESULTS</b>	<b>75</b>
<b>5.1 Establishment of molecular biological methods to demonstrate expression of MT<sub>1</sub> and MT<sub>2</sub> mRNA in rat tissues</b>	<b>75</b>
5.1.1 RNA-Isolation	75
5.1.2 RT-PCR experiments on the isolated RNA	76
5.1.3 RT-qPCR for ACTB, MT <sub>1</sub> and MT <sub>2</sub> mRNA expression	79
<b>5.2 Preparation of rat aorta samples for subsequent PCR experiments</b>	<b>82</b>
5.2.1 RNA isolation	82
5.2.2 Reverse transcription	85
5.2.3 RT-PCR for $\beta$ -actin mRNA expression	85
<b>5.3 Expression of MT<sub>1</sub> mRNA in rat aortas</b>	<b>86</b>
5.3.1 Aortas from two different time points	86
5.3.2 Aortas from SHR and control rats	90
<b>5.4 Expression of MT<sub>2</sub> mRNA in rat aortas</b>	<b>95</b>
5.4.1 RT-PCR for MT <sub>2</sub> mRNA expression according to the established method	95
5.4.2 Sequencing of the MT <sub>2</sub> PCR product from the brain sample	95
5.4.3 Search for and selection of alternative PCR protocols	96
5.4.4 RT-PCR for MT <sub>2</sub> mRNA expression according to the Sugden-protocol	98
5.4.5 Design of new exon spanning primers for MT <sub>2</sub>	100
5.4.6 RT-PCR for MT <sub>2</sub> mRNA expression with the newly designed primers	101
<b>5.5 Expression analysis of MT<sub>1</sub> protein in the rat aorta by IF</b>	<b>105</b>
5.5.1 Single stainings for SM-actin and pecam-1 protein expression	105
5.5.2 Double staining for SM-actin + pecam-1 protein expression	106
5.5.3 Single stainings for MT <sub>1</sub> protein expression on cryo-sections	108
5.5.4 Single stainings for MT <sub>1</sub> protein expression on paraffin sections	110
<b>6 DISCUSSION</b>	<b>121</b>
<b>7 CONCLUSION AND OUTLOOK</b>	<b>125</b>
<b>8 LIST OF ABBREVIATIONS</b>	<b>126</b>
<b>9 REFERENCES</b>	<b>128</b>
<b>10 CURRICULUM VITAE</b>	<b>143</b>





# 1 ABSTRACT / KURZFASSUNG

## English

**Introduction:** Melatonin, known as the hormone of darkness, is a versatile substance produced in the pineal gland from its precursor substance serotonin. Melatonin plays a role in many processes including regulation of the body's internal clock, appetite, sleep, radical scavenging, and supposedly in behavior, tumor suppression, blood pressure and many more. Because of its sleep promoting effect, melatonin is used as a mild hypnotic, even though the effects of orally administered melatonin are limited. During the course of its metabolization, melatonin can scavenge a great number of reactive oxygen species, which is the cause for the extremely potent antioxidative capabilities of this substance. Apart from numerous other binding sites, two G-protein coupled receptors (GPCRs), MT<sub>1</sub> and MT<sub>2</sub>, exist in mammals which recognize melatonin as ligand and mediate many of its functions. Both receptors are coupled to Gi-proteins, but while MT<sub>1</sub> is almost ubiquitously expressed in many tissues, MT<sub>2</sub> is restricted to few regions of the body, like eye and brain. These GPCRs show circadian expression patterns in some tissues. Importantly, MT<sub>1</sub> and MT<sub>2</sub> are expressed in the cardiovascular system, however these data are conflicting and the influence of the GPCRs on, and their expression and location in the cardiovascular system are still not completely understood and remain to be fully characterized. It was suggested that MT<sub>1</sub> mediates vasoconstriction through direct activation of smooth muscle cells, while MT<sub>2</sub> mediates vasodilation through activation of nitric oxide synthase in the endothelium of the blood vessels. In any case, exogenous melatonin lowers blood pressure, both of healthy and hypertensive animals and humans. The mechanisms involved in this blood pressure regulating properties include melatonin's antioxidative capabilities, a dampening influence of melatonin on the central nervous system and the melatonin GPCRs. **Aims:** 1) Establish methods for RT-PCR and RT-qPCR experiments for investigation of MT<sub>1</sub> and MT<sub>2</sub> mRNA expression levels. 2) Investigate whether there is expression of MT<sub>1</sub> and MT<sub>2</sub> mRNA in the rat aorta. 3) Investigate the difference between melatonin GPCR mRNA expression levels in aortas from rats of two different time points. 4) Investigate the difference between melatonin GPCR mRNA expression levels in aortas from spontaneously hypertensive rats (SHR) and control rats. 5) Establish and perform immunofluorescence (IF) stainings to investigate the location of the melatonin GPCRs in the rat aorta. **Methods:** RNA was extracted and reversely transcribed using standard protocols. PCR with diverse primer pairs either retrieved from literature or custom designed was performed for MT<sub>1</sub> and MT<sub>2</sub>. RT-qPCR experiments were performed using commercially available assays for rat MT<sub>1</sub> and MT<sub>2</sub>. For method establishment, pre-frozen rat tissue samples of various organs were used.

16 aorta samples from two different time points – eight from day and eight from the night – were investigated to assess the difference in melatonin GPCR mRNA expression levels depending on the circadian phase state. 16 aorta samples of SHR and control rats – eight each – were investigated to evaluate the difference in melatonin GPCR mRNA expression levels between normotensive and hypertensive animals. Paraffin embedded sections and cryo-sections were used for localization of MT<sub>1</sub> by IF-staining, which was done using two different antibodies directed against MT<sub>1</sub>. Two mouse tissues, brain and intestine, were used as positive controls. **Results:** Observed expression levels of MT<sub>1</sub> and MT<sub>2</sub> in the rat organs did not exactly correlate with the levels in the literature, indicating rat-strain or interindividual differences. MT<sub>1</sub> mRNA was present in almost all aorta samples and showed a high interindividual variability in expression levels, while MT<sub>2</sub> mRNA was not present in aortas at all. There was no significant difference in MT<sub>1</sub> mRNA levels between the daytime and nighttime groups, though a trend toward higher expression in the nighttime group might be observed with a larger sample number. However, a significant difference in expression was found between aortas from SHR, which exhibited about 4 times (0–8) more mRNA for MT<sub>1</sub>, and the aortas from control rats, supporting a function of melatonin in blood pressure reduction. Immunofluorescence showed weak staining for MT<sub>1</sub>, but surprisingly in the tunica adventitia of the aortas, while a strong, region specific, staining in the positive controls was found. This was in contrast to the expected localization of MT<sub>1</sub> in the tunica media. **Conclusion:** We could demonstrate that MT<sub>1</sub> is indeed expressed in the rat aorta as model for the vascular system, while MT<sub>2</sub> is not present at all. It seems that the expression levels for MT<sub>1</sub> mRNA are not dependent on the time of day, although the sample size was too low and the number of time points too few for any final statement. We found a significant difference in expression of MT<sub>1</sub> between normotensive and hypertensive animals, supporting a function of MT<sub>1</sub> in the blood pressure modulating capabilities of melatonin. MT<sub>1</sub> seemed to be mainly located in the tunica adventitia of the aorta and not, as expected, in the tunica media. This localization of MT<sub>1</sub> and the absence of MT<sub>2</sub>, however, are in conflict with the current hypothesis on the influence of the melatonin GPCRs on blood pressure regulation by melatonin and ask for further investigation.

## Deutsch

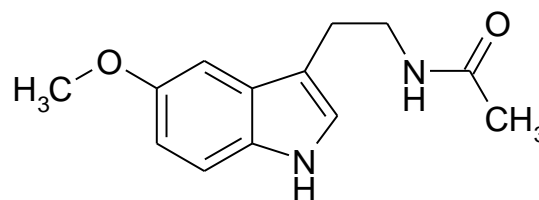
**Einleitung:** Melatonin ist eine sehr vielseitige Substanz, die in der Zirbeldrüse aus Serotonin entsteht und auch als „das Hormon der Dunkelheit“ bezeichnet wird. Zu den vielfältigen Einflussbereichen von Melatonin im Körper gehören zum Beispiel die Regulation der inneren Uhr, des Appetites und des Schlafs sowie das Abfangen freier Radikale. Vermutet wird auch ein Einfluss auf Verhalten, Tumorsuppression, Blutdruck und andere Funktionen des Körpers. Wegen seines schlafvermittelnden Effektes wird Melatonin als mildes Hypnotikum eingesetzt, allerdings ist seine Effektivität bei oraler Anwendung begrenzt. Im Rahmen des Abbaus von Melatonin im Körper können eine große Menge freier Radikale gebunden und somit unschädlich gemacht werden, was die starke antioxidative Wirkung von Melatonin erklärt. Für Melatonin gibt es mehrere Bindungsstellen; zwei davon,  $MT_1$  und  $MT_2$ , sind G-Protein gekoppelte Rezeptoren, die auch in Säugetieren vorkommen. Obwohl beide Rezeptoren vom  $G_i$ -Typ sind, ist  $MT_1$  fast in allen Teilen des Körpers exprimiert, wohingegen  $MT_2$  nur in bestimmten Geweben, wie z.B. Auge oder Gehirn, zu finden ist. Die Expression dieser Rezeptoren zeigt in manchen Geweben einen zirkadianen Rhythmus. Zwar sind  $MT_1$  und  $MT_2$  auch in Blutgefäßen vorhanden, die Datenlage zu deren Lokalisation, Funktion und Expression im vaskulären System ist allerdings widersprüchlich und noch abzuklären. Es wird angenommen, dass  $MT_1$  für Vasokonstriktion durch direkte Aktivierung der glatten Gefäßmuskulatur verantwortlich ist, während  $MT_2$  durch Aktivierung der NO-Synthase in Endothelzellen Vasodilatation vermittelt. Verabreichung von Melatonin führt jedenfalls zu Blutdrucksenkung. Dies wurde sowohl am gesunden und hypertensiven Menschen, wie auch am Tiermodell festgestellt. Diese blutdruckregulierende Wirkung von Melatonin wird unter anderem durch seine antioxidativen Eigenschaften, einen dämpfenden Effekt auf das Zentralnervensystem und die Wirkungen der G-Protein-gekoppelten Rezeptoren erklärt. **Ziele:** 1) Etablierung der Methoden für die RT-PCR und RT-qPCR zur Untersuchung der  $MT_1$ - und  $MT_2$ -Expression. 2) Feststellung, ob  $MT_1$  und  $MT_2$  mRNA in der Ratten-Aorta exprimiert sind. 3) Feststellung des Unterschiedes in der mRNA-Expressionsrate von  $MT_1$  und  $MT_2$  zwischen zwei Gruppen von Ratten-Aorten, die zu unterschiedlichen Tageszeiten gewonnen wurden. 4) Feststellung des Unterschiedes in der mRNA-Expressionsrate von  $MT_1$  und  $MT_2$  zwischen Aorten von spontan-hypertensiven-Ratten (SHR) und Kontroll-Ratten. 5) Etablierung und Durchführung von Immunfluoreszenz- (IF) Färbungen, um die Lokalisation von  $MT_1$  und  $MT_2$  zu bestimmen. **Methoden:** Die RNA der einzelnen Proben wurde nach Standard-Protokollen isoliert und revers transkribiert. PCR-Experimente wurden mit verschiedenen Primer-Paaren, die entweder der Literatur entnommen oder selbst erstellt waren, durchgeführt, um  $MT_1$  und  $MT_2$  mRNA in den Proben nachzuweisen. RT-qPCR wurde mit kommerziell erhältlichen

Testsystemen für  $MT_1$  und  $MT_2$  durchgeführt. Zur Etablierung der einzelnen Methoden wurden Proben von verschiedenen Ratten-Geweben verwendet. Um den Unterschied in der mRNA-Expressionsrate von  $MT_1$  und  $MT_2$  abhängig von der Tageszeit zu überprüfen, wurden 16 Ratten-Aorten, wovon acht bei Tag und acht bei Nacht gewonnen wurden, verwendet. Ebenfalls wurden 16 Ratten-Aorten, acht von SHR und acht von Kontroll-Ratten, verwendet, um den Unterschied in der mRNA-Expressionsrate von  $MT_1$  und  $MT_2$  zwischen hypertensiven und normotensiven Tieren zu bestimmen. Paraffin- und Gefrier-Schnitte von Ratten-Aorten wurden benutzt, um die Lokalisation von  $MT_1$  mittels IF-Färbung zu bestimmen, wobei zwei unterschiedliche Antikörper gegen Ratten- $MT_1$  verwendet wurden. Als Positiv-Kontrollen kamen Maus-Gehirn und Maus-Darm zum Einsatz. **Resultate:** Die beobachteten Expressionsraten von  $MT_1$  und  $MT_2$  in den Ratten-Organen divergieren teilweise von den in der Literatur beschriebenen, was auf interindividuelle Abweichungen oder Unterschiede zwischen verschiedenen Ratten-Arten hindeuten könnte. Es konnte kein signifikanter Unterschied der mRNA-Expressionsraten zwischen den Aorten-Gruppen von zwei unterschiedlichen Tageszeiten festgestellt werden. Dem Trend der Daten folgend, wäre es allerdings möglich, dass eine höhere Expression von  $MT_1$  mRNA in der „Nacht“-Gruppe bei einer größeren Anzahl von Proben in beiden Gruppen zu sehen gewesen wäre. Im Gegensatz dazu konnte ein eindeutiger Unterschied in der Expressionsrate von  $MT_1$  mRNA zwischen den Aorten von SHR und Kontroll-Ratten festgestellt werden, wobei SHR ungefähr 4-mal mehr (0–8) mRNA exprimierten als Kontroll-Ratten. Dies unterstützt den postulierten Einfluss von Melatonin auf die Blutdruckregulation über den G-protein-gekoppelten Rezeptor  $MT_1$ . Die IF-Experimente zeigten eine schwache Färbung von  $MT_1$ -Protein in der Ratten-Aorta, erstaunlicherweise überwiegend in der Tunica adventitia. Die Positiv-Kontrollen zeigten eine starke, region-spezifische Färbung. **Schlussfolgerung:** Wir konnten nachweisen, dass  $MT_1$  mRNA tatsächlich in der Ratten-Aorta – als Modell für das Gefäßsystem – exprimiert ist.  $MT_2$  mRNA hingegen wird in der Ratten-Aorta überhaupt nicht exprimiert. Es scheint, als wäre die Expressionsrate von  $MT_1$  mRNA nicht von zirkadianen Rhythmen abhängig, allerdings war die Anzahl der Proben wohl zu gering, um eindeutige Schlussfolgerungen zu ziehen. Ein eindeutiger Unterschied in der Expressionsrate von  $MT_1$  zwischen normotensiven und hypertensiven Tieren konnte nachgewiesen werden, was eine Funktion von  $MT_1$  im Rahmen der Blutdruck regulierenden Eigenschaften von Melatonin unterstützt.  $MT_1$  scheint hauptsächlich in der Tunica adventitia exprimiert zu sein und nicht, wie angenommen, in der Tunica media. Diese Lokalisation und die Abwesenheit von  $MT_2$  stehen im Gegensatz zu derzeitigen Hypothesen über den Einfluss der Melatonin-Rezeptoren  $MT_1$  und  $MT_2$  und bedürfen weiterer Untersuchung.

## 2 INTRODUCTION

### 2.1 General information about melatonin

Melatonin (chemical name N-acetyl-5-methoxytryptamine or N-[2-(5-methoxy-1H-indol-3-yl)-ethyl]-ethanamide, see Figure 1) is commonly known as the “darkness hormone” because melatonin levels are highly dependent on lighting conditions, being low at day and high at night [1-2]. Melatonin is (in vertebrates) produced in the pineal gland [3] but also in various other areas such as the suprachiasmatic nucleus (SCN) [4], leucocytes [5] the retina, the bone marrow, the skin, the gastro intestinal tract, the skin, and probably others [6-7]. It was first discovered in the year of 1958 by Lerner et al. [8]. Melatonin was named after its ability to lighten the color of melanocytes in certain animals and its precursor serotonin [7-9].



Melatonin

**Figure 1:** Structure of melatonin.

Melatonin has a variety of roles, like control of circadian rhythms and sleep by playing an essential part in the body's internal clock. Thereby, the main function of melatonin is to inform various parts of the body about photoperiods (= day length), so that changes in pigmentation, appetite, sleep etc. can be organized. Other functions of melatonin include vascular and blood pressure (BP) modulation, scavenging of free radicals and reduction of oxidative stress, stimulation of the immune system, regulation of seasonal reproduction and body temperature, inhibition of tumor proliferation, osteolysis inhibition, behavior regulation and others [6-7, 10-12].

Because of this multitude of functions and because of numerous other facts – melatonin's non receptor-dependent antioxidative capability, synthesis in organs other than the pineal gland, and that melatonin can be taken up with food supplementing the endogenous production – Tan et al. [7] point out that melatonin could not only be described as a hormone, but as a vitamin, too.

Melatonin not only occurs in animals, but also in unicellular organisms and fungi [13] as well as in plants, where it exhibits a similar circadian rhythm like in animals, although the data on its function is yet not very conclusive. Various roles, such as that

of an antioxidant, have been hypothesized. The first definite job of melatonin in plants seems to be that of a growth promoter [9].

## 2.2 Melatonin biosynthesis

Melatonin is synthesized from serotonin in two steps (see Figure 2). The first step is acetylation of serotonin to the intermediate N-acetylserotonin by the arylalkylamine-N-transferase (AANAT). The acetyl group is supplied by AcCoA. The second step is methylation of N-acetylserotonin to N-acetyl-5-methoxy-tryptamine (melatonin) by the hydroxyindole-O-methyltransferase (HIOMT) [1]. The methyl group is carried over from S-adenosyl-methionine [2]. Melatonin synthesis is highly dependent on environmental light and therefore follows a circadian rhythm. In low light conditions, melatonin levels are greatly increased, with correspondent increase of AANAT activity. HIOMT activity, on the other hand, is not increased or, at most, to a lesser extent. Nocturnal melatonin synthesis also rapidly diminishes again after exposure to light (see Figure 2) [1, 14].

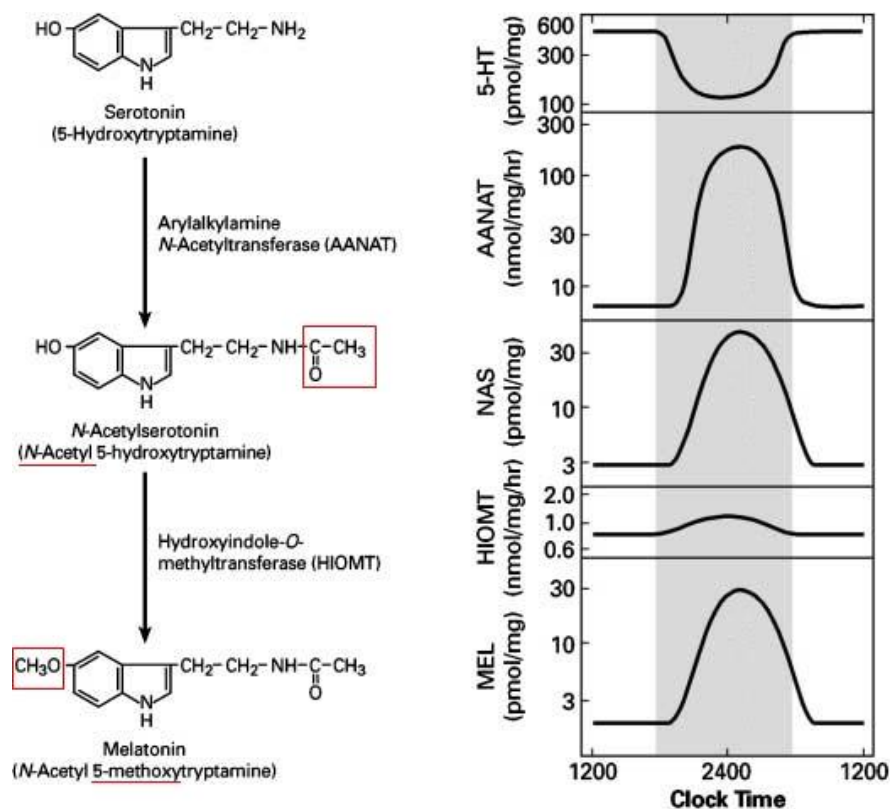


**Figure 2:** Daily rhythm of indoles in the rat pineal gland. Molecular changes are highlighted with red rectangles / lines. Periods of darkness are indicated by gray shading. Nocturnally increased activity of AANAT results in decreased serotonin and increased NAS-levels. HIOMT activity is also increased during nighttime, but to a much lesser extent. As a result, melatonin concentration is greatly elevated during the night. Modified after [1].

### 2.2.1 Adrenergic control of melatonin biosynthesis

Melatonin synthesis in the pineal gland is strongly controlled by adrenergic stimulation via the SCN. The SCN is the main controller of all circadian rhythms in mammals and synchronizes the various more or less autonomous “clocks” in mammals [15]. It is the driving element of the circadian rhythm of melatonin. In the rat, the SCN is largely controlled by lighting conditions [16], but can also function autonomously, when left in complete darkness. Nerves emerging from the SCN ultimately activate sympathetic fibers which in turn innervate the pineal gland [1].

Stimulation of  $\alpha$ 1-adreno-receptors activates proteinkinase C (PKC) via increased  $\text{Ca}^{2+}$  and diacylglycerol (DAG) concentrations in the pineal cells (see Figure 3).

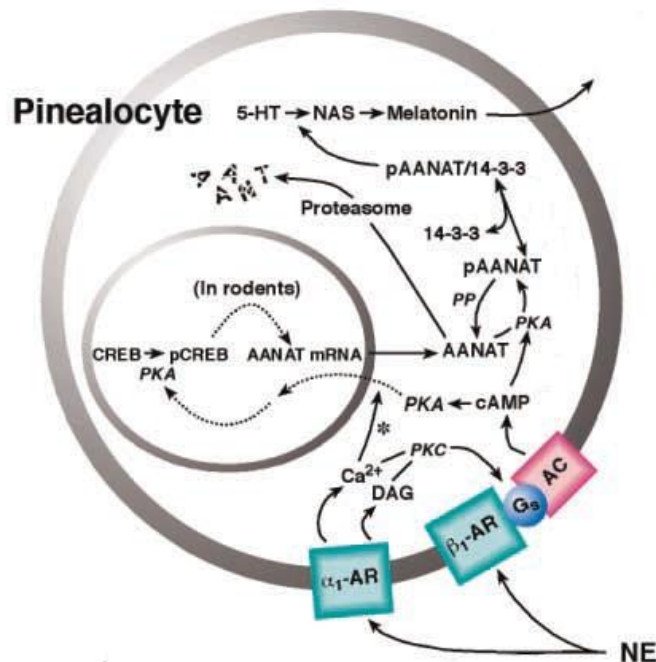


**Figure 3:** Adrenergic regulation of melatonin synthesis. Norepinephrine (NE) binds to  $\alpha$ 1 or  $\beta$ 1 receptors.  $\alpha$ 1 stimulation potentiates the effect of  $\beta$ 1 stimulation by activating protein kinase C (PKC) which in turn activates the adenylate cyclase (AC) of the  $\beta$ 1 receptor. The AC produces cyclic AMP (cAMP) which activates protein kinase A (PKA). PKA has now two different methods of raising AANAT-activity: 1) by phosphorylation of cAMP-response-element-binding-protein (CREB) which then promotes transcription of the AANAT-gene, and 2) by phosphorylation of AANAT which leads to a complex of AANAT with 14-3-3, rendering AANAT insensitive to proteasomal proeteolysis. Modified after [1].

While stimulation of  $\alpha$ 1 alone has no effect on AANAT activity [17], the increased  $\text{Ca}^{2+}$  influx potentiates the effect of protein kinase A (PKA). PKA is activated by cAMP generated through  $\beta$ 1-stimulation, therefore acting as an amplifier for the  $\beta$ 1-adrenergic signal [18]. A cAMP-responsive element binding protein (CREB) has been identified [19], which, together with an adjacent 5-base-box function, acts as a promoter for the

AANAT-gene. Furthermore, PKA acts via direct phosphorylation of AANAT [17], leading to the formation of an AANAT-complex with a 14-3-3 protein, a kind of “shielding protein” which protects the AANAT from proteolysis [20].

In summary, there are two mechanisms for regulation of AANAT activity: increased transcription of AANAT-mRNA and inhibition of preteolysis by coupling with 14-3-3 proteins [14].

## 2.2.2 Melatonin metabolism

Melatonin is metabolized mainly in the liver via the cytochromes CYP1A2 and CYP1B2. Metabolic pathways are 6-hydroxylation to 6-hydroxy-melatonin with subsequent sulfatation and excretion, O-demethylation to N-acetyl-5-hydroxy-tryptamine and non-enzymatic deacetylation to 5-methoxytryptamine [21]. This last, non-enzymatic way for metabolism of melatonin is also called kynuric pathway. It is essential for melatonin's antioxidative abilities. In its course, free radicals such as  $O_2^{\cdot-}$ ,  $CO_3^{\cdot-}$ ,  $NO^{\cdot}$  or  $H_2O_2$  are scavenged [6] (see Figure 4).

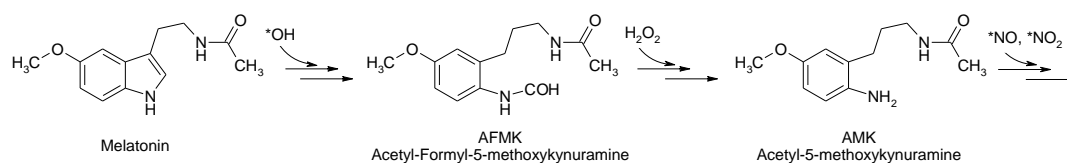


**Figure 4:** Simplified kynuric pathway of melatonin metabolism. After [6].

## 2.3 Melatonin receptors and other melatonin binding proteins

### 2.3.1 $MT_1$ and $MT_2$ – G-protein coupled receptors

In 1994 the first melatonin receptor  $Mel_{1C}$  was found in *Xenopus laevis* (African clawed frog) and discovered to be a G-protein coupled receptor (GPCR) of the  $G_i$ -type, therefore reducing cAMP levels by inhibiting the adenylyl cyclase. It was shown that the receptor was highly affine to melatonin and had a structure of 420 amino acids grouped in 7 hydrophobic elements [22], typical of GPCRs [23]. However,  $Mel_{1C}$  is not expressed in mammals, but only in fish, amphibiae or birds. Two other melatonin receptors have been found shortly afterwards, which were originally called  $Mel_{1A}$  and  $Mel_{1B}$ , respectively, but then re-named melatonin receptor 1 ( $MT_1$ ) and Melatonin receptor 2 ( $MT_2$ ) [24].

$MT_1$  was first discovered in sheep and humans. [25]. The receptor has a size of 350 amino acids (in rats: 353 amino acids [26]) with 7 transmembranic domains [27]



and is also a G-protein coupled receptor of the  $G_i$ -type. The expression of  $MT_1$  is, at least partly, regulated by circadian rhythms controlled by the SCN [24].

One year later,  $MT_2$  was found in humans. The receptor comprises 362 amino acids (in rats: 364 amino acids [26]) and is, again, a G-protein coupled receptor of the  $G_i$ -type [28].

Depending on the cell type in which the receptors are expressed, they also seem to exhibit coupling with  $G_q$ -proteins, indicating possible parallel signaling pathways for these receptors [27]. See Figure 5 for an overview of the proposed signaling pathways of the melatonin receptors.

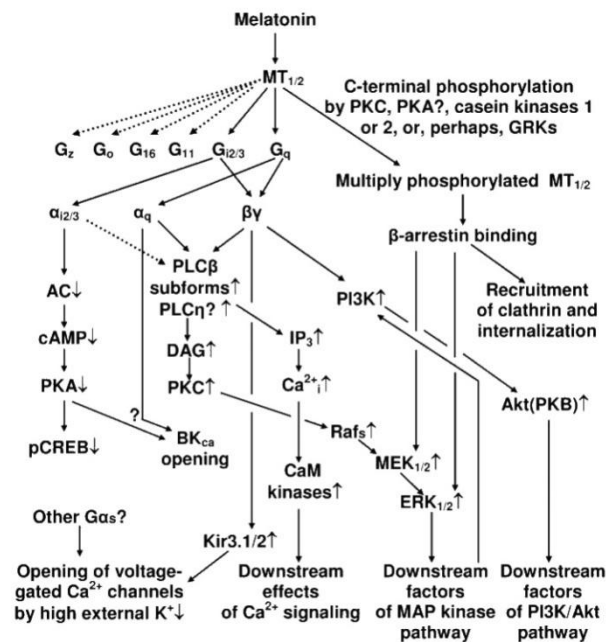


**Figure 5:** Melatonin GPCR signaling cascade. Modified after [27]. Q. v. for detailed information.

The human  $MT_1$  and  $MT_2$  receptors show a different affinity for melatonin ( $K_i$  80.7 vs 383 pM) [29] and other compounds. Some of these substances are important for studies on receptor-mediated melatonin effects. Luzindole (2-benzyl-N-acetyltryptamine), an unselective antagonist for both melatonin GPCRs, was identified by Dubocovich [30] and is often used in studies to suppress receptor-mediated melatonin effects. 4P-ADOT (4-phenyl-2-acetamidotetraline) and 4P-PDOT (4-phenyl-2-propionamidotetralin) serve as relatively selective antagonists of  $MT_2$  [31]. More recently, N-butanoyl-5-methoxy-1-methyl- $\beta,\beta$ -trimethylene-tryptamine, which is an antagonist at  $MT_1$ , but an agonist at  $MT_2$  and N-butanoyl-5-methoxy-1-methyl- $\beta,\beta$ -tetramethylene-tryptamine, which is an antagonist at  $MT_1$  not showing any interaction with  $MT_2$ , thus being selectively antagonistic at  $MT_1$  [32], have been identified and will allow further studies on the function of melatonin's GPCRs.

## Distribution and functions

The distribution of melatonin GPCRs has been investigated in many studies. For humans, studies on mRNA expression via RT-PCR as well as protein expression via western blot or immunohistochemical methods revealed MT<sub>1</sub> and, to a lower extent, MT<sub>2</sub> to be present in regions of the brain, ovary, kidney, intestine and various other organs and cell types [33]. However, while well characterized antibodies are available against human MT<sub>1</sub> and MT<sub>2</sub>, no reliable antibodies for other species have been reported yet. Therefore, most studies concerning melatonin GPCR expression in other species than human, e.g. rat, were performed on the mRNA level [24].

Earlier studies investigating MT<sub>1</sub> and MT<sub>2</sub> mRNA expression in the rat used only incomplete sequences of the receptor's mRNA as template for primer design [34-36]. Addressing these issues, Ishii et al. [26] identified the gene structures including the whole mRNA sequence for both rat MT<sub>1</sub> and MT<sub>2</sub>. Using newly designed exon-spanning primers, designed from the identified mRNA sequences for both receptors, they demonstrated occurrence of MT<sub>1</sub> and MT<sub>2</sub> mRNA – without the risk of false positives through genomic DNA – in a great variety of rat tissues, like lung, kidney and intestine (see Figure 6).

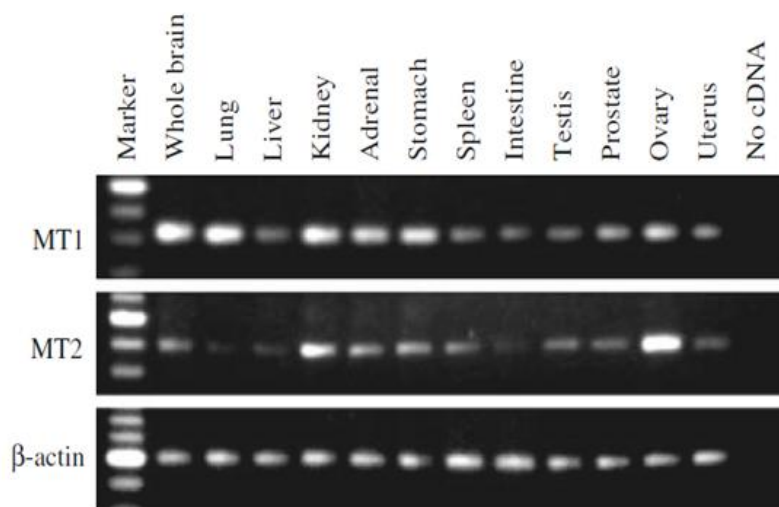


**Figure 6:** RT-PCR analysis of MT<sub>1</sub>, MT<sub>2</sub> and β-actin expression in various rat tissues. Both MT<sub>1</sub> and MT<sub>2</sub> were detected in all tissues. β-actin is used as control. Modified after [26].

Melatonin exhibits an enormous multitude of functions via its known G-protein-coupled-receptors. An extensive discussion of all the effects of the melatonin receptors would go beyond the scope of this introduction. An overview can be seen in Figure 7, details can be found e.g. in [33], [37] or [6]. The expression, distribution and functionality of  $MT_1$  and  $MT_2$  in the cardiovascular system will be discussed in 2.6.

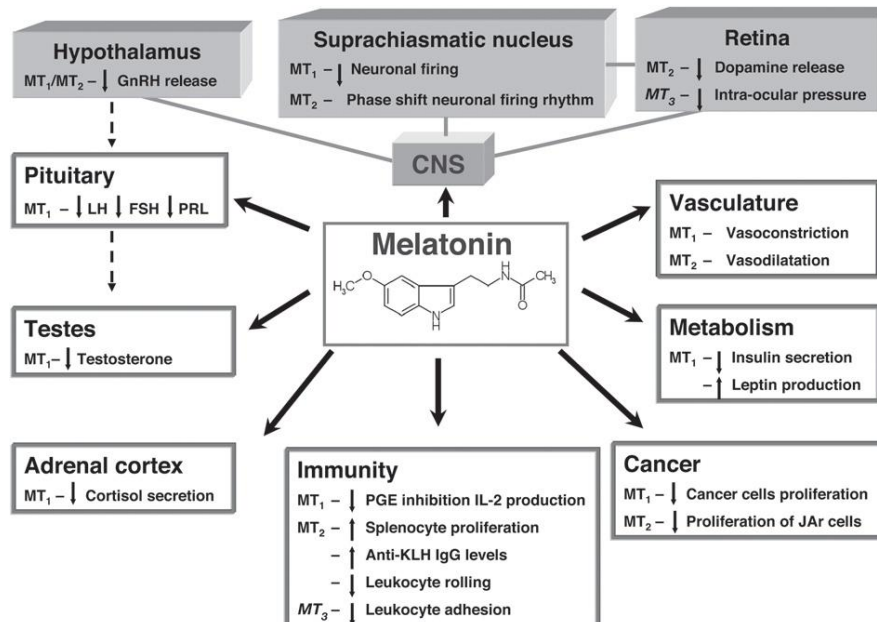


**Figure 7:**  $MT_1$ ,  $MT_2$  and  $MT_3$  (see 2.3.2) responses in the CNS and peripheral tissue [37]. Q.v. for detailed information.

## Structure and functionality

Both the human and rat  $MT_1$  gene consist of two exons. The rat  $MT_2$  gene consists of three exons, whereas the human  $MT_2$  gene contains only two. This suggests that regulation of  $MT_2$  receptor expression might be species specific [26].

All melatonin GPCRs,  $Mel_{1C}$ ,  $MT_1$  and  $MT_2$ , show a high degree of homology with each other: 60 % for the complete sequences, 73 % within the transmembrane sections [28]. The rat receptors exhibit 84.1 % and 78.3 % identity with their human counterparts [26]. As of yet there are no x-ray crystallographic structures available for any of these receptors. The predicted membrane topologies of human  $MT_1$  and  $MT_2$  are shown in Figure 8.

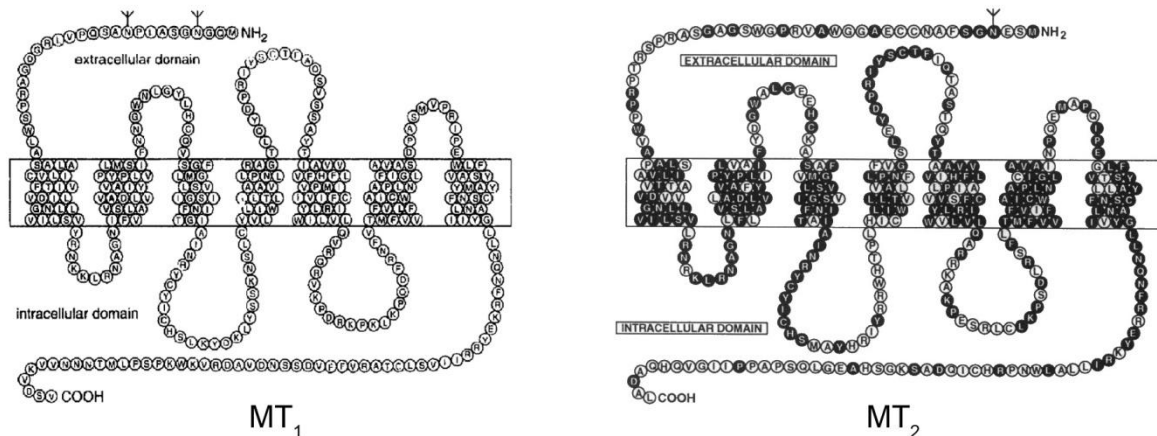


**Figure 8:** Predicted membrane topology of  $MT_1$  and  $MT_2$  with deduced amino acid structures. Y = potential N-linked glycosylation site. Solid dots = identical amino acids in  $MT_1$  and  $MT_2$ .  $MT_1$ : [38];  $MT_2$ : [28].

The C-terminal tails of both  $MT_1$  and  $MT_2$  are necessary for interaction with the G-protein and receptor internalization [27, 39]. For details see [40] and [39]. The C-terminal tail of  $MT_1$  also interacts with the protein MUPP1 amongst others, which joins  $MT_1$  to cAMP regulation and nitric oxygen synthase (NOS). This could explain the fact that NO production is inhibited by melatonin [24]. However, at least in endothelial cells, not the melatonin GPCRs seem to be involved in the reduction of nitric oxide (NO) production [41-42], but interaction with intracellular  $Ca^{2+}$  mobilization [41] or NF- $\kappa$ B inhibition [42]. In addition to the G-proteins,  $MT_1$  and  $MT_2$  interact with a number of other proteins, like the actin binding protein filamin A, and insulin receptor substrate 4 (IRS4), proteins commonly associated with other GPCRs [24].

GPCRs generally tend towards di- or oligomerization [23] and the melatonin GPCRs are no exception [24]. It was demonstrated that the relative propensity of the  $MT_1$  /  $MT_2$  heterodimer and the  $MT_1$  /  $MT_1$  homodimer is similar, but for the  $MT_2$  /  $MT_2$  dimer it is three to four times lower. Heterodimers also interact with selective ligands for  $MT_1$  and  $MT_2$ , resulting in a possible problem with data interpretation of ligand affinities or receptor expression patterns [43].

In 1996, G protein-coupled receptor 50 (GPR50), an orphan GPCR belonging to the melatonin receptor family (45 % identical to  $MT_1$  and  $MT_2$ ), but not interacting with melatonin or any other known ligand, was discovered. It has an unusually long C-terminal tail consisting of over 300 amino acids, but no N-linked glycosylation sites [44]. See Figure 9 for predicted membrane topology.

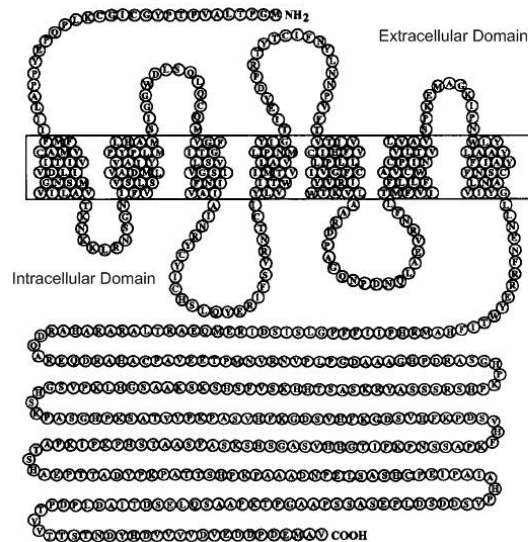


**Figure 9:** Predicted membrane topology of GPR50, with deduced amino acid structure. Modified after [44].

Ten years later, it was shown that GPR50 is as likely to engage in homodimers as in heterodimers with  $MT_1$  or  $MT_2$  but not with  $\beta_2$ -adrenoreceptors or CC chemokine receptors (CCR). Heterodimers of GPR50 with  $MT_2$  did not change the activity of  $MT_2$ , but dimers with  $MT_1$  strongly inhibit receptor function. It seems that the C-terminal tail inhibits the interaction of  $MT_1$  with the G-protein and  $\beta$ -arrestin [24]. Since  $MT_2$  dimers with GPR50 show no decreased activity,  $MT_2$  could act as an endogenous antagonist for GPR50, thus inhibiting the inhibition of  $MT_1$  by GPR50 [45]. For an overview of melatonin GPCR dimerizations see Figure 10.

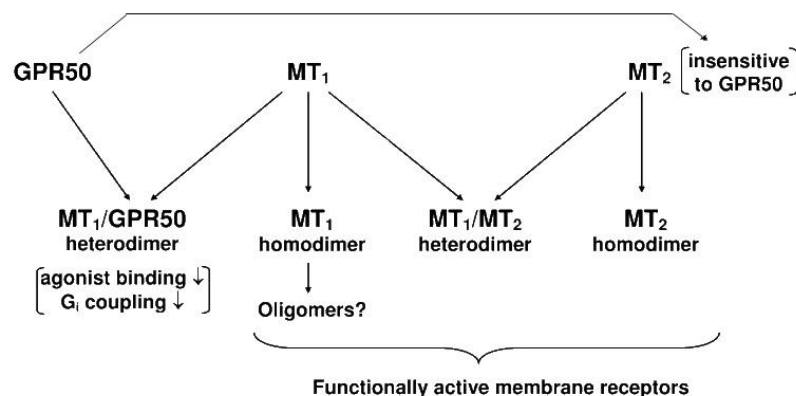


**Figure 10:** Melatonin GPCR dimerizations. Modified after [27].

### 2.3.2 Other melatonin binding sites

Another protein binding and reacting to melatonin is  $MT_3$ , originally named ML2 and discovered in 1988 [24, 46]. Compared to  $MT_1$  and  $MT_2$ , it exhibits a relatively low affinity for melatonin and fast kinetics [24, 47]. In the year 2000,  $MT_3$  could be identified

as the quinone reductase 2 (QR2), a well known enzyme with oxidoreductive properties [48]. X-ray structural analysis of the melatonin / QR2 complex proved the interaction between melatonin and QR2 [49]. QR2 seems to increase cytotoxic effects caused by reactive quinones, seeing that, for example, QR2 knockdown cells are 42–48 % less sensitive to menadione poisoning [50]. While the mechanisms of QR2 and its regulation are still somewhat unclear [27], it seems very probable that some of the beneficial aspects of melatonin such as its antioxidative capability are connected with its binding affinity to the QR2 binding site [24].

In addition to the GPCRs MT<sub>1</sub> and MT<sub>2</sub> as well as QR2, melatonin interacts with numerous other targets. In 1993, Benitez-King et al. [51] demonstrated affinity of melatonin for calmodulin, thus modulating intracellular Ca<sup>2+</sup> functions. It was proved recently that melatonin has a very significant influence on calcium / calmodulin-dependent protein kinases in rat INS-1 cells [52]. Calreticulin, another calcium binding protein, has high affinity for melatonin, too. Calreticulin is a protein of the endoplasmatic reticulum with various functions like chaperon activity or integrin function. There are speculations that melatonin might influence calreticulin's internalization in the nucleus [53].

Melatonin has an (albeit low) affinity for nuclear receptors such as Retinoid-related orphan receptor alpha (ROR $\alpha$ ) 1, 2, and retinoid Z receptors (RZR). While the RORs are probably involved in regulating effects on leucocytes, little is known about RZR [6]. For more details on these nuclear receptors see [27].

Finally, melatonin seems to have some influence on mitochondria; while it seems to modulate electron flux and leakage [27], it also inhibits the mitochondrial transition pore (mtPTP), which plays a role in the development of ischemia. Melatonin reduces infarct volume and neuron loss, so that the inhibition of mtPTP might be a very important feature of the anti-apoptotic effect of melatonin [54].

### **2.4 Antioxidative effects of melatonin**

One of melatonin's most prominent features is its antioxidative capacity. Melatonin is most efficient in scavenging free radicals with almost no pro-oxidant side effects [6]. It was discovered that the O-methyl and N-acetyl groups (see Figure 1) are most important for melatonin's extraordinarily strong direct radical scavenging ability [55]. During the metabolism of melatonin to AFMK (N<sup>1</sup>-acetyl-N<sup>2</sup>-formyl-5-methoxykynuramine), the metabolite apparently most important for radical scavenging, up to four free radicals can be eradicated (see Figure 4). Other metabolites of melatonin or their reactions of formation and degradation accordingly exhibit radical scavenging properties as well [6]. Additional to this antioxidant mechanism are indirect effects via

inhibition of NO production [42], up-regulation of antioxidant enzymes like catalase [56] and down-regulation of pro-oxidant enzymes like myeloperoxidase [57], inducible NO-synthase [56] or superoxide dismutase [58].

Various *in vivo* studies have confirmed melatonin's antioxidative capacity and capability to reduce oxidative stress. For example, it was demonstrated that melatonin reduces renal damage from oxidative stress in rats with artificially induced chronic renal failure [59]. Another example is reduced damage, caused by alcohol induced oxidative stress, in the aorta of melatonin treated rats [60].

Further examples for and information on the oxidative stress related effects of melatonin can be found in a variety of reviews, e.g. [6, 61-63].

## 2.5 Pharmacological aspects of melatonin

As a medication, melatonin has phase shifting effects for sleep or body temperature. This might be beneficial for e.g. jet lag or shift work [64], although the observed effect of oral melatonin has been relatively slim [65]. A large meta-analysis showed an average increase in sleep duration of 12.8 minutes and reduced sleep onset by 4.0 minutes [66]. However, a recent study performed on autistic children showed greater benefits of melatonin on sleep onset (47 minutes) as well as sleep duration (52 minutes) when compared to placebo [67]. Melatonin also shows positive effects when treating depression [64].

Another interesting application for melatonin might be the treatment of poisoning with – or toxic side effects of – various substances like sulfur mustard [68], arsenite [69], mercuric chloride [70-71], nickel [72] or carbon tetrachloride [73], the chemotherapeutic drugs adriamycin [74] and doxorubicin [75] as well as the immunosuppressant cyclosporine A [76]. For doxorubicin, simultaneous treatment with melatonin seems not only to ameliorate the cytotoxic side effects of the doxorubicin, but melatonin also increases the drug's apoptosis inducing effect in hepatoma cells *in vitro* [77].

One more field of application for melatonin might be the treatment of glaucoma [78]. While melatonin does not decrease intraocular pressure, it reduces the destructive effects of ocular hypertension [79].

Many melatoninerous substances have been developed [80], however, few are available for human use. Melatonin itself, available as over-the-counter-medicine in the US and available on prescription in the European Union, is probably safe in low dosages [64]. Agomelatine, an agonist at MT<sub>1</sub> and MT<sub>2</sub> and an antagonist at 5-HT<sub>2C</sub> receptors, is used primarily as an antidepressant with good efficacy even in severely depressed patients, and exhibits relatively few adverse effects [81]. Ramelteon, a

selective MT<sub>1</sub> and MT<sub>2</sub> agonist, is effective in promoting sleep in animals and patients with insomnia by regulating the body's natural clock. Unlike other hypnotics, it does not cause withdrawal symptoms or dependence and has only mild side effects [82]. Finally, another new compound, Tasimelteon, a high affinity MT<sub>1</sub> and MT<sub>2</sub> agonist, has proved in clinical trials to improve sleep quality, onset and duration in patients with transient insomnia. Adverse effects were similar for Tasimelteon and placebo [83].

A very promising field for melatonin treatment might be the prevention or alleviation of damage from cardiovascular diseases. Various studies have shown that in patients with acute myocardial infarction [84], coronary heart disease [85-86] or cardiac syndrome X [87], nighttime melatonin levels are reduced. Therefore, it was investigated, whether exogenous melatonin has a beneficial effect on these conditions. Indeed, on artificially ischemic rodents, exogenous melatonin exhibits dramatic effects: animals pre-treated with melatonin 10 minutes before artificially induced ischemia exhibit more than 50 % reduction of the total number of premature ventricular contractions, duration of ventricular fibrillation and ventricular tachycardia. Infarct size was reduced as well. Mortality decreased from 59 % in rats without melatonin treatment to 0–10 % in rats with pre-occlusion melatonin administration. All these effects were attributed to melatonin's antioxidative capabilities [57]. The protective action of melatonin has been demonstrated by similar studies (e.g. [58]) or studies performed on different organs in similar ischemic conditions (e.g. [88]). Because of these promising results, the phase II MARIA trial is being undertaken to confirm the cardioprotective capability of melatonin for patients with acute myocardial infarction undergoing primary angioplasty [89-90].

For more information about melatonin and its protective influence on the cardiovascular system see [91] or [92].

## **2.6 Melatonin and blood pressure (BP) regulation**

### **2.6.1 General overview on BP regulation**

The regulatory mechanisms of BP are manifold. Three parameters influence BP: heart activity (heart rate and contractile force), blood volume and peripheral resistance of the arterioles and capillaries. Through vasoconstriction of arterioles, BP is elevated, while vasodilation reduces BP[93]. To describe all these parameters and the mechanisms that influence them would go beyond the scope of this work. A simplified overview is given in Figure 11. The reader is directed to the pertinent literature for details [94].





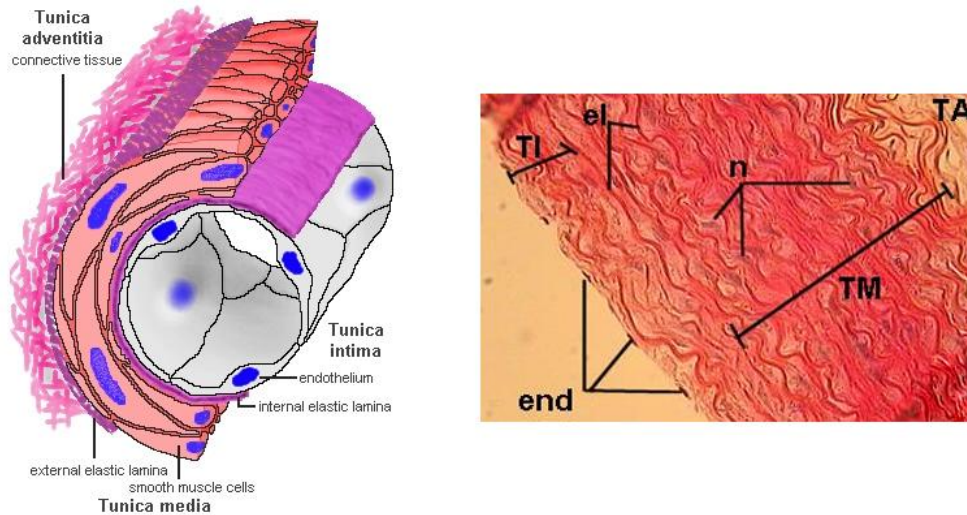


**Figure 12:** Anatomical structure of the aorta. Left panel: schematic depiction of the aorta. Right panel: Histological section of the aorta. TI: tunica intima, end: endothelium, el: elastic lamellae, n: smooth muscle tissue, TM: tunica media, TA: tunica adventitia. Left panel modified after [97], right panel modified after [99].

An important function of the endothelium in blood vessels is the production of nitric oxide (NO), which was identified as the endothelial derived relaxing factor. NO is produced in endothelial cells via NO-synthase and then diffuses in gaseous form in the tunica media where it activates the guanylyl cyclase, which leads to subsequent relaxation of the smooth muscles [100]. Activation of the NO-synthase can be mediated through a variety of factors, including melatonin [61].

In contrast, vasoconstriction is mediated only through direct activation of receptors on the smooth muscle cells. Examples for these substances include norepinephrine or angiotensin II [101], but probably also melatonin [61].

### 2.6.3 Reduced melatonin levels lead to hypertension

Melatonin's physiological function in BP regulation is revealed by the fact that in pinealectomized rats BP increases significantly. Interestingly, the effect is only temporary, as the elevated BP returns to normal values 90 days after the operation [102]. A possibly BP related side effect of pinealectomy is reduced release of vasopressin (a peptide hormone secreted by the pituitary gland regulating water retention and vasoconstriction). Vasopressin levels are significantly lower in pinealectomized rats than in sham operated animals. The osmotic threshold for vasopressin release remains unchanged and only the quantity of released hormone is reduced. This indicates that it is not the actual release of vasopressin that is mediated by melatonin, but the magnitude of the response to altered osmotic conditions, possibly

via some central mechanism not yet discovered [103]. However, since vasopressin action seems to be lower in rats with less melatonin, this fact cannot add to the explanation of the elevated BP in pinealectomized rats.

In patients with nocturnal hypertension, melatonin levels are decreased [104]. This adds to the hypothesis that inhibited melatonin secretion leads to elevated BP, thus suggesting a BP reducing effect of melatonin. Because of this, it seems irritating at first that in other studies, patients with essential hypertension exhibited significantly increased melatonin levels. However, treatment with lacidipine, an antihypertensive drug, not only reduces BP, but the elevated melatonin levels, too [105]. Taken together with the observation that melatonin restores contractile and relaxing functionality in the aorta [106-108], this suggests that BP is not elevated because of the elevated melatonin levels, but in spite of them. Natural melatonin secretion might be increased in hypertensive patients to counteract the elevated BP.

Because of these findings, the use of exogenous melatonin to combat hypertension seems promising.

#### **2.6.4 Influence of melatonin on animal models of hypertension**

Exogenous melatonin exerts a profound influence on hypertension in animals. However, the mechanism of this influence on the BP remains somewhat unclear. As discussed already, melatonin exerts direct influence on smooth muscle tone in blood vessels – and therefore possibly peripheral resistance –, although the data on this influence is conflicting (see 2.6.6).

Apart from this direct influence, melatonin may play a role in mediating central BP regulation as well. Baroreflex responses are improved under melatonin treatment as sympathetic output is decreased. Inhibition via GABAergic fibers from the SCN of areas in the central nervous system responsible for BP regulation might be a possible explanation [61, 109]. In a study performed on rats with stress induced hypertension by electric shocks for two weeks, pre-treatment with melatonin reduced caudal arterial pressure almost to control values. Associated with this reduction was a decrease of angiotensin II levels which was possibly caused by GABA<sub>A</sub> signaling, since the BP and angiotensin II reducing effect of melatonin was nullified when given in combination with bicuculline, a GABA<sub>A</sub> antagonist [109]. This central regulatory mechanism might be receptor-mediated, as another study on the same model of hypertension showed. Under melatonin influence GABA levels in the central nervous system were elevated, while luzindole nullified the effect of melatonin completely [110]. The angiotensin II dependent decrease of BP mentioned before was also observed in rats with angiotensin II levels artificially increased by means of a renal artery clip. Melatonin

treatment reduced the elevated BP and improved the angiotensin II dependent reduced cardiac function [111].

Another factor in melatonin's BP reducing activity might be its antioxidative capability, which prevents structural damage in blood vessels, therefore helping to retain their dilative capabilities [61]. In spontaneously hypertensive rats (SHR; see below), melatonin treated animals exhibit decreased aortic [76] and cardiac [112] collagen content (as opposed to "normal" development of untreated SHR [113]) and thus heart fibrosis is prevented. The apoptosis rate of blood vessel cells is elevated, too, which might be an indicator for increased remodeling of vasculature in response to melatonin [114].

Melatonin treatment of these genetically predisposed hypertensive rats also results in greatly decreased BP in the melatonin treated group (systolic: 149 vs 195 mm Hg in the untreated group). As expected, superoxide and NF- $\kappa$ B levels are reduced [115] in treated animals. Additionally, melatonin improves maximum response of mesenteric arteries of SHR to endothelium dependent vasodilating stimuli like acetylcholine [116].

SHR are a model for essential hypertension; they were originally bred from normal Wistar-Kyoto rats by Okamoto [117]. After reaching adulthood, the systolic BP of SHR reaches 180–200 mm Hg, while after about 40–50 weeks, SHR develop hypertension associated cardiovascular diseases [118]. The cause for this development of hypertension is believed to be of higher central origin [119].

SHR as model of hypertension were also used in the thesis at hand to study the difference in melatonin receptor expression levels in the vascular system between normotensive and hypertensive animals.

### **2.6.5 Influence of melatonin on the BP of humans**

Orally administered melatonin significantly reduced BP together with norepinephrine levels without affecting the heart rate in healthy men [120] and reduced BP in women by about 9 mm Hg [121]. Similar studies on healthy subjects confirmed these findings [122-123]. Prolonged nocturnal melatonin treatment did not change diurnal BP variations [123].

In patients with essential nocturnal hypertension, repeated melatonin treatment at bedtime reduced nocturnal BP by 6 (systolic) and 4 (diastolic) mm Hg. The reduction is most significant during the night (see Figure 13) [124].

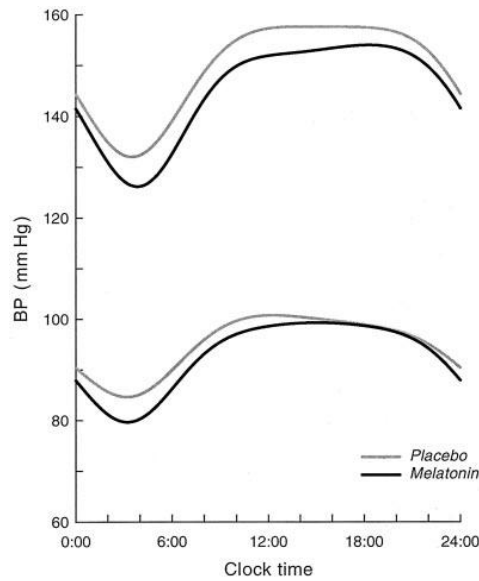


**Figure 13:** Effect of melatonin treatment on the BP of hypertensive patients. The reduction of the diastolic BP is most significant during the night [124].

Similar results were obtained in a study performed on so-called “non-dipper” patients who exhibit an abnormal circadian BP profile, manifesting in elevated BP during the night, but normal BP during the day. Starting from the observation that melatonin levels are decreased during the night in non-dippers [104], 5 mg of melatonin were administered daily before sleep. 35 % of the patients showed complete pattern normalization (vs 15 % in the control group). This effect was not only caused by nighttime BP reduction, but also by daytime BP elevation. Because of these results, the authors of the study recommend close monitoring of the circadian BP profile when using melatonin as antihypertensive medication to avoid the risk of induced arterial hypertension [125]. Another dilemma with long time, high dose melatonin treatment adds to this problem: chronic treatment leads to reduced ROS levels in the blood, but in a long term view this is not only beneficial, since ROS also play important regulatory functions. Reduced ROS levels might lead to reduced NO-synthetase induction and therefore reduced blood vessel dilation, thus again leading to elevated BP [126].

## **2.6.6 Contribution of MT<sub>1</sub> and MT<sub>2</sub> to BP regulation**

### **Expression of MT<sub>1</sub> and MT<sub>2</sub> in the vasculature**

MT<sub>1</sub> and MT<sub>2</sub> were detected in the human vascular system using RT-PCR and western blot [127-128]. MT<sub>1</sub> receptor expression was shown to be highly dependent on circadian rhythm, with the lowest values at night and the highest values in the afternoon [129].

The data on the rat vascular system is conflicting. Pharmacological studies indicated that MT<sub>1</sub> is indeed expressed in the rat's cardiovascular system. Lartaud et al. [56] demonstrated a clear effect of melatonin on rat aortic rings. Melatonin prevented incubation induced loss of contraction which was reversible by the melatonin receptor antagonist luzindole, therefore suggesting present and functional receptors. Similarly, melatonin effects direct vasoconstriction in rat cerebral arteries [130], and the vasoconstriction effect can be reversed by luzindole in rat arterioles. This clearly points to melatonin GPCRs as the responsible element for vasoconstriction in these arteries [131].

Then again, Chucharoen et al. [132] could detect neither MT<sub>1</sub>, nor MT<sub>2</sub> mRNA in rat cerebral arteries, while Masana et al. [36] reported MT<sub>1</sub> and MT<sub>2</sub> mRNA to be present in the rat caudal artery; however, because the primers used in both studies were located only on one exon, it is possible that amplification of genomic DNA influenced the findings. To address this problem, experiments with exon spanning primers are necessary, so that false positives due to amplification of genomic DNA can be excluded.

If MT<sub>1</sub> is indeed expressed in the vasculature of the aorta, the circadian expression pattern observed in humans [129] seems to be organ and / or species specific, as MT<sub>1</sub> expression levels in the rat heart and aorta do not exhibit a diurnal rhythm, as observed on the protein level by Benova et al. [108]. In this study, MT<sub>1</sub> was identified in the aorta of Wistar rats on the protein level by western blot, but of course the problem with antibody specificity [24] remains, putting the results into perspective. Investigations on the mRNA level are necessary to confirm or discard these results on circadian expression of MT<sub>1</sub> and were performed in the course of this thesis..

### **Mechanisms of melatonin influence on the vasculature**

There have been many different reports on melatonin's influences on vasculature and the pathways explaining these influences.

It was suggested that melatonin effects vasoconstriction through blockage of BK<sub>Ca</sub> channels, probably via MT<sub>1</sub> [61], as blockage of these channels inhibited further

constriction by melatonin but not by compounds using a different mechanism of action like the NO-synthase inhibitor L-NAME (N-nitro-L-arginine-methyl-ester) [131].

In contrast to  $MT_1$ ,  $MT_2$  seems to mediate vasodilation: Doolen et al. [133] noted that isolated rat caudal segments showed increased constriction in presence of the  $MT_2$  antagonist 4-phenyl-2-acetamidotetraline.

These findings were confirmed in 2002 by Masana et al. [36] by comparing the contractile responses of the rat arteries in presence of melatonin alone, melatonin compared with 6-chloro-melatonin (10-fold less sensitive to  $MT_1$  than  $MT_2$ ) and melatonin plus 4-Phenyl-2-propionamidotetralin, an antagonist for  $MT_1$  and  $MT_2$ , which is selective for  $MT_2$  in concentrations of about 10 nM. 6-chloro-melatonin ( $MT_2$  agonist) was 10 times less effective in potentiating vasoconstriction than melatonin (Figure 14, left panel), suggesting that  $MT_1$  and not  $MT_2$  is responsible for potentiation of exogenously induced vasoconstriction (in this case by phenylephrine). Selective antagonistic concentrations of 4-Phenyl-2-propionamidotetralin for  $MT_2$  (10 nM) markedly increased the contractile response to melatonin (Figure 14, right panel). This strongly suggests that  $MT_2$  attenuates  $MT_1$  mediated vasoconstriction. Nevertheless, the vasodilating influence of  $MT_2$  is covered by the contracting effect of  $MT_1$ , as melatonin alone had a contracting effect.

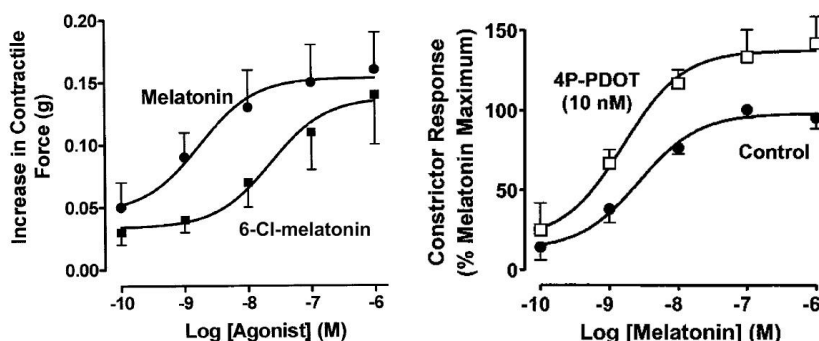


**Figure 14:** Left graph: effect of low affinity  $MT_1$  agonist 6-chloro-melatonin (6-Cl-melatonin) on contractile response compared to melatonin, demonstrating  $MT_1$  dependent increase in contractile force. Right graph: effect of melatonin in presence of a  $MT_2$  selective concentration of 4-Phenyl-2-propionamidotetralin (4P-PDOT) compared to melatonin alone, demonstrating generally elevated contractile force and increased maximum response to melatonin which suggests an attenuating influence of  $MT_2$  on  $MT_1$ . Modified after [36].

So, in summary,  $MT_1$  mediates vasoconstriction and  $MT_2$  vasodilatation, but probably to a lesser extent. It has been proposed that vasoconstriction is triggered through  $G_q$  mediated  $Ca^{2+}$  efflux from the sarcoplasmic reticulum directly into smooth muscle cells. Vasodilation on the other hand is mediated indirectly via melatonin induced activation of NOS in endothelial cells of the blood vessels (see Figure 15).

Details can be found in [61]. See chapter 2.6.2 for basic information on blood vessels. For understanding of these proposed pathways, it is essential to know whether both melatonin receptors are present in the cardiovascular system. The thesis at hand confronts this question.

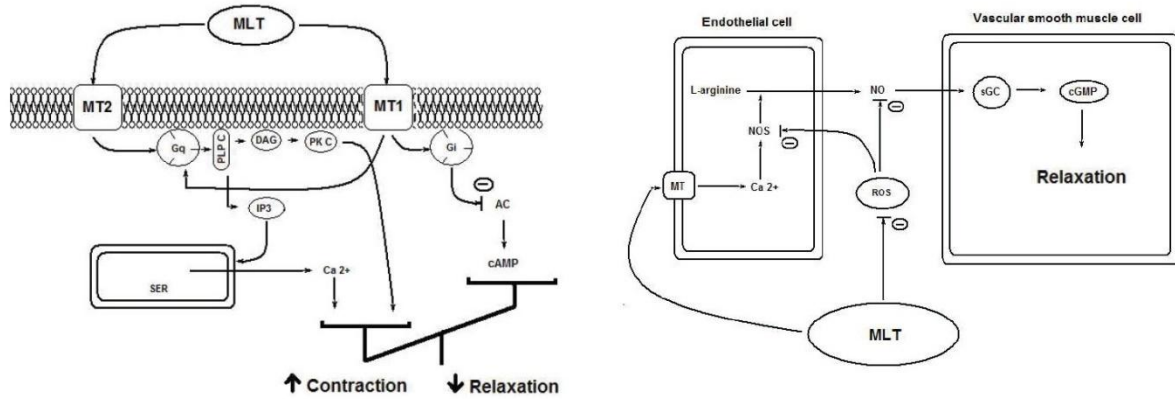


**Figure 15** Left panel: potential pathway mediating melatonin induced vasoconstriction in vivo. Melatonin activates  $MT_1$  (and  $MT_2$ ) directly on smooth muscle cells which both activate a  $G_q$ -protein, leading to  $Ca^{2+}$  efflux from the sarcoplasmic reticulum and subsequent muscle contraction. At the same time  $MT_1$  activates a  $G_i$ -protein which inhibits the formation of cAMP and subsequent muscle relaxation. Right panel: potential pathway mediating melatonin induced vasodilatation in vivo. Melatonin activates  $MT_2$  on endothelial cells, which leads to activation of NOS through increased  $Ca^{2+}$  concentrations. At the same time, melatonin scavenges ROS that normally intercepts NO in the tissue. Both modified after [61]. Q. v. for abbreviations, literature and detailed information.



### 3 AIMS

Melatonin is known to influence BP and this influence is, at least partly, mediated by the G-protein coupled receptors (GPCRs)  $MT_1$  and  $MT_2$  [61].

Because the vascular system plays an integral role in BP regulation and melatonin is known to influence vascular tone, both dilating and contracting (e.g. [36, 56, 108, 131, 134]), it is of interest to know how these responses are mediated. The data on melatonin GPCR expression in the vascular system in general and the aorta as a model is conflicting. Both  $MT_1$  and  $MT_2$  have been found as well as not found in various studies with various vascular models including the aorta [56, 108, 127, 132, 135]. Most of these experiments were performed on the protein level or via pharmacological studies and it has to be noted that the antibodies for rat melatonin GPCRs are not well characterized [24]. The few RT-PCR studies [36] were performed with intra-exon primers designed from non-complete sequences of the mRNA of both receptors. Recently, Ishii et al. [26] demonstrated the expression of rat  $MT_1$  and  $MT_2$  mRNA in many rat tissues by RT-PCR using exon spanning primers derived from the complete mRNA sequences. Starting from the findings and methods of that study [26], in the thesis at hand the expression of  $MT_1$  and  $MT_2$  in the rat aorta were to be characterized, pursuing the following aims.

#### 1) Establishment of molecular biological methods for demonstrating $MT_1$ and $MT_2$ mRNA expression

The first aim of the thesis was to establish the RT-PCR and RT-qPCR protocols for detection of rat  $MT_1$  and  $MT_2$  mRNA. To achieve this goal, we had to establish the method for RNA extraction and reverse transcription and test the published RT-PCR method by Ishii et al. [26] and an RT-qPCR method on various rat organs as well as adjust the methods as necessary to achieve consistent results.

#### 2) Investigating the expression of $MT_1$ and $MT_2$ in the rat aorta

Following the establishment of the methods, RT-PCR experiments to investigate the expression of  $MT_1$  and  $MT_2$  mRNA in the rat aorta as a model system for arterial blood vessels were performed.

**3) Quantification of MT<sub>1</sub> and MT<sub>2</sub> mRNA expression difference in the rat aorta depending on the time of day**

The melatonin GPCRs are known to exhibit circadian expression patterns in some organs [136]. Because BP is subjected to high diurnal variations [137] and the regulating influence of melatonin on BP is known [61], it was of interest to assess whether the expression levels of MT<sub>1</sub> and / or MT<sub>2</sub> were different in the vascular system depending on the time of day. The data on this is conflicting, as a diurnal variation has been demonstrated for human coronary arteries [129], while in the rat aorta, no circadian rhythms were observed at the protein level [108]. Consequently, as a third aim of the thesis, we performed RT-PCR and RT-qPCR experiments to evaluate a possible difference in receptor expression at the mRNA level between rat aortas of two time groups.

**4) Quantification of MT<sub>1</sub> and MT<sub>2</sub> mRNA expression difference in the rat aorta depending on BP**

Because the mechanisms of BP regulation by melatonin are still somewhat unclear [61], it is of interest to know whether there is an expression difference of melatonin GPCRs – if they are present – in the vascular system between normotensive and hypertensive animals. As of yet, the only data available is from L-NAME induced hypertensive rats, where no difference in expression was found on the protein level [108]. Therefore, as a fourth aim of the thesis, we performed RT-PCR and RT-qPCR experiments on aortas of control and spontaneously hypertensive rats (SHR) to assess if there was such a difference at the mRNA level.

**5) Localization of MT<sub>1</sub> and MT<sub>2</sub> protein in the rat aorta**

If the melatonin GPCRs can be found on the mRNA level because of the proposed different signaling and regulating mechanisms of MT<sub>1</sub> and MT<sub>2</sub> [61], it is of interest to know the allocation of MT<sub>1</sub> and / or MT<sub>2</sub> within the aorta. Some studies on the localization of the melatonin GPCRs have been performed [135, 138], but so far only on human and chicken samples and using immunohistochemistry and radio assays respectively. To better understand the effects of melatonin on MT<sub>1</sub> and MT<sub>2</sub> in blood vessels, immunofluorescence (IF) stainings to localize MT<sub>1</sub> and MT<sub>2</sub> in the structure of the rat aorta were performed as the fifth aim of the thesis.

## **4 MATERIALS AND METHODS**

### **4.1 Samples**

#### **4.1.1 Various rat organs for PCR method establishment**

Various rat organs (brain, eye, heart, intestine, kidney, liver, lung, skeletal muscle, testes and thymus) have been prepared and frozen in 2008 by M. Svoboda (Department of Pathophysiology, Medical University Vienna). These tissues were used for establishing the methods for RNA-isolation, RT-PCR, RT-qPCR.

#### **4.1.2 Rat aortas from two different time points**

Sixteen prepared aortas of normal (Wistar) rats were kindly provided by Professor M. Zeman, Comenius University of Bratislava, Slovakia. Prior to dissection, the animals were kept in a 12 / 12 day / night rhythm (lights off at 22:00 hours and lights on at 10:00 hours). Half of the aortas were obtained in operations 2 hours before lights on (nighttime group; A75, A76, A77, A79, A81, A82, A83, A88) and 2 hours before lights off (daytime group; A31, A32, A33, A34, A35, A36, A37, A38), respectively. The aortas were then frozen at -80 °C and finally transferred to Vienna on dry ice.

These aortas were used to examine whether melatonin receptor expression follows a circadian rhythm in the rat aorta by usage of PCR experiments.

The names of the aortas are taken from the nomenclature used by the Comenius University of Bratislava and kept for better traceability of the samples.

#### **4.1.3 Rat aortas from SHR and control rats**

Sixteen prepared aortas of SHR (ASHR 01–ASHR 08) and control (Wistar; ACTRL 01–ACTRL 08) rats were kindly provided by Professor M. Zeman, Comenius University of Bratislava, Slovakia. After dissection, a part of each aorta was fixated in HOPE® solution (DCS, Hamburg, Germany) and transferred to Vienna on blue ice, while the other part was frozen at -80 °C and transferred to Vienna on dry ice. The HOPE® fixated parts of the aortas were then paraffin-sectioned by H. Uhrova (Department of Pathophysiology, Medical University Vienna), while the other part was used for RNA extraction and the subsequent PCR experiments.

These aortas were used to examine whether the expression of MT<sub>1</sub> and MT<sub>2</sub> is different in the aortas of hypertensive and normotensive rats by usage of PCR and IF experiments with paraffin-sections.

### **4.1.4 Additional rat aortas for IF experiments**

These aortas were prepared for cryo-sectioning in 2008 by M. Benova (Comenius University of Bratislava, Slovakia; during a research stay at Department of Pathophysiology, Medical University Vienna) and stem from SHR (A\_cryo4–A\_cryo6) and control (Wistar; A\_cryo1–A\_cryo3) rats. These tissues were used for IF method establishment to examine the difference in melatonin receptor expression by usage of IF experiments with cryo-sections.

### **4.1.5 Mouse organs for IF experiments**

The organs (brain and intestine) were prepared by H. Uhrova, R. Stumberger and C. Brünner-Kubath and then HOPE® fixated and paraffin-sectioned by H. Uhrova (all Department of Pathophysiology and Allergy Research, Medical University Vienna). These organs were used as positive controls in some IF experiments.

## **4.2 RNA isolation from frozen tissues**

### **4.2.1 Background**

After [139].

In order to demonstrate the occurrence of specific mRNA, the first step is to isolate the total RNA of all tissues that are to be investigated. The total RNA of a tissue is isolated by extracting it from deep frozen or freshly prepared tissue samples, which are first pulverized and then subjected to peqGOLD TriFast™ treatment. PeqGOLD TriFast™ treatment is an optimized guanidineisothiocyanate / phenol method, suitable for RNA, DNA and protein extraction. After extraction and homogenization with PeqGOLD TriFast™, chloroform is added to the mixture, where the DNA and protein fraction will enrich, while the more hydrophilic RNA will stay in the aqueous phase. The RNA can then be precipitated using isopropanol, washed with ethanol and finally solved in DNase, RNase, DNA free water (“PCR water”). The isolated and purified RNA can then be stored over a long period of time at -80 °C.

## 4.2.2 Materials

- Box with ice
- Chloroform (Merck, 2445)
- Coolable Centrifuge (Eppendorf, Centrifuge 5415R)
- DNase, RNase, DNA free distilled water, "PCR water", (Gibco, 0977035)
- DNase, RNase, DNA free pipette tips
  - 1250 µL (Biozym, Safe seal tips® professional, 770600)
  - 200 µL (Biozym, 770280)
- DNase, RNase, DNA free tubes 1,5 mL (Biozym, 710310)
- Ethanol 70% (diluted from Ethanol absolute, VWR Prolabo, 20821.310)
- Forceps
- gloves for cryogenic work (handling of liquid N<sub>2</sub>, Tempshield, Cryogloves®)
- Heating block (Eppendorf, Thermomixer 5436)
- Homogenizer (IKA® Werke, T10 basic Ultra Turrax®, 3420000)
- Isopropanol (Merck, 1.09634.1011)
- Latex gloves (Hartmann, Peha-Soft® powderfree, 942162)
- Liquid N<sub>2</sub>
- Mortar + pistil
- Paper towels
- peqGOLD Trifast™ (peqLAB, 30-20XX)
- Polystyrene (styrofoam) boxes (two) with lids
- Polystyrene rack
- Protective glasses
- Small flasks (Greiner bio-one, scintillation vial 27.0/60.0 mm, 619301; saw off neck)
- Vortexer (Labinco, L24)

### 4.2.3 Method

1. Preparation
  - a. Fill the Styrofoam boxes with liquid N<sub>2</sub>
  - b. Put the Styrofoam rack in the box
  - c. Put the small flasks in the styrofoam rack
  - d. Put the sample(s) (from -80 °C cooling unit) in the styrofoam box
  - e. Put the mortar into the second styrofoam box and fill mortar and box with some liquid N<sub>2</sub>
2. Sample preparation
  - a. Put 50–100 mg or about 5x5x1 mm of tissue (break if necessary) into the mortar (with liquid N<sub>2</sub>)
  - b. Pulverize the tissue with the pistil and avoid complete evaporation of the N<sub>2</sub> in the mortar
  - c. Transfer the crushed tissue plus some liquid N<sub>2</sub> into a flask (scintillation vial with sawed off neck)
  - d. Keep the flask containing the sample in the Styrofoam box with liquid N<sub>2</sub> and avoid drying out of the liquid N<sub>2</sub> in the flask
3. TriFast™ utilization
  - a. When all samples are homogenized, let the N<sub>2</sub> in the flask evaporate and add 1 mL of Trifast™ reagent (per max. 100 mg of tissue) to the flask (one flask at a time!)
  - b. Transfer the flask from the Styrofoam box to ice
  - c. Homogenize for 30 seconds with UltraTurrax® (avoid excess heat generation)
  - d. Transfer the homogenated tissue into one 1.5 mL tube (per 1 mL Trifast™) and ...
  - e. ... put the tube immediately on ice and incubate for 5 min
  - f. Incubate for 5 min at rt – from now on, work in a bench designated for RNA extraction (storage is now possible at -80 °C)
4. RNA isolation
  - a. Add 200 µL chloroform
  - b. Vortex for 15 sec
  - c. Incubate for 5 min at rt
  - d. Centrifuge for 15 min at 12,000 x g / 4 °C → phase separation
  - e. Transfer the upper aqueous phase (containing RNA) to a fresh tube
  - f. Centrifuge again for 15 min at 12,000 x g / 4 °C, meanwhile ...
5. RNA precipitation

- a. ... prepare a fresh tube and fill it with 500  $\mu\text{L}$  isopropanol
  - b. Transfer the aqueous phase (containing RNA) to the tube with isopropanol
  - c. Vortex for 10 sec
  - d. Incubate for 10 min on ice
  - e. Centrifuge for 15 min at  $12,000 \times g / 4 \text{ }^\circ\text{C}$
  - f. Remove the isopropanol from the precipitate
6. RNA washing
- a. Wash the pellet with 1 mL ethanol 70 % (v / v) by vortexing
  - b. Centrifuge for 10 min at  $12,000 \times g / 4 \text{ }^\circ\text{C}$
  - c. Remove the ethanol thoroughly from the pellet
  - d. Repeat steps 6a through 6c once, then continue to step 7a
7. Solving and storing
- a. Dry the pellet in a heating block at  $55 \text{ }^\circ\text{C}$  for 1 (max. 3) min with opened lid
  - b. Add 20  $\mu\text{L}$  PCR water
  - c. Pipette up and down a few times until the RNA is dissolved
  - d. Incubate at  $55 \text{ }^\circ\text{C}$  for 5 min
  - e. Store RNA at  $-80 \text{ }^\circ\text{C}$

## 4.3 Quantification and purity assessment of RNA and DNA

### 4.3.1 Background

The quantity of RNA or DNA is then determined by UV/VIS spectrophotometry. The ratio of the samples' absorbance at 260 nm and 280 nm ( $A_{260} / A_{280}$ ) is used to assess its purity. For extracted RNA, the PeqGOLD TriFast™ instruction manual [139] specifies an achievable ratio of 1.60–2.00, depending on the type of tissue and certain other factors.

### 4.3.2 Materials

- Box with ice (for transportation of samples)
- DNase, RNase, DNA free pipette tips
  - 10  $\mu\text{L}$  (Biozym, 770010)
  - 20  $\mu\text{L}$  (Peqlab, 81-1020)
- Paper towels
- Soft paper wipes (Kleenex®)

- Solvent, 10  $\mu\text{L}$  (here: DNase, RNase, DNA free distilled water, “PCR water”; Gibco, 0977035) for blank measurements
- Spectrophotometer (Thermo Fisher Scientific, NanoDrop™ 1000)
- Vortexer (Labinco, L24)

### 4.3.3 Method

1. Start the ND-1000 program
2. Choose the appropriate user name from the drop down menu (enter a password if necessary) and then choose the button “Nucleic Acid”
3. The software prompts to load a water sample
4. Sample loading procedure
  - a. Open the instrument’s arm
  - b. Apply a volume of the sample (1–2  $\mu\text{L}$ ) to the lower measurement pedestal
  - c. Carefully close the instrument’s arm (do not use force)
5. Click “OK”
6. Load a water sample (PCR water)
7. After initialization of the instrument is complete, wipe the residue from the upper and lower pedestals with a soft wipe.
8. Select the appropriate calculation method (DNA-50 or RNA-40) for the type of sample (DNA or RNA) using the drop down menu
9. Load a blank sample (here: 1  $\mu\text{L}$  PCR water)
10. Click “Blank”
11. Clean the pedestals
12. Load 1  $\mu\text{L}$  of sample
13. Click “Measure”
14. Take down the readings (concentration,  $A_{260} / A_{280}$  ratio)
15. Clean the pedestals
16. Repeat steps 11–14 for all samples
17. Load a blank sample (here: 1  $\mu\text{L}$  PCR water)
18. Click “Measure” – the spectrum should exhibit a relatively flat bottom line
19. Clean the pedestals and do not forget to close the sample arm
20. Click “Exit”, then “Exit” again to close the program



## 4.4 Agarose gel-electrophoresis (GE)

### 4.4.1 Background

GE is employed to separate nucleic acids like RNA and DNA by their size. As the name suggests, the gels employed in this method are made of dissolved and re-solidified agarose in TRIS-acetic-acid-EDTA (TAE) buffer. The samples are mixed with loading dye, which contains dyes that migrate at the same speed as nucleotides of a certain length and also serves the purpose of increasing the samples' specific weight, so it will not be washed out of the gel pocket. The sample-loading dye mixtures are then loaded in the pockets of the gel, which is submerged in TAE buffer. After the loading procedure, a current is applied along the gel. Because RNA and DNA are negatively charged, they will be drawn to the anode. The gel retains this migration, larger nucleic acid molecules being more strongly retained than smaller ones. After a certain time, the current is switched off and the separated nucleic acids appear as bands along the migration route.

To make these bands visible, the gel contains ethidium bromide, which intercalates with DNA or RNA molecules. This intercalation results in orange fluorescence if the molecule complex is subjected to UV light. Therefore, while (trans-)illuminating the gel with UV light, nucleic acid bands can be seen and photographed.

When used for testing the intactness of isolated total RNA, two distinct bands will appear for the 28S and 18S rRNA (ribosomal RNA, accounting for over 98 % of the total RNA in a cell) if the RNA is not degraded. If the RNA is degraded – through contamination with RNase – GE will show a smear of low molecular weight bands.

When used for analysis of (RT-) PCR products, a marker, containing a defined amount of DNA fragments of several defined lengths, should be used to assess the size of the PCR product.

### 4.4.2 Buffers and solutions

#### 0.5 M EDTA solution

##### *Materials*

- Aqua bidest.
- EDTA, Na-salt (Merck, 1.08418.1000)
- NaOH (Merck, 1.06498.1000)
- pH-meter (Metrohm, pH-Lab 827)

### *Method*

1. Solve 93.05 g EDTA, Na-salt in 400 mL aqua bidest.
2. Adjust the pH to 8.0 with NaOH
3. Adjust the volume to 500 mL with aqua bidest.
4. Store at rt

### **TAE stock solution (50x)**

#### *Materials*

- 0.5 M EDTA solution (see above)
- Aqua bidest.
- Glacial acetic acid (Merck, 8.18755.2500)
- Tris (Merck, 1.08382.1000)

#### *Method*

1. Solve 242 g of Tris in 750 mL aqua bidest.
2. Add 57.1 mL of glacial acetic acid
3. Add 100 mL of 0.5 M EDTA
4. Fill to 1000 mL with aqua bidest.
5. Store at rt

### **1x TAE buffer**

#### *Materials*

- TAE stock solution (50x) (see above)
- Aqua bidest.

#### *Method*

1. Dilute one part TAE stock solution (50x) with 49 parts aqua bidest. (1 : 50)
2. Store at rt

### **Ethidium bromide solution 10 mg / mL**

#### *Materials*

- Aqua bidest.
- Ethidium bromide (Amresco, 0492-56)
- Latex gloves (Hartmann, Peha-Soft® powderfree, 942162)
- Nitrile gloves (Meditrade Medicare, Senso Nitril®, 14211)

*Method*

1. Solve 10 mg ethidium bromide in 1 mL aqua bidest.
2. Store at rt

**6x loading dye***Materials*

- Bromphenolblue (Amresco, 0449)
- Xylene cyanol FF (Amresco, 0819)
- Glycerol (Merck, 1.04094.0500)
- DNase, RNase, DNA free distilled water, "PCR water" (Gibco, 0977035)
- Latex gloves (Hartmann, Peha-Soft® powderfree, 942162)

*Method*

1. Mix 0.25 % (w / v) of bromphenolblue
2. 0.25 % (w / v) xylene cyanol FF
3. 30 % (v / v) glycerol
4. and 69.5 % (v / v) PCR water
5. Store in aliquots at -20 °C

**4.4.3 Preparation of agarose gels***Materials*

- 1x TAE buffer (see 4.4.2)
- Agarose (Invitrogen, 10975-035)
- Combs and walls fitting for the GE chamber
  - Wall (Peqlab, 41-1325-Wall)
  - Comb 28 well (Peqlab, 41-1325-28D)
  - Comb 20 well (Peqlab, 41-1325-20D)
  - Comb 16 well (Peqlab, 41-1325-16D)
- Ethidium bromide solution 10 mg / mL (see 4.4.2)
- GE chamber (Peqlab, 41-1325)
- Latex gloves (Hartmann, Peha-Soft® powderfree, 942162)
- Microwave oven (Moulinex® Micro-Chef Mo 55)
- Nitrile gloves (Meditrade Medicare, Senso Nitril®, 1421I)
- Saran wrap

### *Method*

1. Prepare the GE chamber (combs and side walls)
2. According to the desired concentration of the gel, mix the respective amount of agarose with 1x TAE buffer (e.g. 2.625 g agarose in 175 mL 1x TAE buffer for a 1.5 % gel)
3. Microwave the solution until the first boiling appears
4. Shake the solution and let it cool down until it is not steaming any more
5. Add 0.007 % of ethidium bromide solution (10 mg / mL; e.g. 12.5 µL in 175 mL gel solution)
6. Pour the gel into the prepared GE chamber and let the gel solidify
7. Add walls to the GE chamber if applicable
8. Remove the gel(s) and store them in plastic foil at 4° C

### **4.4.4 Electrophoresis**

#### *Materials*

- GE chamber (Peqlab, 41-1325)
- GE power supply (Peqlab, EV231)
- Agarose gel with ethidium bromide (see 4.4.3)
- UV transillumination imaging equipment (Biozym, Chemilmager 4400)
- Latex gloves (Hartmann, Peha-Soft® powderfree, 942162)
- Ladder (Fermentas, GeneRuler™, SM0323)
- Nitrile gloves (Meditrade Medicare, Senso Nitril®, 14211)
- DNase, RNase, DNA free pipette tips
  - 10 µL (Biozym, 770010)
  - 20 µL (Peqlab, 81-1020)
  - 100 µL (ART®, 100E, 2065E)
- DNase, RNase, DNA free distilled water, “PCR water” (Gibco, 0977035)
- 6x loading dye (see 4.4.2)
- Sterile 96 well plates (Greiner Labortechnik, PS-Mikrotiterplatte, 96K, kobaltsteril, 655161)
- Aqua bidest.

*Method*

1. Gel-electrophoresis
  - a. Mix a volume of sample (depending on the size of the gel pockets) with one sixth of loading dye in a well of a 96 well plate (pipette up and down to mix)
  - b. Repeat step a. for all samples
  - c. Load the gel
  - d. Ensure correct alignment of the gel in the GE rack and close the lid
  - e. Connect the GE electrodes to the GE power supply
  - f. Run the gel (suggested conditions: 150 V, 1:30 h; check the propagation of the loading dye during the run)
2. Analysis of the gel
  - a. Open the hatch of the transilluminator and place the gel on the surface for UV illumination
  - b. Start the chemi-Imager 4400 program
  - c. Click on "Acquire"
  - d. Activate epi-white, ensure that the aperture is not set too low
  - e. Align the gel and magnification so that it fills the preview completely
  - f. Click on "Exposure Preview"
  - g. Close the hatch, deactivate epi-white and activate UV
  - h. Change the exposure time and aperture so that the gel is correctly exposed
  - i. Click on "Capture Image"
  - j. After the image is taken, deactivate UV and click "Print"
  - k. Exit the program
  - l. Open the hatch, remove the gel, clean the UV surface with aqua bidest. and close the hatch again

## 4.5 Reverse Transcription

### 4.5.1 Background

After [140-141].

Because RNA itself is not suitable for PCR, it has to be converted to DNA first. This is done using reverse transcription, where RNA, e.g. total isolated RNA extracted from tissue, is reversely transcribed to single stranded complementary DNA (cDNA). This is done by adding dNTPs, random primers and reverse transcriptase, an enzyme gained from retro viruses, to the RNA sample. RNase inhibitor can be added, too, to prevent the degradation of the template RNA due to minute contamination with RNases. To avoid mix-ups and pipetting error, all components except for the samples are pre-mixed in a mastermix and added to the separate samples just before reaction.

The reaction mixture is warmed to 37 °C for two hours, during which the random primers bind to the RNA and the reverse transcriptase synthesizes a complementary strand of cDNA in 3' direction. After the two hours, the mixture is heated shortly to 85 °C to permanently inactivate the enzyme. The cDNA can then be stored over a long period of time at -20 °C and used for subsequent PCR or qPCR experiments.

### 4.5.2 Materials

- -20 °C storage box (for reverse transcriptase and RNase inhibitor)
- Box with ice
- DNase, RNase, DNA free distilled water, "PCR water" (Gibco, 0977035)
- DNase, RNase, DNA free pipette tips
  - 10 µL (Biozym, 770010)
  - 20 µL (Pepqlab, 81-1020)
  - 100 µL (ART®, 100E, 2065E)
- DNase, RNase, DNA free tubes with flat lid 0.2 mL (Biozym, 710920)
- Latex gloves (Hartmann, Peha-Soft® powderfree, 942162)
- RT Kit (Applied Biosystems, "High capacity cDNA reverse transcription kit", 4368814), contains:
  - 10x RT buffer
  - 10x RT random primers
  - 25x dNTP Mix (100 mM)
  - Multiscribe™ Reverse Transcriptase 50 U / µL
  - RNase inhibitor
- Thermal cycler (Eppendorf mastercycler personal, 53332 000.014)
- Vortexer (Labinco, L24)

### 4.5.3 Method

1. Preparation of 10  $\mu\text{L}$  of the RT 2x mastermix (per 20  $\mu\text{L}$  reaction)
  - a. Let the components thaw slowly on ice, do not take the enzymes out of the refrigerator yet!
  - b. Calculate the necessary amounts of reagent according to the number of samples plus one aliquot in excess
  - c. Prepare the RT 2x mastermix according to the following table (add the enzymes last, take them out of the refrigerator only in the  $-20\text{ }^{\circ}\text{C}$  storage box and put them back in the refrigerator as soon as possible!)

**Table 1:** Recipe for 10  $\mu\text{L}$  2x reverse transcription mastermix using the high capacity cDNA reverse transcription kit [142].

Vol [ $\mu\text{L}$ ]	Component
2.0	10x RT buffer
0.8	10x dNTP mix
2.0	10x RT random primers
3.2	PCR water
1.0	Reverse transcriptase
1.0	RNAse inhibitor

- d. Vortex the RT 2x mastermix for a short while and put it on ice
2. Preparation of the samples
  - a. Pipette an aliquot of RNA sample (containing 2  $\mu\text{g}$  of RNA) in a 0.2 mL tube
  - b. Add PCR water for a total volume of 10  $\mu\text{L}$
  - c. Add 10  $\mu\text{L}$  of RT mastermix and pipette up and down a few times to mix
  - d. Keep the prepared sample on ice
  - e. Repeat steps a–d for all samples
3. Reverse transcription
  - a. Put all the samples in the thermal cycler
  - b. Use the following temperature program:

**Table 2:** Temperature program for reverse transcription using the high capacity cDNA reverse transcription kit [142].

Step	Time	T [°C]
1	10 min	25
2	120 min	37
3	5 s	85
4	Hold	4

- c. Run the program
- d. After the program is finished, store the transcription products (cDNA) at -20 °C

## 4.6 PCR – Polymerase chain reaction

### 4.6.1 Background

After [143].

DNA or cDNA can be amplified using polymerase chain reaction (PCR). PCR was invented in 1983 and is now a fundamental tool in the life sciences [141]. dNTPs, target specific primers for the nucleotide sequence of interest, and the enzyme Taq-polymerase (from the bacterium *thermus aquaticus*) are added to the (c)DNA of the sample. To stabilize the enzyme, MgCl<sub>2</sub> is added to the reaction mixture. To avoid mix-ups and pipetting error, all components except for the samples are pre-mixed in a mastermix and added to the separate samples just before reaction.

Initially, the reaction mixture is heated to about 95 °C for a few minutes to completely denaturize all double strands of DNA.

The samples are then subjected to three steps of different temperatures for different periods of time: 1) Denaturation: 95 °C for about 30 seconds to one minute for complete denaturation of the double strands of the DNA. 2) Annealing: a reaction-specific annealing temperature (often about 55–60 °C) for about 30 seconds. At this temperature, the primers will anneal to the specific complement area of the target DNA strand. After the primer has annealed to its target, the Taq-polymerase will bind to the primer / target-complex and starts elongation of the template strand's complement in 3' direction. The annealing temperature depends on the primers and should be about 5 °C lower than the lowest melting temperature (= temperature where the primer denaturizes from the template) of the primer pair's two primers. If the temperature is too low, the PCR will become unspecific and multiple strands of DNA will be amplified, because the primers can bind to non-perfect complements. If the temperature is too high, the primers will not be able to anneal to anything at all, resulting in no



amplification whatsoever. 3) Elongation: the temperature is raised to about 72 °C for about 30 seconds. At this temperature, the Taq-polymerase will work most efficiently, so that (at least in theory) the target sequence is doubled at the end of the elongation step. Then, the cycle starts over with denaturation again for a specified number of times, which depend on the amount of original template DNA and have to be determined empirically. After the last cycle, the sample is again incubated at 72 °C for a few minutes of final elongation and then stored at 4° C until removed from the thermocycler.

After PCR, the amplified DNA can be examined by applying GE or stored at -20 °C over a long period of time.

When amplifying cDNA obtained through RT, the complete procedure is consequently called RT-PCR. When performing RT-PCR, it is essential to keep the RNA and subsequent cDNA free from contaminating genomic DNA, which would cover up the presence or lack of cDNA obtained through RT. One way of ensuring that only cDNA is amplified is the use of specially designed primer pairs, where both primers lie on two different adjoining exons (exon spanning primers). When using such primers, only the amplicon from cDNA templates will be of the correct size, because the introns, which are present in the genomic DNA, will be spliced out in the mRNA and thus the respective cDNA.

Because interpretation of GE can lead to false identifications of the bands (in case of unspecific amplification, amplicons can appear that seem to be at the same length as the target of interest), there are ways of ensuring an observed band's identity.

One possible method is the use of a so called "nested" PCR, where two PCRs are performed consecutively: the primer pairs for both PCRs lie, as the name suggests, nested in each other. The "outer" primers amplify their specific product. After this "outer" reaction is complete, a small aliquot of the reaction mixture is re-amplified using the "inner" primers, but with much fewer cycles. Because the target of the inner primers is the amplicon from the "outer" PCR, it should be greatly enriched if the amplification was specific. Therefore the "inner" PCR will result in a smaller product of high quantity. If both reactions were specific, GE of the "inner" product will show a band at a shorter length than GE of the "outer" product. If both products are of the expected size, it is highly probable that the amplification was specific. Another advantage of the nested PCR is that PCR products with very low yield can be amplified to a much greater extent, making bands visible that were not or hardly before [144].

Other ways to ensure specificity of a PCR is sequencing the respective PCR product (see 4.8) or restriction enzyme digestion (not performed in this thesis).

To ensure correct interpretation of the results from a PCR experiment, there are three types of control samples that can be included in every PCR reaction batch. The first type is a blind sample, containing no sample, but only PCR mastermix and water, to exclude that any observed bands derive from contamination of the reagents. This type of control should be included every time. The second type is the -RT sample, containing non-reversely transcribed RNA. This control sample is best prepared by performing an RT reaction with all components except the enzyme reverse transcriptase. It should be included in methods using intra-exon primers, to exclude amplification of genomic DNA and can be included in other methods as well. The third type of control sample is a positive control, which contains cDNA of the desired target in high and reliable concentration. This is very helpful if there is none or very little template in the samples of interest, so that one can ensure the success of the PCR.

### 4.6.2 General procedure

#### *Materials*

- -20 °C storage box (for the Taq-polymerase)
- 10 mM dNTP Mix (Fermentas, R0192)
- Box with ice
- DNase, RNase, DNA free distilled water, “PCR water” (Gibco, 0977035)
- DNase, RNase, DNA free pipette tips
  - 10 µL (Biozym, 770010)
  - 20 µL (Peqlab, 81-1020)
  - 100 µL (ART®, 100E, 2065E)
  - 200 µL (Biozym, 770280)
- DNase, RNase, DNA free tubes with convex lid 0.2 mL (Biozym, 710900)
- Forward and reverse primer (see 4.6.3)
- Latex gloves (Hartmann, Peha-Soft® powderfree, 942162)
- Taq-Polymerase (Fermentas, Taq DNA Polymerase (recombinant), EP0404), supplied with:
  - 10x PCR buffer (Taq Buffer with KCl or Taq Buffer with (NH<sub>4</sub>)<sub>2</sub>SO<sub>4</sub>)
  - 25 mM MgCl<sub>2</sub>
- Thermal cycler (Eppendorf Mastercycler personal, 53332 000.014)
- Vortexer (Labinco, L24)

*Method*

1. Preparation of PCR 2x mastermix (per reaction)
  - a. Let the components thaw slowly on ice, do not take the enzymes out of the refrigerator yet!
  - b. Calculate the necessary amounts of reagent according to the number of samples plus one aliquot in excess
  - c. Prepare the PCR 2x mastermix (add the enzymes last, take them out of the refrigerator only in the -20 °C storage box and put them back in the refrigerator as soon as possible!). See 4.6.3 for the mastermix recipes.
  - d. Vortex the PCR 2x mastermix for a short while and put it on ice
2. Preparation of the samples
  - a. Pipette an aliquot of cDNA sample (containing the desired amount of corresponding RNA)
  - b. Add PCR water to the desired total volume
  - c. Prepare a blind sample (PCR water only)
  - d. Add the appropriate amount of PCR 2x mastermix and pipette up and down a few times to mix
  - e. Store the prepared sample on ice
  - f. Repeat steps a–e for all samples (prepare only one blind!)
3. Polymerase chain reaction
  - a. Put all the samples in the thermal cycler
  - b. Use the appropriate temperature program for the experiment (see 4.6.3)
  - c. Run the program
  - d. After the program is finished, store the PCR products at -20 °C

**4.6.3 Primers, mastermixes and temperature programs****PCR method for MT<sub>1</sub>, MT<sub>2</sub> and  $\beta$ -actin according to Ishii et al. [26]**

The sequences of the primers, the respective mastermix recipe and temperature program were taken from Ishii et al. [26]. These methods were originally supposed to suffice for all RT-PCR experiments in the course of this work. The primers are designed as exon spanning and therefore amplification of genomic DNA should be excluded. These primer pairs will be henceforth referred to as “Ishii primers”.

Primers were custom synthesized by Eurofins, MWG operon (Ebersberg, Germany)

### Primers

**Table 3:** PCR primers according to Ishii et al. [26].

Name	Sequence	Product size
rat MT1 fwd.	5' -ATGGCCCTGGCTGTGCTGCGGTAAG-3'	316 bp
rat MT1 rev.	5' -TAAGTATAGACGTCAGCGCCAAGGGAAATG-3'	
rat MT2 fwd.	5' -GGAGCGCCCCAAGCAGTG-3'	390 bp
rat MT2 rev.	5' -GGATCTCCCAAGTACCCAACCGTCAT-3'	
rat $\beta$ -actin fwd.	5' -GTCCACACCCGCCACCAGT-3'	496 bp
rat $\beta$ -actin rev.	5' -CGTCTCCGGAGTCCATCACAAT-3'	

### Mastermix recipe

25  $\mu$ L reactions are used in this method, therefore, 12.5  $\mu$ L mastermix are prepared per sample. All three primer pairs are used with the same temperature program and mastermix recipes.

**Table 4:** Recipe for 12.5  $\mu$ L of 2x PCR mastermix for PCR experiments according to the method described by Ishii et al. [26].

C	Vol [ $\mu$ L]	Component
0.2 mM	0.5	10 mM dNTP mix
0.2 $\mu$ M	0.05	forward primer
0.2 $\mu$ M	0.05	reverse primer
	2.5	10x buffer with KCl
1.5 mM	1.5	25 mM MgCl <sub>2</sub>
	6.9	PCR water
1 U	1.0	Taq-Polymerase

*Modified mastermix recipe for MT<sub>2</sub>*

This mastermix recipe was only used in one experiment (see 5.1.2).

**Table 5:** Modified recipe for 12.5  $\mu\text{L}$  of 2x PCR mastermix for one PCR experiment concerning MT<sub>2</sub> according to the method described by Ishii et al. [26].

C	Vol [ $\mu\text{L}$ ]	Component
0.2 mM	0.5	10 mM dNTP mix
0.2 $\mu\text{M}$	0.05	forward primer
0.2 $\mu\text{M}$	0.05	reverse primer
	2.5	10x buffer with $(\text{NH}_4)_2\text{SO}_4$
2.0 mM	2.0	25 mM $\text{MgCl}_2$
	6.4	PCR water
1 U	1.0	Taq-Polymerase

*Temperature program*

**Table 6:** Temperature program for PCR experiments according to the method described by Ishii et al. [26]. This temperature program was used for  $\beta$ -actin, MT<sub>1</sub> and MT<sub>2</sub> in initial experiments, but was for MT<sub>2</sub> replaced by the one described in below because of unsatisfactory results (see 5.1.2).

Step	Cycles	Time	T [ $^{\circ}\text{C}$ ]
1	1	2 min	95
2	$\beta$ -actin: 25 MT1: 40 (MT2: 40)	30 s	95
3		20 s	60
4		30 s	72
5	1	5 min	72
6	1	Hold	4

*Modified temperature program for MT<sub>2</sub>*

**Table 7:** Modified temperature program for PCR experiments according to the method described by Ishii et al. [26].

Step	Cycles	Time	T [°C]
1	1	2 min	95
2	40	30 s	95
3		20 s	57
4		30 s	72
5	1	5 min	72
6	1	Hold	4

**PCR method for MT<sub>2</sub> (modified after Sugden et al. [34])**

The sequences of the primers, the respective mastermix recipe and temperature program were taken from [34]. The primers are designed for a nested PCR and as both pairs lie in one exon, amplification of contaminating genomic DNA is possible. The primer pairs will be henceforth referred to as “Sugden primers” in general or as “Sug out MT2” for the outer primers of the nested PCR and “Sug nes MT2” for the inner primers of the nested PCR. See 5.4.3 for the primer selection process. Primers were custom synthesized by Eurofins, MWG operon (Ebersberg, Germany).

*Primers*

**Table 8:** Primers for experiments conducted according to the method described by Sugden et al. [34].

Name	Sequence	Product
Sug out MT2 fwd.	5' -ATCTGTCACAGTGCACCTACC-3'	292 bp
Sug out MT2 rev.	5' -TTCTCTCAGCCTTTGCCTTC-3'	
Sug nes MT2 fwd.	5' -AGCCTCATCTGGCTTCTCAC-3'	154 bp
Sug nes MT2 rev	5' -TTGGAAGGAGGAAGTGGATG-3'	

*Mastermix recipe*

20  $\mu\text{L}$  reactions are used in this method, therefore, 10  $\mu\text{L}$  mastermix are prepared per sample. Both primer pairs are used with the same temperature program and mastermix recipes.

**Table 9:** Recipe for 10  $\mu\text{L}$  of 2x PCR mastermix for PCR experiments according to the method described by Sugden et al. [34].

C	Vol [ $\mu\text{L}$ ]	Component
0.1 mM	0.2	10 mM dNTP mix
0.5 $\mu\text{M}$	0.1	forward primer
0.5 $\mu\text{M}$	0.1	reverse primer
	2.0	10x buffer with KCl
1.5 mM	1.2	25 mM $\text{MgCl}_2$
	5.4	PCR water
1 U	1.0	Taq-Polymerase

*Temperature program*

**Table 10:** Temperature program for PCR experiments according to the method described by Sugden et al. [34].

Step	Cycles	Time	T [ $^{\circ}\text{C}$ ]
1	1	2 min	94
2	Sug out MT2: 40 Sug nes MT2: 20	1 min	94
3		1 min	55
4		2 min	72
5	1	10 min	72
6	1	Hold	4

**PCR method for  $\text{MT}_2$  (self-designed)**

See 5.4.5 for the primer design process. The primer pairs will be henceforth referred to as MS1\_rMT2 and MS2\_rMT2. Both custom designed primer pairs share the same reverse primer. Primers were custom synthesized by Eurofins, MWG operon (Ebersberg, Germany). The mastermix recipe and temperature program were both custom designed, following the recommendations in the manufacturer's instructions of the Taq-Polymerase [143].

### Primers

**Table 11:** Self designed primers for rat  $MT_2$  amplification. MS1\_rMT2 rev. and MS2\_rMT2 rev. are identical.

Name	Sequence	Product
MS1_rMT2 fwd.	5' - TAGCACTTGCTGGGCGGGGA-3'	540 bp
MS1_rMT2 rev.	5' - AGGCTCGGTGGTAGGTCGCA-3'	
MS2_rMT2 fwd.	5' - GCGCATCTATCCCGGGCTGC-3'	483 bp
MS1_rMT2 rev.	5' - AGGCTCGGTGGTAGGTCGCA-3'	

### Mastermix recipe

**Table 12:** Self-designed recipe for 12.5  $\mu$ L of 2x PCR mastermix for use with the self designed primers for rat  $MT_2$ .

C	Vol [ $\mu$ L]	Component
0.2 mM	0.5	10 mM dNTP mix
0.2 $\mu$ M	0.05	forward primer
0.2 $\mu$ M	0.05	reverse primer
	2.5	10x buffer with KCl
1.5 mM	1.5	25 mM $MgCl_2$
	6.9	PCR water
1 U	1.0	Taq-Polymerase

### Temperature program

**Table 13:** Self-designed temperature program for use with the self-designed primers for rat  $MT_2$ .

Step	Cycles	Time	T [ $^{\circ}$ C]
1	1	3 min	95
2	40	1 min	95
3		1 min	57
4		1 min	72
5	1	10 min	72
6	1	Hold	4



## 4.7 DNase treatment of RNA samples

### 4.7.1 Background

To avoid amplification of genomic DNA when using non exon spanning primers in PCR, the RNA is treated before the RT with DNase, which should degrade present DNA contaminations in the isolated RNA samples but leaving the RNA intact.

### 4.7.2 Materials

- -20 °C storage box (for DNase)
- DNase I, Amplification Grade (Invitrogen, 18068-015), supplied with:
  - 10x DNase I Reaction buffer
  - 25 mM EDTA (pH 8.0)
  - DNase I, Amp Grade, 1 U /  $\mu$ L
- DNase, RNase, DNA free distilled water, “PCR water” (Gibco, 0977035)
- DNase, RNase, DNA free pipette tips
  - 10  $\mu$ L (Biozym, 770010)
- DNase, RNase, DNA free tubes with flat lid 0.2 mL (Biozym, 710920)
- Latex gloves (Hartmann, Peha-Soft® powderfree, 942162)
- Thermal cycler (Eppendorf mastercycler personal, 53332 000.014)

### 4.7.3 Method

According to manufacturer’s instruction [145].

1. Pipette an aliquot of RNA sample in a 0.2 mL tube containing 1  $\mu$ g of RNA
2. Add 1  $\mu$ L of DNase I reaction buffer
3. Add 1  $\mu$ L DNase I, Amp Grade, 1 U /  $\mu$ L
4. Fill with PCR water to 10  $\mu$ L
5. Incubate for 15 minutes at rt
6. Add 1  $\mu$ L of 25 mM EDTA solution
7. Heat for 10 minutes at 65 °C (thermocycler)
8. Add the RT mastermix (minus 1  $\mu$ L of PCR water per sample) for direct RT or store at -20 °C

Note that the total volume of the DNase treated samples is 11  $\mu$ L. The volume of PCR water in the RT-mastermix has therefore to be reduced by 1  $\mu$ L (from 3.2 to 2.2  $\mu$ L per reaction). See 4.5 for information about reverse transcription.

## 4.8 DNA extraction and purification from agarose gels

### 4.8.1 Background

After [146].

The length of the PCR product alone is not enough to safely determine the identity of observed bands from a PCR experiment, because a different fragment of similar size might be mistaken for the expected one. Therefore, in addition to performing a nested PCR, sequencing of the isolated amplicon is a safe way to ensure its identity.

In order to sequence an isolated DNA band from an agarose gel, the band has to be excised from the gel, the gel has to be dissolved and the DNA extracted from the mixture, using a DNA gel extraction kit (QIAquick®, Gel Extraction Kit).

The principle of the kit's method of operation is a centrifugeable column filled with a silica membrane, which adsorbs the DNA, but not impurities and contaminations. The gel slice is first dissolved in lysis buffer, which contains a pH indicator to enable easy checking of the optimal pH (< 7.5). If the pH is too basic, the DNA will not adsorb on the silica membrane. Residual buffer and impurities are then washed away using washing buffer. Because adsorption of the DNA to the silica matrix occurs only at acidic pH, the DNA can be eluted from the column using pure water or 5 mM Tris.HCl (pH 8.5) buffer.

To ensure the success of the extraction, the concentration of the DNA is quantified using spectrophotometry (see 4.3) and a small amount of the DNA solution can be checked for intactness via GE (see 4.4).

### 4.8.2 Materials

- Centrifuge (Eppendorf, Centrifuge 5417R)
- DNase, RNase, DNA free distilled water, "PCR water" (Gibco, 0977035)
- DNase, RNase, DNA free pipette tips
  - 100 µL (ART®, 100E, 2065E)
- DNase, RNase, DNA free tubes 1.5 mL (Biozym, 710310)
- Heating block (Eppendorf, Thermomixer 5436)
- Isopropanol (Merck, 1.09634.1011)
- Latex gloves (Hartmann, Peha-Soft® powderfree, 942162)
- Pipette tips
  - 1000 µL (Biozym, 721000)
  - 200 µL (Biozym, 720230)
- QIAquick® Gel Extraction Kit (Qiagen, 28704), contains:
  - Buffer EB

- Buffer PE
- Buffer QG
- Spin columns + 2 mL collection tubes
- Na-acetate (Merck, 6268)
- Vortexer (Labinco, L24)

### 4.8.3 Method

1. Excise the DNA fragment(s) from the agarose gel (minimize excess gel)
2. Weigh the gel slice(s) (approx.)
3. Add 3 volumes of Buffer QG to per volume of gel (100 µg equals 100 µL)
4. Note: If the concentration of the agarose gel is 2 % or higher, use 6 volumes of buffer QG
5. Note: One spin column can take up to 400 mg of gel. If the weight of the gel slice(s) exceed(s) 400 mg, divide it in appropriate parts and use multiple spin columns
6. Incubate at 50 °C for 10 min and vortex every 2–3 min until the gel slice(s) is (are) dissolved
7. If the color of the mixture is orange or red, add 10 µL of 3 M Na-acetate (pH 5.0)
8. Add 1 gel volume of isopropanol to the sample and vortex
9. Place a QIAquick® spin column in a 2 mL collection tube
10. Apply the sample to the column and centrifuge for 1 min at 17,900 x *g*
11. If the volume of the sample exceeds 800 µL, centrifuge twice using the same column
12. Discard the flow-through and place the column back in the collection tube
13. Add 0.5 mL of Buffer QG to the column and centrifuge for 1 min at 17,900 x *g*
14. Discard the flow-through and place the column back in the collection tube
15. Add 0.75 mL of Buffer PE to the column and centrifuge for 1 min at 17,900 x *g*
16. Discard the flow-through and centrifuge again for 1 minute at 17,900 x *g*
17. Place the column in a DNase, RNase, DNA free 1.5 mL tube (cut off cap!)
18. Add 50 µL of Buffer EB or PCR water to the center of the column membrane and centrifuge for 1 minute at 17,900 x *g*
19. Note: alternatively, 30 µL might be used – the column should then stand for 1 minute prior to centrifugation
20. Transfer the eluate (with a DNase, RNase, DNA free 100 µL pipette tip) from the tube with the cut off cap to a fresh DNase, RNase, DNA free tube.
21. Store at -20 °C.

## 4.9 DNA Sequencing and sequence comparison

After extraction and purification from agarose gels (see 4.8) the DNA is sent to MWG Eurofins Operon (Ebersberg, Germany) for sequencing. The sequencing results are then analyzed by the BLASTn program from the National Center for Biotechnology Information [147-148].

## 4.10 Real time PCR (qPCR)

### 4.10.1 Background

After [149].

Real-time PCR, abbreviated as “qPCR” (for “quantitative PCR”) to avoid mix-ups with RT-PCR, is a technique to quantify the amount of amplicon accumulated during the PCR process. Therefore, the amplification can be tracked “live” (thus the name “real-time”), in contrast to qualitative PCR, where the result of the amplification can be analyzed only at the end of the complete reaction. Also, real-time PCR is much more sensitive, because the increase in amplicon is measured through increasing fluorescence by the machine and not through manual optical inspection of a gel, as in conventional qualitative PCR.

With real-time PCR the concentration of the template can be measured as absolute (as copies of the template) or relative (compared to a standard gene). Real time PCR can of course also be used in conjunction with reverse transcription (RT-qPCR).

As mentioned before, the amplification is detected through the increase in fluorescence of the sample. This is achieved through one of the following two methods: One possibility is the exploitation of unspecific intercalation of a fluorescent dye with the DNA (e.g. SYBR® green I). The second option is the usage of sequence specific DNA probes (e.g. Taq-Man®) which will bind to the DNA and release a fluorescent dye (reporter) from the vicinity of a quencher after the polymerase (exhibiting exonuclease activity) “cleaves” the probe off (see Figure 16). This increase in fluorescence is then measured by photodiodes in the real-time PCR machine. Because of the sensitivity of the method, the components of the reaction mixture have to be very carefully balanced, so normally pre-fabricated mastermixes and primer kits, as well as standardized reaction plates, are used.

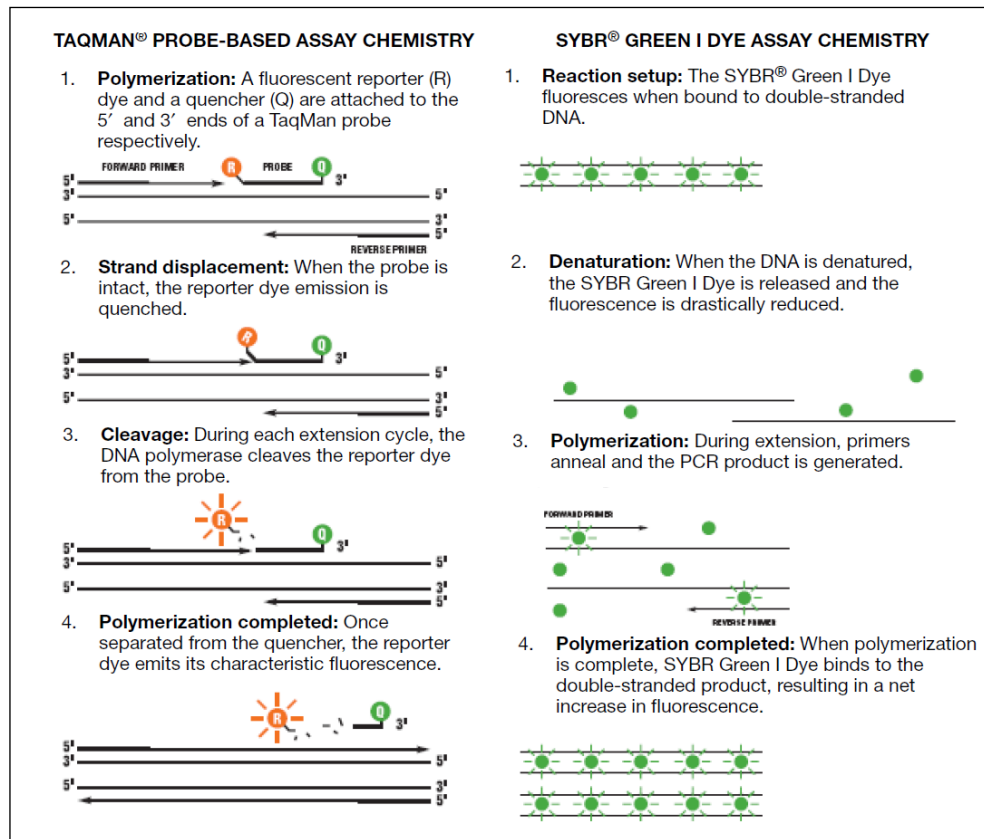


**Figure 16:** The two methods for amplification measurement by increased fluorescence [149].

#### 4.10.2 Materials

- Box with ice
- Centrifuge (Sigma 4K15C, 10742)
- DNase, RNase, DNA free distilled water, “PCR water” (Gibco, 0977035)
- DNase, RNase, DNA free pipette tips
  - 10  $\mu$ L (Biozym, 770010)
  - 100  $\mu$ L (ART<sup>®</sup>, 100E, 2065E)
  - 20  $\mu$ L (Pepqab, 81-1020)
- DNase, RNase, DNA free tubes with flat lid 0.2 mL (Biozym, 710920)
- Fast 96-well reaction plate 0.1 mL (Applied Biosystems, 346907)
- Latex gloves (Hartmann, Peha-Soft<sup>®</sup> powderfree, 942162)
- MicroAmp<sup>™</sup> Optical Adhesive Film (Applied Biosystems, 4311971)
- StepOnePlus<sup>™</sup> Real Time PCR System with Tower Computer (Applied Biosystems, 4376599)
- Taq-Man<sup>®</sup> Gene Expression Assay(s) (20x Mix)
- Taq-Man<sup>®</sup> Gene Expression Master Mix (Applied Biosystems, 4369016)
- Vortexer (Labinco, L24)

### 4.10.3 Method

20  $\mu\text{L}$  reactions were used in this thesis. For other volumes (10–50  $\mu\text{L}$  are possible), the respective volumes of the reaction components have to be adjusted accordingly..

#### Mastermix

**Table 14:** Mastermix recipe for 20  $\mu\text{L}$  qPCR reactions (after [150]).

Vol [ $\mu\text{L}$ ]	Component
10	Taq-Man® 2x Master Mix
1	Taq-Man® Assay 20x
4	PCR water

#### Gene expression assays

**Table 15:** Gene expression assays used in qPCR experiments in this thesis. VIC: Taq-Man® VIC; FAM: 6-Carboxyfluorescein.

Target	Assay	Reporter
ACTB ( $\beta$ -actin)	Rat ACTB (Applied Biosystems, 4352340E-0805007)	VIC
MT <sub>1</sub>	Rat Mtnr1a (Applied Biosystems 626218 G10)	FAM
MT <sub>2</sub>	Rat Mtnr1b (Applied Biosystems 626217 G5)	FAM

#### Instructions

For detailed instructions consult the manufacturer's manual [151].

1. Theoretical preparation
  - a. Select the samples, targets of interest and number of repetitions.  
Include negative (-RT) and blind samples (water only) as well.
  - b. Prepare a clearly laid out plate layout
  - c. Calculate the amount of cDNA necessary for the sum of all respective wells of all targets. Add one aliquot of cDNA to compensate for pipetting errors.
2. Practical preparation (work on ice)
  - a. Prepare dilutions of the samples (the aspired amount of cDNA per sample should be contained in 5  $\mu\text{L}$  of PCR water)
  - b. Prepare the mastermixes for all targets; always add 1–2 aliquots to compensate for pipetting error

- c. Pipette all diluted samples (and blinds / negatives) in their respective wells (use a fresh tip for each well to ensure volume conformity) in a 96 well reaction plate
  - d. Add the mastermixes to the respective wells
  - e. Seal the reaction plate with the optical adhesive film
  - f. Remove the opaque cover foil from the back of the film
  - g. Place the film centered on the plate
  - h. Use a scraper to flatten the film
  - i. Remove the holding flaps of the film by holding down the film on the plate with the scraper with one hand and pulling on the flap with the other hand
  - j. Make sure that the seal between plate and film is tight
  - k. Centrifuge the plate at 2000 x g for 1 minute
  - l. Remove dust from the bottom of the plate by blowing or a brush
3. Real time PCR
- a. Insert the plate into the instrument and close the hatch
  - b. Start the program "StepOne Software v2.0"
  - c. Click on "Advanced Setup"
  - d. Choose "Standard (~2 hours to complete a run)" under "rampspeed"
  - e. Choose "Quantitation – Comparative CT ( $\Delta\Delta CT$ )"
  - f. Name the experiment
  - g. Go to "Plate Setup"
  - h. Name all targets and choose the appropriate reporter (specified in the assays data sheet)
  - i. Name all samples
  - j. Click on the tab "Assign Targets and Samples"
  - k. Select all wells of one target and activate the checkbox next to the respective target name
  - l. Select the blind samples of the target and click on "N" next to the sample name
  - m. Repeat steps k–l for all targets
  - n. Select all wells of a sample and activate the checkbox next to the respective sample name
  - o. Repeat step n for all samples
  - p. Select the reference sample and the endogenous control
  - q. Go to "Run Method"
  - r. Set the reaction volume per well to 20  $\mu\text{L}$

- s. Click on “START Run”
  - t. Wait for the instrument to complete the run
  - u. After completion of the run, take the plate out of the instrument and close the hatch again
4. Subsequent work after the run is completed
- a. Select “Analysis”
  - b. Go to “Amplification Plot”
  - c. Select “Graph Type: Log”
  - d. Check “Show threshold”
  - e. Select a target
  - f. Uncheck “Auto” and set the threshold within the exponential phase of the amplification (drag the line with the mouse)
  - g. Repeat steps e–f for all targets
  - h. Click on “Export” and save the data to an appropriate location (e.g. USB-stick)
  - i. Close the program, when asked to save the unsaved data, click “yes” and save at an appropriate location

### 4.10.4 Analysis of results

After [149, 151].

The amount of quantified DNA can be expressed in multiple ways. One of the most common ones is the  $\Delta CT$  value. The CT (cycle threshold) value is the number of PCR cycles necessary for a template in a sample to become detectable (so the fluorescence of the sample exceeds the threshold of the background fluorescence). The  $\Delta CT$  value then specifies the difference between the CT of the template in question and a reference gene (e.g. beta actin) which is expressed equally in all the samples. Since the relative ratio of the standard and the template in question does not change, this difference (the  $\Delta CT$  value) is used to “normalize” the CT values and account for discrepancies in pipetting, sample concentration, etc. The  $\Delta CT$  values can be converted from base 2 to base 10 using the formula from Figure 17.

$$E_n = 2^{-\Delta CT}$$

**Figure 17:** Conversion of the expression difference of a target to a the reference gene from the base 2  $\Delta CT$  values to the  $n$ -fold ( $E_n$ ; base 10) value.

The  $\Delta CT$  can then again be measured against other  $\Delta CT$  values, e.g. a placebo group against a verum group. This value is then called  $\Delta\Delta CT$  and specifies the



difference in gene (or mRNA in case of qRT-PCR) expression between the two groups. This difference can then be converted from a base 2 system (CT) to a base 10 system using the formula from Figure 18.

$$E_n = 2^{-\Delta\Delta CT}$$

**Figure 18:** Conversion of the expression difference of two targets from the base 2  $\Delta\Delta CT$  values to the  $n$ -fold ( $E_n$ ; base 10) value.

Of course, this simple conversion works only if the expression efficiency of the amplification reaction is (near) 100 % and the same for all targets. For short amplicon lengths (< 150 bp, true for all TAQMan® Assays), these requirements are met (Applied Biosystems, User Bulletin #2: Relative Quantitation of Gene Expression (Applied Biosystems Inc., Part Number 4303859B)).

A standard sample (of all measured samples) can be chosen to act as a reference. The expression of various samples can then be indicated as  $E_n$ -fold expression of the reference.

All samples should be measured at least in duplicates (better are triplicates or even quadruplicates) to increase the accuracy of the method. The  $\Delta CT$  values are then indicated as mean  $\Delta CT$  of the repeats. To ensure primer specificity and correct amplification, -RT and negative samples should be included for all template groups.

## 4.11 Immunofluorescence (IF)

### 4.11.1 Background

IF is a method used to visualize the location or occurrence of proteins in tissues or cells by use of fluorescence microscopy.

Staining of tissue sections is done in two steps: first, the primary antibody is applied to the tissue. The primary AB recognizes specific antigens (e.g. smooth muscle actin or the melatonin  $MT_1$  receptor) and binds to them. It is created in a host species and can be either poly- or monoclonal. After the primary antibody has bound to its target, a secondary antibody is applied, which recognizes the primary antibody based on the primary AB's host species. This secondary antibody is conjugated with a fluorescent dye, which glows during excitation with light of a specific frequency.

To exclude that the observed fluorescence stems from unspecific binding of the secondary antibody to the tissue, a negative control, with only the secondary antibody applied, should be included in each experiment.

Before the staining, the tissue has to be fixated. This can be done using a variety of methods; examples are the usage of formaldehyde (PFA) or the new HOPE®-solution (DCS, Hamburg, Germany). For sectioning, the tissue needs to be either frozen (in liquid N<sub>2</sub>) or embedded in paraffin. Accordingly, the tissue is then either cryo-sectioned or paraffin sectioned. Afterwards different steps are necessary to prepare it for staining depending on the method used for sectioning. In case of a cryo-sections the tissue only needs to be rehydrated (using PBS) and then bathed in an ammonium-chloride (50 mM) solution to remove any excess PFA remaining in the tissue. With paraffin sections the procedure is more complex, because the paraffin has to be removed and the rehydration has to be done using a descending alcohol series. HOPE®-fixated paraffin sections are somewhat easier to rehydrate, as only two isopropanol and acetone steps are necessary. Also, if a tissue was embedded in paraffin, normally antigen retrieval has to be done, because paraffin in conjunction with PFA can mask antigens. This is done by boiling the sections in citrate buffer, citraconic anhydride, or by using proteases.

After rehydration, the tissue has to be permeabilized to ensure that the primary antibody can “reach” its target and is not hindered by membranes, etc. Also, unspecific binding sites have to be blocked using blocking serum (serum from the animal the second antibody was derived from, or, if this is not possible, with a protein dissolved in buffer such as bovine serum albumin (BSA)) to reduce the background fluorescence. These two steps are normally done at the same time by incubating the tissue with serum containing small amounts of a detergent (Saponin, Triton-X 100 or Tween 20).

If more than one protein, or if the relative positions of two proteins in a tissue, are of interest, double, triple, or even quadruple stainings are possible. The primary antibodies against the different proteins have to be derived from different species, of course. This can be achieved using two different approaches, which both have specific advantages and disadvantages.

The first approach is parallel staining, where the primary and secondary antibodies, respectively, are mixed and applied together. The advantage is that the amount of time for the procedure is the same as for a single staining and that all primary antibodies can be applied overnight, so staining should be strong for all targets. However, the primary antibodies (and secondary antibodies, respectively) may influence each other if they are dissolved in the same solution.

The second approach is sequential staining, where the staining procedure is repeated for each primary / secondary AB combination. The advantage is that the antibodies have less chance of influencing each other and the stainings are usually more reliable. The disadvantage is a proportional increase in time necessary for each

further target, since all washing and incubation steps have to be repeated for each antibody duo.

After the staining procedure with all the antibodies is completed, the tissue is usually dyed for nucleic acids, therefore making the nuclei of the cells visible. This is done with chemicals which intercalate in DNA, which results in fluorescence. An example for such a “nucleic acid dye” is 4',6-diamidino-2-phenylindole (DAPI).

When all dyeing steps are completed, the tissue is embedded in a mounting medium which is pervious for a broad range of light frequencies, ideally for the whole UV/VIS/IR spectrum. An example for such a medium is Mowiol.

### **4.11.2 Tissue sectioning**

#### **General remarks**

For IF staining, thin sections of tissue (1–15  $\mu\text{m}$ ) are necessary. This can be done by cryo-sectioning, where the tissue is cut in a frozen state. The tissue is embedded in TissueTek™, a substance based on polyvinyl alcohol, which is liquid at rt, but freezes to a solid, sliceable mass at low temperatures. All tissues cut and used for cryo-sectioning in this work were fixated and frozen in TissueTek™ in 2008 by M. Benova (Institute for Pathophysiology, Medical University Vienna). Therefore, the method for fixating the tissue prior to initial freezing will not be discussed in this work.

Alternatively, paraffin-sections, where the tissue is embedded in paraffin and cut at rt can be used. All paraffin sections used for IF experiments in this work were fixated, embedded and cut in 2010 by H. Uhrova (Institute of Pathophysiology and Allergy Research, Medical University Vienna). Therefore, the methods for paraffin embedding and sectioning will not be discussed in this work.

#### **Cryo-sectioning**

##### *Materials*

- Acetone (Merck, 1.00014.2500)
- Cryomicrotome (Microm, 500 O-M)
- Cryomicrotome blade (Microm Sec 35, 152200)
- Latex gloves (Meditrade Gentle Skin sensitive, 1221)
- Paper towels
- Positively precharged slides (Thermo Scientific Superfrost® Plus Gold, K5800AMNZ)
- Scalpel, brush, forceps
- TissueTek™ (Sakura, 4583)

### *Method*

1. Switch on the microtome by activating “Light”, “Motor”, and “Object”
2. Mount the TissueTek™ embedded tissue on one of the stamps in the instrument by applying TissueTek™ on the stamp, letting it solidify for a moment, then adding the embedded tissue
3. Check the orientation of the tissue, correct by thawing and reorientation if necessary
4. Let the tissue with the TissueTek™ freeze completely inside the microtome
5. Apply more TissueTek™ on the stamp so that a large area around the embedded tissue is covered with TissueTek™; avoid protruding parts of the tissue
6. Repeat steps 3–5 for all samples
7. Insert a microtome blade in the blade holder
8. Insert a stamp with embedded tissue in the stamp-holder and fasten the holding screw
9. Adjust the angle of the blade and / or the stamp, if necessary
10. Move the stamp away from the blade by using the [↑] button
11. Set the section thickness to 40 μm
12. Use the motor to approach the blade with the section
13. Slice off TissueTek™ at 40 μm until the tissue is cut together with the TissueTek™
14. Set the section thickness to 1–15 μm (7 μm for aorta sections)
15. Slice off a few sections to adapt the microtome to the new thickness
16. Carefully cut a section off using the hand-wheel (clockwise) – while the section is being cut, gently pull the section away from the blade using a brush; try to keep a flat, undisrupted section
17. Lower a positively precharged slide parallel over the section – at about 10–5 mm, the section will be “sucked” onto the slide
18. Keep the slide with the tissue at rt for about 10 min
19. Store the slide at -20 °C
20. Repeat steps 16–19 for all sections of the sample
21. Clean the blade every few sections with acetone
22. Move the stamp away from the blade by using the [↑] button and remove the stamp after releasing the holding screw
23. Remove the remaining tissue (still embedded in TissueTek™) from the stamp using the scalpel
24. Store the remaining tissue at -80°C (still embedded in TissueTek™)

25. Repeat steps 8–24 for all samples
26. Remove the microtome blade and store or discard it
27. Clean the microtome using brushes and acetone soaked towels
28. Switch off the microtome by deactivating “Light”, “Motor” and “Object”, but do not deactivate “Box”

### 4.11.3 Buffers, solutions and reagents

#### PBS (phosphate buffered saline)

##### *Materials*

- KCl (Merck, 4936.1000)
- NaCl (Merck, 1.06404.1000)
- $\text{KH}_2\text{PO}_4$  (Merck, 1.04873.1000)
- $\text{Na}_2\text{HPO}_4 \cdot 2\text{H}_2\text{O}$  (Merck, 1.06580.1000)
- Aqua bidest.
- Osmometer (Osmomat 030, Gonotec)
- pH-meter (Metrohm, pH-Lab 827)

##### *Method*

1. Solve in 800 mL aqua bidest
  - a. 0.2 g KCl
  - b. 8.01 g NaCl
  - c. 0.21 g  $\text{KH}_2\text{PO}_4$
  - d. 1.44 g  $\text{Na}_2\text{HPO}_4 \cdot 2\text{H}_2\text{O}$
2. Adjust pH to 7.4 with HCl or NaOH
3. Fill to 1000 mL with aqua bidest.
4. Osmolarity should be between 0.280–0.305 osmol / kg
5. Store at 4 °C

#### 50 mM $\text{NH}_4\text{Cl}$ in PBS

##### *Materials*

- $\text{NH}_4\text{Cl}$  (Merck, 1.01142.1000)
- PBS (see above)

##### *Method*

1. Dissolve 2.67 g of  $\text{NH}_4\text{Cl}$  in 1000 mL aqua bidest.
2. Store at rt

## 10 mM citrate buffer

### Materials

- Aqua bidest.
- Citric acid monohydrate (Merck, 244)
- pH-meter (Metrohm, pH-Lab 827)
- Tri-sodium citrate dihydrate (Sigma C-8532)

### Method

1. Mix
  - a. 8.5 mL of a 0.1 M solution of citric acid monohydrate:
    - i. 21.06 g citric acid monohydrate
    - ii. 1000 mL aqua bidest.
  - b. 41.5 mL of a 0.1 M solution of tri-sodium citrate dehydrate:
    - i. 29.41 g tri-sodium citrate dihydrate
    - ii. 1000 mL aqua bidest.
2. Adjust to 500 mL with aqua bidest.
3. Adjust to pH 6 with solution a or b
4. Store at 4 °C

## Mowiol mounting medium

### Materials

- Centrifuge (Rotixa, Hettich)
- Centrifuge tubes 50 mL (VWR, 50 ml Super Clear® Centrifuge tubes, 525-0307)
- Disposable sterile syringe filters, 25 mm, 0.20 Micron, cellulose acetate membrane acrylic (IWAKI 2052-025)
- Glycerol 87 % (Merck 1.04094.0500)
- Hydrochloric acid, fuming 37 % (Merck 1.00314.1000)
- Magnetic hot plate stirrer
- Mowiol 4-88 (FLUKA 81381)
- $\text{NaN}_3$  (Sigma S-8032)
- Syringes, single use, 10 mL (B. Braun, Melsungen AG H4606108V)
- Tris (Merck 1.08382.1000)
- Tubes 1.5 mL (Biozym, 710160)
- Waterbath (GFL, 1083)

*Method*

1. Mix in a 50 mL tube
  - a. 6 g glycerol
  - b. 2.4 g Mowiol 4-88
2. Let the mixture disperse for 1 h at rt under frequent shaking
3. Add 6 mL aqua bidest.
4. Stir for 1 h at rt
5. Add 12 mL 0.2 M Tris/HCl pH 8.5 + 0.02 % (v / w)  $\text{NaN}_3$
6. Incubate for 2 h in the waterbath at 50 °C and stir every 20 min
7. Centrifuge at 5,000 x g for 15 min
8. Filtrate through a 0.2  $\mu\text{m}$  syringe filter
9. Prepare 1 mL aliquots
10. Store at -20 °C

**4.11.4 Staining procedures for cryo-sections****Materials**

- Aluminum foil
- Blocking serum (sera) from host animal of secondary AB(s) (5 % in PBS + 0.05 % saponin; see 4.11.6)
- Antibodies (see 4.11.6)
- Box with ice
- Coolable Centrifuge (Eppendorf, Centrifuge 5415R)
- Coverslips (Menzel-Gläser)
- DakoPen (Dako, S2002)
- DAPI (4',6-diamidino-2-phenylindole; Roche 10236276001) 1:10,000 in PBS
- Dyeing trays (plastic or glass)
- Forceps
- Latex gloves (Meditrade Gentle Skin sensitive, 1221)
- Mowiol (Roth, 07031)
- pipette tips
  - 10  $\mu\text{L}$  (Biozym, 720031)
  - 200  $\mu\text{L}$  (Biozym, 720230)
  - 1000  $\mu\text{L}$  (Biozym, 721000)
- Solutions and buffers
  - 50 mM  $\text{NH}_4\text{Cl}$  (see 4.11.3)
  - PBS (see 4.11.3)

- Tubes 1.5 mL (Biozym, 710160)
- Vortexer (Labinco, L24)
- Wet chamber

### Notes

- ✓ Washing steps are performed in dyeing trays and always for 5 minutes unless otherwise stated
- ✓ Incubation steps are always performed in a wet chamber, the solution the tissue is incubated with is applied directly on the tissue with a pipette
- ✓ Always take the slides out of the trays very slowly to avoid detaching of the sections
- ✓ Always keep the tissue wet
- ✓ Antibodies (primary and secondary) are always diluted in blocking buffer (5 % animal serum of the respective secondary AB + 0.05 % saponin in PBS or 1 % BSA + 0.05 % saponin in PBS). Use the serum from the host animal of the secondary antibody.



**Single-staining procedure**

1. Tissue preparation (rehydration and blocking)
  - a. Wash once for 10 min in 50 mM NH<sub>4</sub>Cl
  - b. Wash 3 times in PBS
  - c. Draw a circle around the tissue(s) with the Dako-Pen
  - d. Incubate with blocking buffer for 1 h at rt
2. Primary antibody
  - a. Centrifuge the antibody at 14.000 x g for 5 min
  - b. Dilute the antibody in blocking buffer
  - c. Incubate with primary antibody in a wet chamber for 1 h–24 h
  - d. Wash 5 times in PBS
3. Secondary antibody (work in the dark!)
  - a. Centrifuge the antibody at 14.000 x g for 5 min
  - b. Dilute the antibody in blocking buffer
  - c. Incubate with secondary antibody in a wet chamber for 1 h
4. Nuclei staining
  - a. Wash twice in PBS
  - b. Incubate for 10 min with DAPI
  - c. Wash twice in PBS
  - d. Rinse once in aqua bidest. (in and out)
5. Embedding
  - a. Apply an appropriate volume of Mowiol on the tissue and the slide
  - b. Cover with coverslip
  - c. Dry for 24 h in the dark at rt
6. Store the slides at 4 °C in the dark

## Double-staining procedures

### *Parallel staining*

1. Tissue preparation (rehydration and blocking)
  - a. Wash once for 10 min in 50 mM NH<sub>4</sub>Cl
  - b. Wash 3 times in PBS
  - c. Draw a circle around the tissue(s) with the Dako-Pen
  - d. Incubate with blocking buffer (use 1 % BSA in PBS + 0.05 % saponin, if the host animals for the secondary ABs are not identical)
2. Primary antibodies
  - a. Centrifuge the antibodies at 14,000 x *g* for 5 min
  - b. Dilute the antibodies in blocking buffer (use 1 % BSA in PBS + 0.05 % saponin, if the host animals for the secondary ABs are not identical) and mix them
  - c. Incubate with primary antibody mixture in a wet chamber for 1 h–24 h
  - d. Wash 5 times in PBS
3. Secondary antibodies (from now on, work in the dark!)
  - a. Centrifuge the antibodies at 14,000 x *g* for 5 min
  - b. Dilute the antibodies in blocking buffer (use 1 % BSA in PBS + 0.05 % saponin, if the host animals for the secondary ABs are not identical) and mix them
  - c. Incubate with secondary antibody mixture in a wet chamber for 1 h
4. Nuclei staining
  - a. Wash twice in PBS
  - b. Incubate for 10 min with DAPI
  - c. Wash twice in PBS and rinse once in aqua bidest. (in and out)
5. Embedding
  - a. Apply an appropriate volume of Mowiol on the tissue and the slide
  - b. Cover with coverslip and dry for 24 h in the dark at rt
6. Store the slides at 4 °C in the dark

*Sequential staining*

1. Tissue preparation (rehydratization and blocking)
  - a. Wash once for 10 min in 50 mM NH<sub>4</sub>Cl
  - b. Wash 3 times in PBS
  - c. Draw a circle around the tissue(s) with the Dako-Pen
  - d. Incubate with blocking buffer (use the serum of the host animal for the first secondary antibody; if this is not possible because of cross reactions with the other antibodies, use 1 % BSA in PBS + 0.05 % saponin)
2. First primary antibody
  - a. Centrifuge the antibody at 14,000 x g for 5 min
  - b. Dilute the antibody in blocking buffer (use the serum of the host animal for the first secondary antibody; if this is not possible because of cross reactions with the other antibodies, use 1 % BSA in PBS + 0.05 % saponin)
  - c. Incubate with primary antibody in a wet chamber for 1 h–24 h
  - d. Wash 5 times in PBS
3. First secondary antibody (from now on, work in the dark!)
  - a. Centrifuge the antibody at 14,000 x g for 5 min
  - b. Dilute the antibody in blocking buffer (use the serum of the host animal for the second secondary antibody; if this is not possible because of cross reactions with the other antibodies, use 1 % BSA in PBS + 0.05 % saponin)
  - c. Incubate with secondary antibody in a wet chamber for 1 h
  - d. Wash 5 times in PBS
4. Second primary antibody
  - a. Centrifuge the antibody at 14,000 x g for 5 min
  - b. Dilute the antibody in blocking buffer (use the serum of the host animal for the first secondary antibody; if this is not possible because of cross reactions with the other antibodies, use 1 % BSA in PBS + 0.05 % saponin)
  - c. Incubate with primary antibody in a wet chamber for 1 h–24 h
  - d. Wash 5 times in PBS
5. Second secondary antibody
  - a. Centrifuge the antibody at 14,000 x g for 5 min
  - b. Dilute the antibody in blocking serum
  - c. Incubate with secondary antibody in a wet chamber for 1 h

6. Nuclei staining
  - a. Wash twice in PBS
  - b. Incubate for 10 min with DAPI
  - c. Wash twice in PBS
  - d. Rinse once in aqua bidest. (in and out)
7. Embedding
  - a. Apply an appropriate volume of Mowiol on the tissue and the slide
  - b. Cover with coverslip
  - c. Dry for 24 h in the dark at rt
8. Store the slides at 4 °C in the dark

### 4.11.5 Staining procedures for HOPE®-fixated paraffin sections

#### *Materials*

- 10 mM citrate buffer, pH 6 (see 4.11.3)
- Acetone (Merck, 1.00014.2500)
- Aqua bidest.
- Dyeing trays (plastic and glass)
- Isopropanol (Merck, 1.09634.1011)
- Oven (Mammert, TV15u), kept at 60 °C
- PBS (see 4.11.3)
- Refrigerator
- Steamer (Braun, MultiGourmet Type 3-216)
- Further materials: see 4.11.4

#### *Method*

1. Deparaffination
  - a. Incubate the slides with the sections for 10 min in warm isopropanol (60 °C)
  - b. Wash with fresh, warm isopropanol (60 °C)
2. Rehydration
  - a. Incubate 2x for 10 min in 70 % cold (4 °C) acetone (keep in refrigerator)
  - b. Wash 2x with aqua bidest.
3. Incubate for 5 min in aqua bidest.
4. Antigen retrieval
  - a. Fill a plastic dyeing tray with 10 mM citrate buffer and put it in the steamer
  - b. Pre-heat the citrate buffer for 20 min

- c. Incubate the slides for 15 min in the hot citrate buffer in the steamer
  - d. Take the tray out of the steamer and let it cool to RT
  - e. Wash twice in PBS (5 min each)
5. The further procedure is identical with the ones for single staining or double staining of cryo-sections (see 4.11.4)

#### 4.11.6 Antibodies and blocking buffers

The respective antibodies used in the experiments are given in the results chapter (5.5). As blocking buffer, always 5 % animal serum of the respective secondary AB + 0.05 % saponin in PBS is used. Santa Cruz is abbreviated as SC.

#### Primary antibodies

**Table 16:** Primary antibodies used in this thesis. All dilutions of the antibodies are given, as well as information about the origin of the respective antibody (modified after the datasheets of the respective antibodies [152-155]).

Antibody	Dilutions	Information
Goat Anti MT1 (SC, sc-13186)	1:50, 1:20, 1:10	Affinity purified goat polyclonal antibody raised against a peptide mapping near the C-terminus of MT <sub>2</sub> of rat origin; 200 µg / mL
Rabbit Anti MT1 (Abbiotec, 250761)	1:50, 1:10	Affinity purified rabbit polyclonal antibody raised against a KLH-conjugated synthetic peptide encompassing a sequence within the center region of MT <sub>1</sub> of human origin
Rabbit Anti Pecam-1 (SC, sc-1506)	1:50	Affinity purified rabbit polyclonal antibody raised against a peptide mapping at the C-terminus of PECAM-1 of mouse origin; 200 µg / mL
Mouse Anti SM Actin (Sigma, A2547)	1:1000	Mouse monoclonal antibody raised against a KLH-conjugated synthetic decapeptide encompassing the N-terminus of α-smooth muscle actin

## Secondary antibodies

**Table 17:** Secondary antibodies used in this thesis. All dilutions of the antibodies are given, as well as information about the respective antibody (modified after the data sheets of the respective antibodies[156-158]). All secondary antibodies are mixed 1:1 with glycerol (Merck, 1.04094.0500).

Antibody	Dilution	Information
Donkey Anti Goat Alexa Fluor® 568 (Invitrogen, A11057)	1:1000	Affinity purified donkey antibodies against goat IgG heavy chains and all classes of Ig light chains, conjugated to Alexa Fluor® 568 dye; mixed 1:1 with glycerol
Donkey Anti Goat Alexa Fluor® 647 (Invitrogen, A21447)	1:1000	Affinity purified donkey antibodies against goat IgG heavy chains and all classes of Ig light chains, conjugated to Alexa Fluor® 647 dye; mixed 1:1 with glycerol
Goat Anti Mouse Alexa Fluor® 568 (Invitrogen, A21042)	1:1000	Affinity purified goat antibodies against mouse IgG heavy chains and all classes of Ig light chains, conjugated to Alexa Fluor® 568 dye; mixed 1:1 with glycerol
Goat Anti Rabbit Alexa Fluor® 568 (Invitrogen, A11011)	1:1000	Affinity purified goat antibodies against rabbit IgG heavy chains and all classes of Ig light chains, conjugated to Alexa Fluor® 568 dye; mixed 1:1 with glycerol
Goat Anti Rabbit Alexa Fluor® 647 (Invitrogen, A21244)	1:1000	Affinity purified goat antibodies against rabbit IgG heavy chains and all classes of Ig light chains, conjugated to Alexa Fluor® 647 dye; mixed 1:1 with glycerol

## Blocking buffers

### Materials

- Animal serums / BSA
  - Donkey (Jackson Immuno Research, 017-000-121)
  - Goat (Jackson Immuno Research, 005-000-121)
- PBS (see 4.11.3)
- Saponin (Sigma S-1252)
- 50 mL tubes (VWR, 50 ml Super Clear® Centrifuge tubes, 525-0307)

### Method

1. Mix
  - a. 25 mL animal serum
  - b. 400 mL PBS
  - c. 250 µL saponin
2. Adjust to 500 mL with PBS
3. Prepare 50 mL aliquots
4. Store at -20 °C

### 4.11.7 Photography of IF-stained sections

#### *Materials*

- ZEISS Axio Imager Z1 microscope equipped with TissueFAXS, TissueGnostics GmbH (TF)
  - Objectives
    - EC-Plan Neofluar 2.5 x / 0.07
    - EC-Plan Neofluar 20 x / 0.5
  - Camara (PCO Pixelfly)
- Ethanol 70 % (v / v), diluted from Ethanol 96 % (v / v) (Merck, 1.00983.1000)

#### *Method*

1. Clean the slides using Ethanol 70 % (v / v)
2. Insert the slides in the slide holder
3. Insert the slide holder into the stage
4. Start the TissueFaxes application
5. Acquire all areas of interest\*
6. Remove the slides from the slide holder and store them at 4 °C

\*To describe the process of using the TF image acquisition system in detail would go beyond the scope of this work. See the instructions of the TF for detailed information.

#### *Notes*

- ✓ Images are saved as PNG
- ✓ All parameters for image acquisition (exposure time, lamp intensity, thresholds, gain ...) are recorded for each channel and each experiment and are stated with the respective image series in the results section.
- ✓ The tonality of all IF-images in this work have been adjusted by the same amount for better clarity in print (10 / 1.25 / 200) in Adobe® Photoshop®
- ✓ If not specified otherwise, all pictures consist of the overlay of the respective channel(s) of the secondary AB(s) and the DAPI channel
- ✓ All images are captured using the 20 x objective

## 4.11.8 Experiment parameters

### Single stainings for SM-actin and pecam-1

**Table 18:** Experiment parameters for single staining of aorta sections stained for SM-actin with Alexa Fluor® 568. Blocking buffer and ABs: see 4.11.6, incubation times and dilution(s) are stated; o/n: overnight; Tex: name of the channel for acquisition of 568 stained images; LT: lower threshold (parameter to reduce background in the TF software).

<b>Type</b>	Single staining
<b>Blocking buffer</b>	5 % goat serum + 0.05 % saponin in PBS
<b>Primary AB</b>	o/n 1:500 Mouse Anti SM Actin
<b>Secondary AB</b>	1 h 1:1000 Goat Anti Mouse Alexa Fluor® 568
<b>Acquisition parameters</b>	DAPI: 30 ms, Tex: 150 ms + LT 250

**Table 19:** Experiment parameters for single staining of aorta sections stained for pecam-1 with Alexa Fluor® 568. Blocking buffer and ABs: see 4.11.6, incubation times and dilution(s) are stated; o/n: overnight; Tex: name of the channel for acquisition of 568 stained images; LT: lower threshold (parameter to reduce background in the TF software).

<b>Type</b>	Single staining
<b>Blocking buffer</b>	5 % goat serum + 0.05 % saponin in PBS
<b>Primary AB</b>	o/n 1:50 Rabbit Anti Pecam
<b>Secondary AB</b>	1 h 1:1000 Goat Anti Rabbit Alexa Fluor® 647
<b>Acquisition parameters</b>	DAPI: 30 ms, Tex: 150 ms + LT 250



## Double stainings for SM-actin + pecam-1

**Table 20:** Experiment parameters for double staining of aorta sections stained for SM-actin + pecam-1 with Alexa Fluor® 568 and Alexa Fluor 647. Blocking buffer and ABs: see 4.11.6, incubation times and dilution(s) are stated; o/n: overnight; Tex: name of the channel for acquisition of 568 stained images; Cy5: name of the channel for acquisition of 647 stained images; LT: lower threshold (parameter to reduce background in the TF software); G: gain (parameter for signal amplification in the TF software).

Type	Double staining		
<b>Blocking buffer</b>	5 % goat serum + 0.05 % saponin in PBS		
<b>1<sup>st</sup> Primary AB</b>	o/n / 1h	1:500	Mouse Anti SM Actin
<b>1<sup>st</sup> Secondary AB</b>	1 h	1:1000	Goat Anti Mouse Alexa Fluor® 568
<b>2<sup>nd</sup> Primary AB</b>	o/n / 1h	1:50	Rabbit Anti Pecam
<b>2<sup>nd</sup> Secondary AB</b>	1 h	1:1000	Goat Anti Rabbit Alexa Fluor® 647
<b>Acquisition parameters</b>	DAPI: 30 ms, Tex: 150 ms + LT 250, Cy5: 450 ms + G + LT 150		

## Single stainings for MT<sub>1</sub> protein expression on cryo-sections

**Table 21:** Experiment parameters for single staining of aorta sections stained for MT<sub>1</sub> using the Abbiotec AB with Alexa Fluor® 568. Blocking buffer and ABs: see 4.11.6, incubation times and dilution(s) are stated; o/n: overnight; Tex: name of the channel for acquisition of 568 stained images.

Type	Single staining		
<b>Blocking buffer</b>	5 % goat serum + 0.05 % saponin in PBS		
<b>Primary AB</b>	o/n	1:200	Rabbit Anti MT1 (Abbiotec)
<b>Secondary AB</b>	1 h	1:1000	Goat Anti Rabbit Alexa Fluor® 568
<b>Acquisition parameters</b>	DAPI: 50 ms, Tex: 400 ms		

**Table 22:** Experiment parameters for single staining of aorta sections stained for MT<sub>1</sub> using the SC AB with Alexa Fluor® 568. Blocking buffer and ABs: see 4.11.6, incubation times and dilution(s) are stated; o/n: overnight; Tex: name of the channel for acquisition of 568 stained images.

Type	Single staining		
<b>Blocking buffer</b>	5 % donkey serum + 0.05 % saponin in PBS		
<b>Primary AB</b>	o/n	1:50	Goat Anti MT1 (SC)
<b>Secondary AB</b>	1 h	1:1000	Donkey Anti Goat Alexa Fluor® 568
<b>Acquisition parameters</b>	DAPI: 50 ms, Tex: 400 ms		

## 4 Materials and methods

---

**Table 23:** Experiment parameters for single staining of aorta sections stained for MT<sub>1</sub> using the SC AB with Alexa Fluor® 647. Blocking buffer and ABs: see 4.11.6, incubation times and dilution(s) are stated; o/n: overnight; Cy5: name of the channel for acquisition of 647 stained images; G: gain (parameter for signal amplification in the TF software).

<b>Type</b>	Single staining
<b>Blocking buffer</b>	5 % donkey serum + 0.05 % saponin in PBS
<b>Primary AB</b>	o/n 1:50, 1:20 Goat Anti MT1 (SC)
<b>Secondary AB</b>	1 h 1:1000 Donkey Anti Goat Alexa Fluor® 647
<b>Acquisition parameters</b>	DAPI: 20 ms, Cy5: 400 ms + G

### Single stainings for MT<sub>1</sub> protein expression on paraffin sections

**Table 24:** Experiment parameters for single staining of aorta and control paraffin sections stained for MT<sub>1</sub> using the Abbotec AB in two different concentrations with Alexa Fluor® 647. Blocking buffer and ABs: see 4.11.6, incubation times and dilution(s) are stated; o/n: overnight; Cy5: name of the channel for acquisition of 647 stained images; G: gain (parameter for signal amplification in the TF software).

<b>Type</b>	Single staining
<b>Blocking buffer</b>	5 % goat serum + 0.05 % saponin in PBS
<b>Primary AB</b>	o/n 1:50, 1:10 Rabbit Anti MT1 (Abbotec)
<b>Secondary AB</b>	1 h 1:1000 Goat Anti Rabbit Alexa Fluor® 647
<b>Acquisition parameters</b>	DAPI: 40 ms, Cy5: 500 ms + G

**Table 25:** Experiment parameters for single staining of aorta and control paraffin sections stained for MT<sub>1</sub> using the SC AB in two different concentrations with Alexa Fluor® 647. Blocking buffer and ABs: see 4.11.6, incubation times and dilution(s) are stated; o/n: overnight; Cy5: name of the channel for acquisition of 647 stained images; G: gain (parameter for signal amplification in the TF software); Trans: transmitted light.

<b>Type</b>	Single staining
<b>Blocking buffer</b>	5 % donkey serum + 0.05 % saponin in PBS
<b>Primary AB</b>	o/n 1:50, 1:20 Goat Anti MT1 (SC)
<b>Secondary AB</b>	1 h 1:1000 Donkey Anti Goat Alexa Fluor® 647
<b>Acquisition parameters</b>	DAPI: 20 ms, Cy5: 400 ms + G, Trans: 75 ms / 5.9 V

## 5 RESULTS

### 5.1 Establishment of molecular biological methods to demonstrate expression of MT<sub>1</sub> and MT<sub>2</sub> mRNA in rat tissues

In order to achieve the primary goal of this thesis, i.e. the confirmation of melatonin receptor mRNA expression in the rat aorta, the methods for RNA isolation, purity assessment, reverse transcription and PCR experiments had to be established. Ishii et al. [26] have recently demonstrated the occurrence of MT<sub>1</sub> and MT<sub>2</sub> mRNA in a variety of rat tissues.

Accordingly, several rat organs where expression of either MT<sub>1</sub> or MT<sub>2</sub> had been established were used as positive control (see 4.1.1). The RNA from these organs was extracted (see 5.1.1), transcribed into cDNA (see 5.1.2) and MT<sub>1</sub> as well as MT<sub>2</sub> mRNA expression was demonstrated by subsequent PCR (see 5.1.2) and qPCR (see 5.1.3).

#### 5.1.1 RNA-Isolation

The RNA of ten different rat organs (see 4.1.1) was isolated (see 4.2). Photometric measurement of all samples (see 4.3) revealed acceptable purity ( $A_{260} / A_{280} > 1.6$ ) of the isolated RNAs. Yields of total RNA (see Table 26) varied, even though the same amount of tissue from each organ was used for RNA extraction (about 70 mg). GE (see 4.4) of the isolated RNA showed that it was intact for all organs and exhibited no signs of degradation (see Figure 19).

**Table 26:** Concentration, purity and yield of extracted RNA from various rat organs. Skeletal m.: skeletal muscle.

Organ	C [ng / $\mu$ L]	$A_{260} / A_{280}$	RNA yield [ $\mu$ g]
Brain	827.1	1.68	16.54
Eye	1212.5	1.77	24.25
Heart	1529.4	1.80	30.59
Intestine	3926.7	1.86	264.68
Kidney	3116.2	1.75	65.11
Liver	1880.6	1.97	188.06
Lung	1012.1	1.80	20.24
Skeletal m.	1978.8	1.88	39.58
Testes	4050.8	1.90	133.55
Thymus	545.5	1.65	10.91

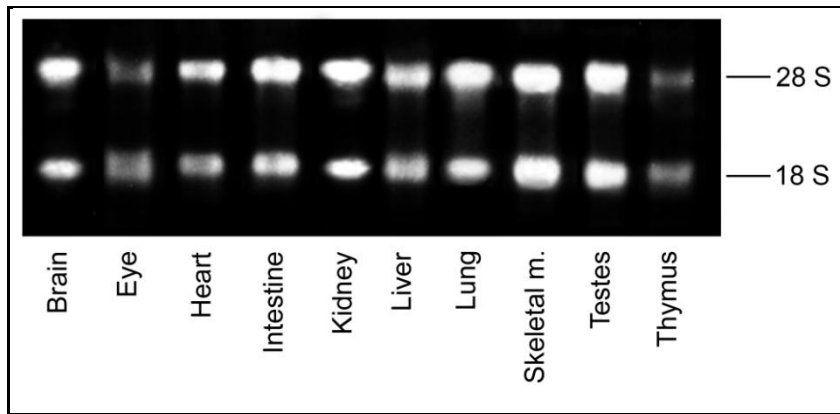


**Figure 19:** Integrity control of total RNA from all extracted organs by GE. The isolated RNA of all organs is intact as judged by intact 28 S and 18 S rRNA bands.

### 5.1.2 RT-PCR experiments on the isolated RNA

Reverse transcription was performed (see 4.5). The obtained cDNAs were used for all following PCR experiments addressing  $\beta$ -actin,  $MT_1$  and  $MT_2$  expression in the rat organs.

#### RT-PCR for $\beta$ -actin mRNA expression to prove successful RT

The first PCR experiment was executed for  $\beta$ -actin to confirm the success of the reverse transcription.  $\beta$ -actin is a so-called “housekeeping gene”, i.e. a gene that is common in all tissue and expressed ubiquitously in high concentrations. Primers and protocol were selected according to Ishii et al. [26]. 200 ng cDNA or water (no cDNA) were subjected to the PCR reaction. See 4.6.2 for the general protocol and 4.6.3 for experiment specific conditions. The experiment shows successful amplification of  $\beta$ -actin mRNA in all samples (see Figure 20), confirming success of the RT and – once more – integrity of the isolated RNA. Strengths of the observed bands were similar.

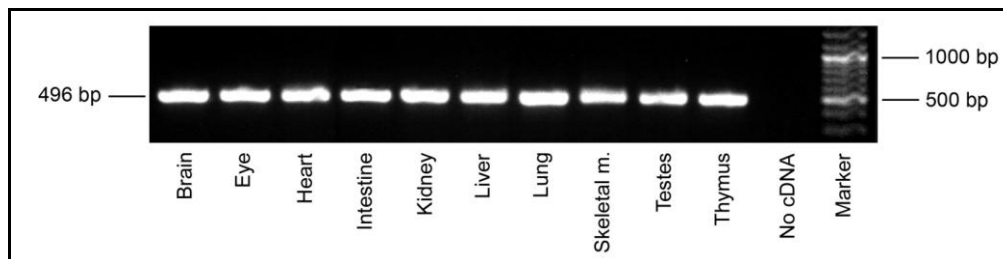


**Figure 20:**  $\beta$ -actin mRNA expression in various rat organs analyzed by RT-PCR, confirming the success of the reverse transcription. Expected length of the PCR product was 496 bp.

### RT-PCR for MT<sub>1</sub> mRNA expression

The next step was amplification of MT<sub>1</sub> mRNA in the rat organs, following the procedure from Ishii et al. [26]. However, using identical settings, only the eye and intestine samples showed very weak bands at the expected size. For all other organs (including e.g. testes, liver or kidney, which exhibited strong bands for MT<sub>1</sub> in the original experiment by Ishii et al. [26]) there were no bands visible at all (data not shown).

Because of this weak amplification, we conducted a new PCR experiment, using double the amount of template cDNA (400 ng instead of 200 ng; RNA equivalent) per sample, and more cycles (increased from 35 to 40). See 4.6.2 for the general protocol and 4.6.3 for experiment specific conditions. The results of this modification can be seen in Figure 21, which shows bands of varying intensity for MT<sub>1</sub> in all tissues, with exception of the liver. Congruent with the results of the last experiment, eye and intestine samples show the strongest bands.

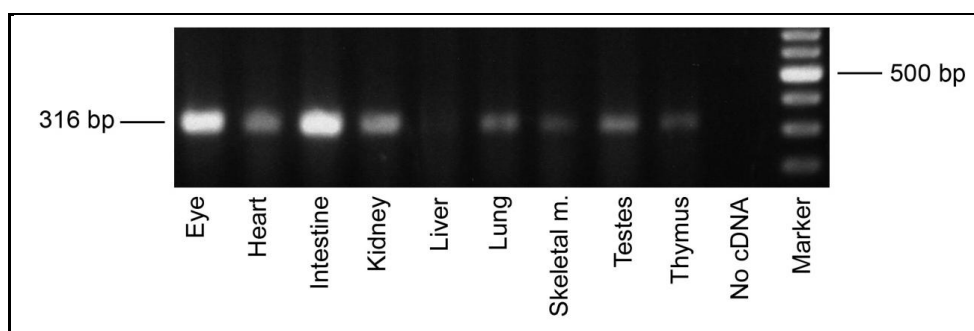


**Figure 21:** MT<sub>1</sub> mRNA expression in various rat organs analyzed by RT-PCR. Expected length of the PCR product was 316 bp.

### RT-PCR for MT<sub>2</sub> mRNA expression

All rat organs were next tested for MT<sub>2</sub> expression, following exactly the procedure described by Ishii et al. [26]. 400 ng of cDNA (RNA equivalent) or water (no cDNA) were subjected to PCR. See 4.6.2 for the general protocol and 4.6.3 for experiment specific conditions.

Unexpectedly, no bands appeared for any organ (data not shown). To exclude methodical error, the procedure was repeated and yielded the same negative results (data not shown).

To address this problem, the protocol was modified using another PCR reaction buffer with NH<sub>4</sub>SO<sub>2</sub>, which should provide higher primer specificity and product yields [143]. To conserve material, this experiment was only performed on three selected samples (kidney, eye and intestine). However, this experiment again failed to

demonstrate MT<sub>2</sub> expression in any of the three tested organs, as a PCR product was detected neither at the expected length of 390 bp nor at any other length (data not shown).

As a final measure to verify MT<sub>2</sub> mRNA expression in brain and eye [24, 26], in the next experiment the annealing temperature of the PCR was reduced from 60 °C to 57 °C. See 4.6.2 for the general protocol and 4.6.3 for experiment specific conditions.

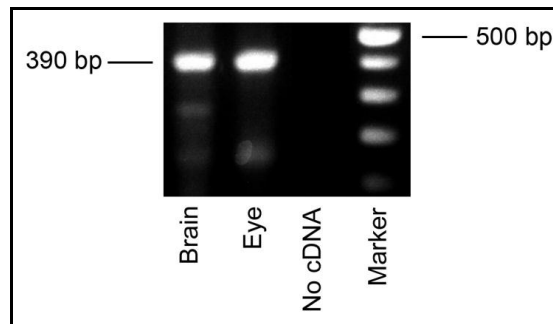


**Figure 22:** MT<sub>2</sub> mRNA expression in rat brain and eye analyzed by RT-PCR. Expected length of the PCR product was 390 bp.

As shown in Figure 22 by the appearance of a major band at 390 bp, this time, amplification was successful for the eye and brain samples. Probably due to the decreased annealing temperature, some other (but much weaker) bands appeared for both samples. Nevertheless, since the main bands were clearly at the correct length and of great intensity, the adapted method with the decreased annealing temperature was chosen to demonstrate MT<sub>2</sub> mRNA expression in the aorta.

### 5.1.3 RT-qPCR for ACTB, MT<sub>1</sub> and MT<sub>2</sub> mRNA expression

Next, the method for qPCR was established according to the procedure described in 4.10. Using qPCR, it is possible to discern the expression levels of various targets at a much greater sensitivity than with conventional “qualitative” PCR.

ACTB ( $\beta$ -actin) was used as reference gene, as it seems to be evenly expressed in all tissues (see Figure 20). Both MT<sub>1</sub> and MT<sub>2</sub> were analyzed in this experiment.

In addition to a negative sample (no cDNA), a -RT sample (intestine RNA treated like the other samples, except that no reverse transcriptase was added to the reaction mixture) was included as well. If the observed amplifications had been due to amplification of genomic DNA, the -RT sample would have shown the same or similar CT values as the reversely transcribed samples.

All samples, each containing 100 ng of the cDNA synthesized in 5.1.2, were prepared in triplicates. The mean of all CT values was calculated (CT<sub>m</sub>) and used as base for the following data analysis.

With respect to ACTB, the experiment went well for all samples except the eye, where ACTB did not show any expression. This can probably be attributed to a preparation error. Because of this, the  $\Delta$ CT values for the eye could not be calculated, while CT values for all other samples are shown in Table 27.

According to the calculation, MT<sub>1</sub> mRNA expression was found in all samples at varying levels, highest in brain, lowest in lung (see Figure 23), correlating quite well with the expression levels observed in the qualitative PCR (see Figure 21). MT<sub>2</sub> mRNA expression was found in brain, kidney, testes and thymus, while the other samples did not exhibit amplification. The highest CT value for MT<sub>2</sub> was found in the eye, confirming MT<sub>2</sub> mRNA expression, but as noted before, no  $\Delta$ CT values can be given because of the failed ACTB amplification.

It is obvious that the CT<sub>m</sub> values for all samples were very high, especially for MT<sub>2</sub>, indicative of rather low expression of the receptors. They also exhibit relatively high standard deviations (CTS<sub>d</sub>) – therefore the comparison of expression levels is to be interpreted with caution. The -RT and negative samples showed amplification for ACTB as well, indicating some trace contamination. However, the difference in expression levels between them and the positively reverse-transcribed samples was so high (15–19 CT) that the contaminants’ influence on the result is negligible. For MT<sub>1</sub> and MT<sub>2</sub>, the -RT and negative samples showed no amplification.

## 5 Results

**Table 27:** ACTB ( $\beta$ -actin), MT<sub>1</sub> and MT<sub>2</sub> mRNA expression in various rat organs analyzed by RT-qPCR. Amplification failed for ACTB in the eye sample, therefore no  $\Delta$ CT values could be calculated. The respective values are printed in gray. Empty cells indicate failed amplification. CT<sub>m</sub>: mean CT value from three repeats; CT<sub>m</sub>Sd: standard deviation for CT<sub>m</sub>;  $\Delta$ CT<sub>m</sub>: mean  $\Delta$ CT value based on the ACTB CT<sub>m</sub> values as reference;  $\Delta$ CT<sub>m</sub>Sd: cumulative standard deviation for  $\Delta$ CT<sub>m</sub>; D(ACTB): decimal difference in expression related to ACTB ( $\Delta$ CT<sub>m</sub> converted from base 2 to base 10, assuming a linear amplification efficiency of 100 %);  $\Delta\Delta$ CT<sub>m</sub>: mean  $\Delta\Delta$ CT value for MT<sub>2</sub> related to MT<sub>1</sub> (difference  $\Delta$ CT<sub>m</sub> for MT<sub>1</sub> and MT<sub>2</sub>);  $\Delta\Delta$ CT<sub>m</sub>Sd: cumulative standard deviation for  $\Delta\Delta$ CT<sub>m</sub>; D(MT1): decimal difference in expression related to MT1 ( $\Delta\Delta$ CT<sub>m</sub> converted from base 2 to base 10, assuming a linear amplification efficiency of 100 %), only given for MT<sub>2</sub> expressing samples.

Sample	Target	CT <sub>m</sub>	CT <sub>m</sub> Sd	$\Delta$ CT <sub>m</sub>	$\Delta$ CT <sub>m</sub> Sd	D(ACTB)	$\Delta\Delta$ CT <sub>m</sub>	$\Delta\Delta$ CT <sub>m</sub> Sd	D(MT1)
Brain	ACTB	17.07	0.06						
Eye	ACTB								
Heart	ACTB	17.10	0.74						
Intestine	ACTB	15.66	0.15						
Kidney	ACTB	17.11	0.06						
Lung	ACTB	15.10	0.41						
Liver	ACTB	18.52	0.25						
Skeletal m.	ACTB	19.15	0.24						
Testes	ACTB	17.39	1.32						
Thymus	ACTB	17.89	0.18						
No cDNA	ACTB	34.22	0.32						
-RT	ACTB	34.16	0.63						
Brain	MT1	31.59	0.11	14.53	0.17	4.2E-05			
Eye	MT1	32.43	0.14						
Heart	MT1	35.61	0.35	18.51	1.09	2.7E-06			
Intestine	MT1	32.25	0.16	16.60	0.31	1.0E-05			
Kidney	MT1	35.32	0.47	18.21	0.53	3.3E-06			
Lung	MT1	36.65	1.09	21.55	1.50	3.3E-07			
Liver	MT1	38.34		19.82		1.1E-06			
Skeletal m.	MT1	36.72		17.57		5.1E-06			
Testes	MT1	34.45	0.98	17.06	2.31	7.3E-06			
Thymus	MT1	35.42	0.60	17.53	0.78	5.3E-06			
No cDNA	MT1								
-RT	MT1								
Brain	MT2	34.58	0.55	17.52	0.60	5.3E-06	2.99	0.77	1.3E-01
Eye	MT2	32.79	0.10						
Heart	MT2								
Intestine	MT2								
Kidney	MT2	38.02		20.91		5.1E-07	2.70	0.53	1.5E-01
Lung	MT2								
Liver	MT2								
Skeletal m.	MT2								
Testes	MT2	38.16		20.77		5.6E-07	3.71	2.31	7.6E-02
Thymus	MT2	38.39	0.60	20.50	0.77	6.7E-07	2.97	1.55	1.3E-01
No cDNA	MT2								
-RT	MT2								



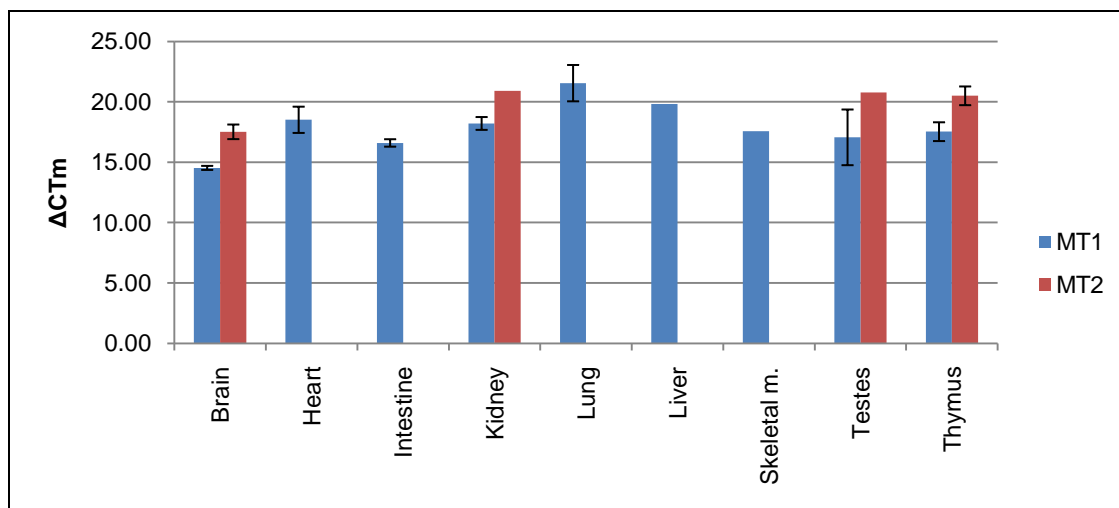


**Figure 23:** The diagram shows the mean  $\Delta CT$  values of  $MT_1$  and  $MT_2$  mRNA expression in relation to  $ACTB$  ( $\beta$ -actin) mRNA expression in various rat organs as calculated from the results of RT-qPCR. The lines on the top of the bars indicate the respective standard deviation; the indicators are missing in case of only one of the three repeats succeeding. Higher bars mean less expression. The missing bars for  $MT_2$  in many organs indicate failed amplification.  $\Delta CT_m$ : mean  $\Delta CT$  value based on the  $ACTB$   $CT_m$  values as reference.

For those samples where amplification for  $MT_1$  and  $MT_2$  was successful the  $\Delta\Delta CT$  values for  $MT_2$  related to  $MT_1$  were calculated as reference. The difference in expression between  $MT_1$  and  $MT_2$  ranged from 2.7 to 3.7 CT (or 0.15–0.076 converted to base 10, assuming a linear amplification efficiency of 100 %), indicating an about ten-fold difference in expression on average (see Figure 24).

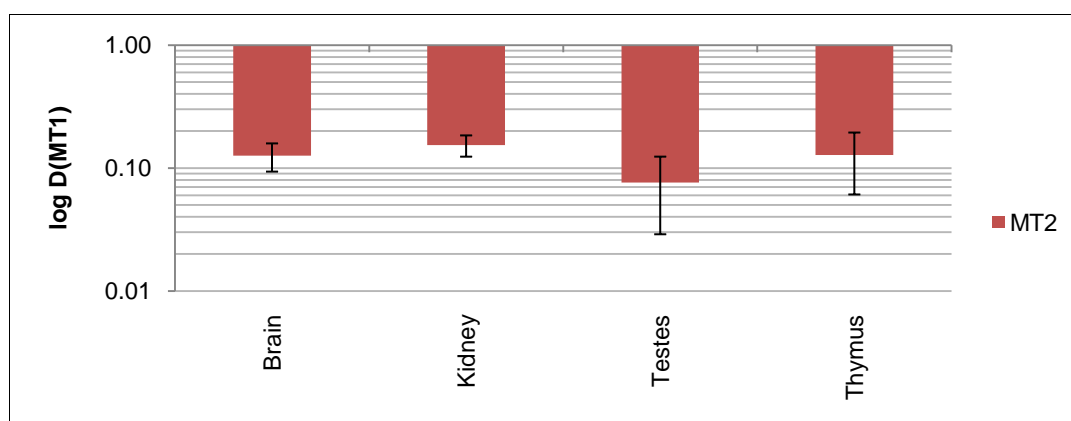


**Figure 24:** The diagram shows the logarithmic difference in  $MT_2$  expression in relation to  $MT_1$  from RT-qPCR analysis of  $ACTB$  ( $\beta$ -actin),  $MT_1$  and  $MT_2$  mRNA expression in various rat organs. Base  $MT_1$  expression is 1.00.  $D(MT_1)$ : decimal difference in expression related to  $MT_1$  ( $\Delta\Delta CT_m$  converted from base 2 to base 10, assuming a linear amplification efficiency of 100 %).

To summarize, methods (RT-PCR, RT-qPCR) for demonstration of  $MT_1$  and  $MT_2$  mRNA in rat tissues had been successfully established.

## 5.2 Preparation of rat aorta samples for subsequent PCR experiments

Two different groups of aortas with two subgroups each were investigated (see 4.1.2 and 4.1.3) The two groups each served as basis for the different aims (see chapter 3) of the thesis.

### 5.2.1 RNA isolation

#### Aortas from two different time points

The RNA was extracted and measured by photometry in two batches (batch 1: A31, A32, A33, A75, A76 and A77, batch 2: A34, A35, A36, A37, A38, A79, A81, A82, A83 and A88) according to the described procedures (see 4.2 and 4.3). Because the amount of tissue was in some cases very small, the concentrations and total isolated amounts of RNA were rather low (see Table 28). Five samples were below the specified range for the  $A_{260} / A_{280}$  ratio (1.6–2.0; A32, A33, A75, A76 and A77). 300 ng RNA were used for GE (see 4.4) to prove intactness of all samples' RNA (see Figure 25).

**Table 28:** Concentration, purity and yield of RNA extracted from rat aortas from two different time points. Daytime group (orange): A31–A38; nighttime group (blue): A75–A88.

Sample	Group	C [ng / $\mu$ L]	$A_{260} / A_{280}$	Isolated amount [ $\mu$ g]
A31	Daytime	730.1	1.82	14.60
A32	Daytime	235.1	1.56	4.70
A33	Daytime	136.3	1.52	2.73
A34	Daytime	295.3	1.64	5.91
A35	Daytime	711.7	1.80	14.23
A36	Daytime	574.0	1.89	11.48
A37	Daytime	703.9	1.83	14.08
A38	Daytime	361.4	1.72	7.23
A75	Nighttime	370.9	1.52	7.42
A76	Nighttime	159.8	1.55	3.20
A77	Nighttime	141.9	1.55	2.84
A79	Nighttime	324.0	1.80	6.48
A81	Nighttime	743.6	1.83	14.87
A82	Nighttime	299.5	1.64	5.99
A83	Nighttime	716.2	1.76	14.32
A88	Nighttime	623.2	1.88	12.46

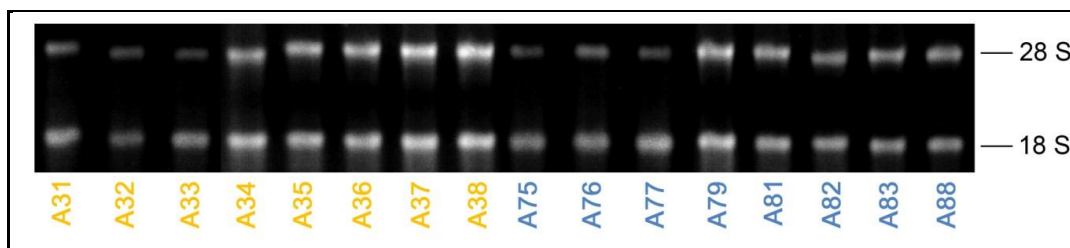


**Figure 25:** Integrity control of total RNA of rat aortas from two different time points by GE. The isolated RNA of all samples is intact as judged by intact 28 S and 18 S rRNAs. Because the RNA was extracted and analyzed in two batches (see main text), their respective lanes show different saturations. Daytime group (orange): A31–A38; nighttime group (blue): A75–A88.

### Aortas from SHR and control rats

The RNA was extracted and measured by photometry according to the described procedures (see 4.2, 4.3 and 4.4). Because the amount of tissue was in some cases very small, the concentrations and total isolated amounts of RNA were so low that for four samples (ASHR 04, ASHR 08, ACTRL 01 and ACTRL 04), too little isolated RNA remained for further experiments (see Table 29). Therefore, they could not be used in any of the subsequent procedures concerning the SHR and control aortas.

With exception of ASHR 07, all samples that were being used for further experiments lay within the specified  $A_{260} / A_{280}$  range (1.6–2.0). To conserve RNA, only 100 ng were used for GE (see 4.4), which proved intactness of all samples' RNA (see Figure 26).

**Table 29:** Concentration, purity and yield of RNA extracted from aortas of SHR and control rats. For four samples (ASHR 04, ASHR 08, ACTRL 01 and ACTRL 04) the total isolated amount was too low for further analysis (see main text). The respective entries in the table are printed in gray.

Sample	Group	C [ng / $\mu$ L]	A <sub>260</sub> / A <sub>280</sub>	Isolated amount [ $\mu$ g]
ASHR 01	SHR	99,0	1,6	1,98
ASHR 02	SHR	257,7	1,62	5,15
ASHR 03	SHR	95,2	1,6	1,90
ASHR 04	SHR	17,4	1,46	0,35
ASHR 05	SHR	175,1	1,73	3,50
ASHR 06	SHR	53,7	1,59	1,07
ASHR 07	SHR	47,3	1,55	0,95
ASHR 08	SHR	3,8	1,23	0,08
ACTRL 01	Control	39,1	1,76	0,78
ACTRL 02	Control	164,3	1,67	3,29
ACTRL 03	Control	253,8	1,71	5,08
ACTRL 04	Control	39,3	1,45	0,79
ACTRL 05	Control	160,4	1,65	3,21
ACTRL 06	Control	83,6	1,63	1,67
ACTRL 07	Control	184,8	1,6	3,70
ACTRL 08	Control	157,8	1,79	3,16

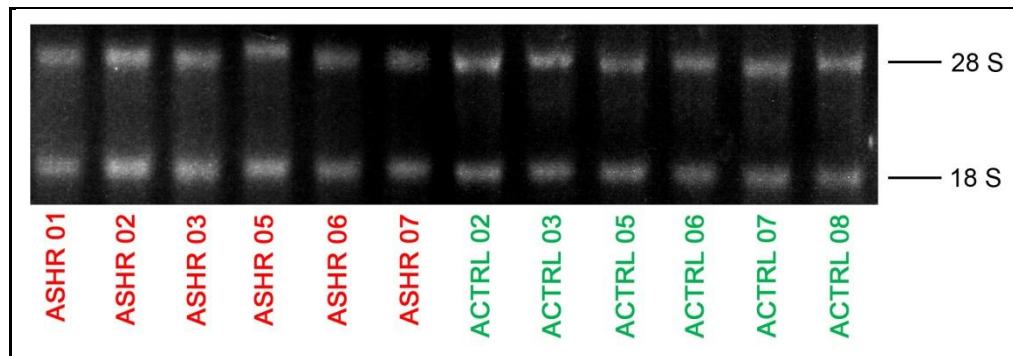


**Figure 26:** Integrity control of total RNA of aortas from SHR (red) and control (green) rats by GE. The isolated RNA of all samples was intact as judged by intact 28 S and 18 S rRNAs.

## 5.2.2 Reverse transcription

All samples of the aortas from two different time points were reversely transcribed according to the described procedure (see 4.5). Reverse transcription was performed in two batches (see 5.2.1 for the break-up). All samples from the SHR and control rats, excepting those with too little isolated RNA (see 5.2.1), were reversely transcribed according to the described procedure (see 4.5).

## 5.2.3 RT-PCR for $\beta$ -actin mRNA expression

To demonstrate the success of the RTs, 50 ng of all aorta samples or water (no cDNA) were tested for  $\beta$ -actin mRNA expression. See 4.6.2 for the general protocol and 4.6.3 for experiment specific conditions. The experiment shows successful amplification of  $\beta$ -actin mRNA in all samples (see Figure 27 and Figure 28). To make sure that the observed amplicons were not caused by genomic DNA (which is thought to be impossible since the primers are exon spanning [26]), -RT samples (A35 and ASHR 02, respectively) were included in the experiments as well. As shown in the respective figures, the -RT sample exhibited no amplification.

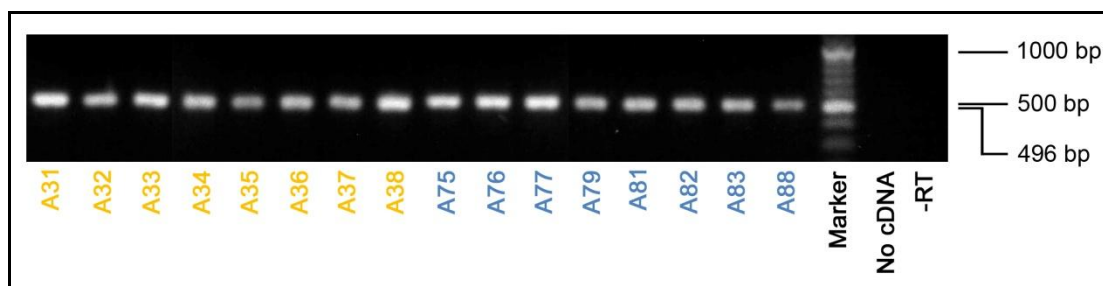


**Figure 27:**  $\beta$ -actin mRNA expression in rat aortas from two different time points analyzed by RT-PCR, confirming the success of the reverse transcription. Expected length of the PCR product was 496 bp. Daytime group (orange): A31–A38; nighttime group (blue): A75–A88.

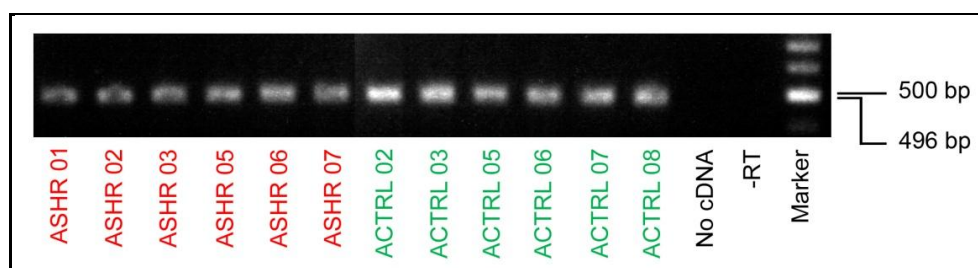


**Figure 28:**  $\beta$ -actin mRNA expression in aortas of SHR (red) and control (green) rats analyzed by RT-PCR, confirming the success of the reverse transcription. Expected length of the PCR product was 496 bp.

## 5.3 Expression of MT<sub>1</sub> mRNA in rat aortas

### 5.3.1 Aortas from two different time points

#### RT-PCR for MT<sub>1</sub> mRNA expression

Next, aortas from different time points were examined for the presence of MT<sub>1</sub> mRNA in the rat aorta and for an overview of expression levels between the two aorta groups. 400 ng of cDNA (RNA equivalent) per sample or water (no cDNA) were subjected to PCR. A -RT sample (A35) was included as well. See 4.6.2 for the general protocol and 4.6.3 for experiment specific conditions.

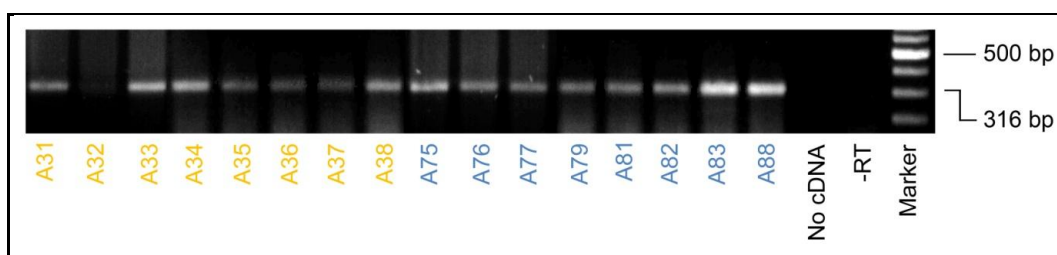


**Figure 29:** MT<sub>1</sub> mRNA expression in aortas from two different time points analyzed by RT-PCR. Expected length of the PCR product was 316 bp. Daytime group (orange): A31–A38; nighttime group (blue): A75–A88.

Bands of the expected length for MT<sub>1</sub> were present in all samples but one (A32). Taken together, the bands in the daytime group (A31–A38) appeared less intense than those in the nighttime group (A75–A88). Especially A83 and A88 (both of the nighttime group) exhibited very strong bands (Figure 29). It has to be noted that the varying intensities and absences could have resulted from outside factors as well, such as pipetting errors, varying cDNA concentrations after RT, contaminations, etc. To confront these possible sources of error, a qPCR was performed at a later stage (see below).

Because there were no bands present in the -RT sample, amplification of genomic DNA could be excluded. The blind sample exhibits no bands either, excluding contamination of the reagents.

To confirm the identity of the observed bands they were cut out of the gel and processed for sequencing.

#### Sequencing of MT<sub>1</sub> RT-PCR-products

To extract a sufficient amount of DNA for sequencing, the excised bands of A33, A34, A38, A75, A83 and A88 were pooled and the DNA was extracted and purified according to the described procedure (see 4.8). Concentration measurement of the

eluated DNA by photometry (see 4.3) revealed a concentration of 8.8 ng /  $\mu\text{L}$ . 5  $\mu\text{L}$  of the eluate were analyzed using GE to determine the extracted DNA's purity. Only a single band at the expected length of 316 bp was visible (not shown). The eluate was then sent to MWG Eurofins Operon (Ebersberg, Germany) for sequencing (see 4.9) together with aliquots containing 30 pmol of each primer (rat\_MT1\_fwd and rat\_MT1\_rev, see 4.6.3).

MT1	169	TGGCCCTGGCTGTGCTGCGGTAAGTCACCCAGGGGACCATGAAGGGCAATGTCAGCGAGC	228
fwd	1	AATGTCAGCGAGC	13
rev	274	TGGCCCTGGCTGTGCTGCGGTAAGTCACCCAGGGGACCATGAAGGGCAATGTCAGCGAGC	215
MT1	229	TTCTCAACGCCTCTCAGCAGGCTCCAGGCGCGGGGAGGAAATAAGATCGCGGCCGTCGT	288
fwd	14	TTCTCAACGCCTCTCAGCAGGCTCCAGGCGCGGGGAGGAAATAAGATCGCGGCCGTCGT	73
rev	214	TTCTCAACGCCTCTCAGCAGGCTCCAGGCGCGGGGAGGAAATAAGATCGCGGCCGTCGT	155
MT1	289	GGCTGGCCTCTACACTGGCCTTCATCCTCATCTTTACTATCGTGGTGGACATCCTGGGCA	348
fwd	74	GGCTGGCCTCTACACTGGCCTTCATCCTCATCTTTACTATCGTGGTGGACATCCTGGGCA	133
rev	154	GGCTGGCCTCTACACTGGCCTTCATCCTCATCTTTACTATCGTGGTGGACATCCTGGGCA	95
MT1	349	ACCTGCTGGTCATCCTGTCTGTGTATCGCAACAAGAAGCTCAGGAACGCAGGGGAATATAT	408
fwd	134	ACCTGCTGGTCATCCTGTCTGTGTATCGCAACAAGAAGCTCAGGAACGCAGGGGAATATAT	193
rev	94	ACCTGCTGGTCATCCTGTCTGTGTATCGCAACAAGAAGCTCAGGAACGCAGGGGAATATAT	35
MT1	409	TTGTGGTGAGTTTAGCTGTGGCAGACCTCGTGGTGGCTATTTACCCATTTCCCTTGGCGC	468
fwd	194	TTGTGGTGAGTTTAGCTGTGGCAGACCTCGTGGTGGCTATTTACCCATTTCCCTTGGCGC	253
rev	34	TTGTGGTGAGTTTAGCTGTGGCAGACCTCGTGGT	1
MT1	469	TGACGTCTATACTTAA	484
fwd	254	TGACGTCTATACTTAA	269

**Figure 30:** Comparison of the sequencing results from the MT<sub>1</sub> RT-PCR products and the published sequence for MT<sub>1</sub> mRNA (RefSeq: NM\_053676.1). Combined length of the sequencing results of both primers: 315 bp. E-values: fwd = 6E-145, rev = 1E-147; fwd: rat\_MT1\_fwd; rev: rat\_MT1\_rev.

Sequencing worked well and comparison with the published sequence for the rat MT<sub>1</sub> mRNA ([26], RefSeq: NM\_053676.1) showed 100 % identity over a length of 315 bp (expected: 316 bp). This result confirmed the identity of the observed amplicons as MT<sub>1</sub>.

### RT-qPCR for quantification of MT<sub>1</sub> mRNA expression

Having proven that MT<sub>1</sub> mRNA is indeed expressed in the rat aorta, a real-time PCR experiment was performed to investigate the suggestion from the qualitative PCR (see above) that there might be a difference in expression levels between aortas collected at different time points.

RT-qPCR was executed after the described method (see 4.10) using 100 ng of cDNA (RNA equivalent) per sample. The samples were prepared in duplicates (ACTB) and triplicates (MT<sub>1</sub>). A positive control (eye) from the various rat tissues already investigated (see 5.1.2) was also included as reference. No -RT samples were included

## 5 Results

because the previous RT-qPCR experiment (see 5.1.3) had already proven that the assays are specific for cDNA.

The blind samples were clean for MT<sub>1</sub>, but showed an expression of ACTB at very high CT levels. However, the difference in expression levels in comparison was so big that the contamination did not affect analysis of the data (see Table 30).

**Table 30:** ACTB ( $\beta$ -actin), MT<sub>1</sub> and MT<sub>2</sub> mRNA expression in rat aortas from two different time points and rat eye as positive control analyzed by RT-qPCR. Empty cells indicate failed amplification. CT<sub>m</sub>: mean CT value from two (ACTB) or three (MT<sub>1</sub>) repeats; CT<sub>m</sub>Sd: standard deviation for CT<sub>m</sub>;  $\Delta$ CT<sub>m</sub>: mean  $\Delta$ CT value based on the ACTB CT<sub>m</sub> values as reference;  $\Delta$ CT<sub>m</sub>Sd: cumulative standard deviation for  $\Delta$ CT<sub>m</sub>; D(ACTB): decimal difference in expression related to ACTB ( $\Delta$ CT<sub>m</sub> converted from base 2 to base 10, assuming a linear amplification efficiency of 100 %);  $\Delta\Delta$ CT<sub>m</sub>: mean  $\Delta\Delta$ CT value for MT<sub>1</sub> related to eye as positive control (difference  $\Delta$ CT<sub>m</sub> for MT<sub>1</sub> in the aortas and MT<sub>1</sub> in the eye);  $\Delta\Delta$ CT<sub>m</sub>Sd: cumulative standard deviation for  $\Delta\Delta$ CT<sub>m</sub>; D(Eye): decimal difference in expression related to MT<sub>1</sub> expression in the eye ( $\Delta\Delta$ CT<sub>m</sub> converted from base 2 to base 10, assuming a linear amplification efficiency of 100 %).

Sample	Target	CT <sub>m</sub>	CT <sub>m</sub> Sd	$\Delta$ CT <sub>m</sub>	$\Delta$ CT <sub>m</sub> Sd	D(ACTB)	$\Delta\Delta$ CT <sub>m</sub>	$\Delta\Delta$ CT <sub>m</sub> Sd	D(Eye)
A31	ACTB	15.951	0.055						
A32	ACTB	15.733	0.064						
A33	ACTB	14.770	0.059						
A34	ACTB	15.582	0.004						
A35	ACTB	16.708	0.120						
A36	ACTB	15.736	0.022						
A37	ACTB	15.897	0.075						
A38	ACTB	14.878	0.072						
A75	ACTB	15.414	0.001						
A76	ACTB	15.048	0.085						
A77	ACTB	15.094	0.029						
A79	ACTB	16.617	0.070						
A81	ACTB	16.294	0.169						
A82	ACTB	15.692	0.008						
A83	ACTB	15.749	0.000						
A88	ACTB	15.730	0.000						
E2	ACTB	15.967	0.036						
No cDNA	ACTB	32.387	0.371						
A31	MT1	36.960	0.716	21.008	0.771	4.7E-07	4.953	1.015	3.2E-02
A32	MT1	38.158	0.096	22.425	0.160	1.8E-07	6.370	0.404	1.2E-02
A33	MT1	37.477	0.162	22.707	0.221	1.5E-07	6.651	0.465	1.0E-02
A34	MT1	36.753	1.287	21.171	1.290	4.2E-07	5.116	1.534	2.9E-02
A35	MT1	37.739	1.238	21.031	1.358	4.7E-07	4.975	1.602	3.2E-02
A36	MT1	38.352	0.132	22.616	0.154	1.6E-07	6.560	0.397	1.1E-02
A37	MT1	37.010	0.412	21.113	0.487	4.4E-07	5.058	0.731	3.0E-02
A38	MT1	37.537	0.824	22.659	0.896	1.5E-07	6.604	1.140	1.0E-02
A75	MT1	37.200	1.831	21.786	1.832	2.8E-07	5.730	2.076	1.9E-02
A76	MT1	37.133	0.933	22.086	1.018	2.2E-07	6.030	1.261	1.5E-02
A77	MT1	38.052	1.076	22.957	1.104	1.2E-07	6.902	1.348	8.4E-03
A79	MT1	38.180		21.564		3.2E-07	5.508	0.244	2.2E-02
A81	MT1	38.175	0.637	21.882	0.805	2.6E-07	5.826	1.049	1.8E-02
A82	MT1	36.914	0.614	21.222	0.622	4.1E-07	5.167	0.865	2.8E-02
A83	MT1	37.054	0.984	21.304	0.984	3.9E-07	5.249	1.228	2.6E-02
A88	MT1	35.752				9.4E-07	3.967	0.501	6.4E-02
E2	MT1	32.023				1.5E-05			
No cDNA	MT1								



Calculated (see 4.10) decimal differences between  $MT_1$  expression in the eye and the samples can be seen in Figure 31. All aorta samples showed expression of  $MT_1$ , the amount of expression varying strongly between the individual samples. The same observation had been made before in the course of the qualitative PCR. However, the individual discerned  $MT_1$  expression levels of the aortas did not correlate with the results from the qualitative PCR. The positive control (eye) showed the highest expression of  $MT_1$ , which is again congruent with the results from the qualitative PCR (see above). As in the previous qPCR experiment, the CT values for  $MT_1$  in the aortas were very high (35–38), indicating low expression of  $MT_1$  mRNA.

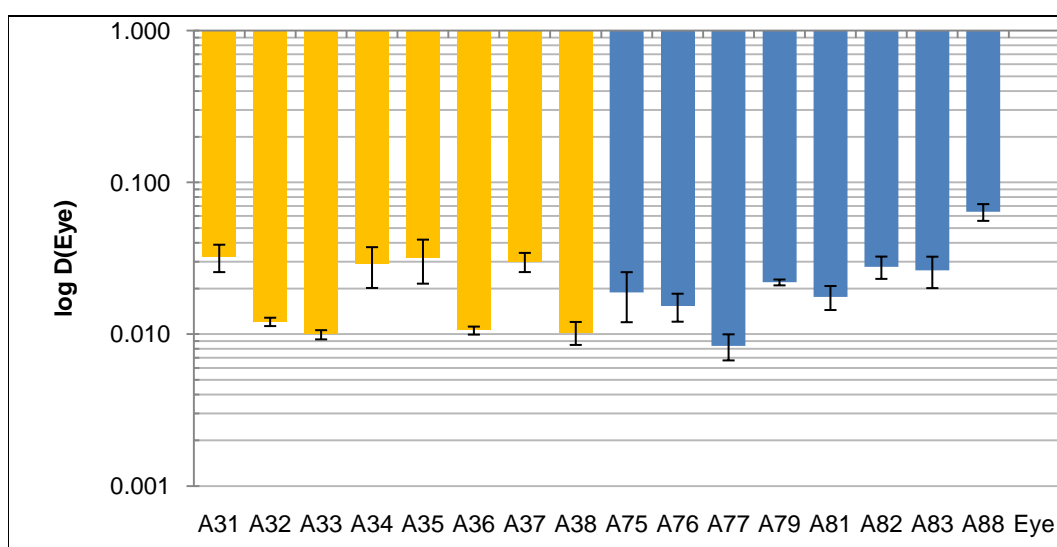


**Figure 31:** Diagram showing the logarithmic difference in  $MT_1$  mRNA expression in the aortas from two different time points in relation to  $MT_1$  mRNA expression in the eye. Base  $MT_1$  expression of the eye is 1.00. The lines on the lower ends of the bars indicate the respective standard deviations. Lower reaching bars mean less expression. Groups: bars of samples belonging to the daylight group are printed in orange, bars of samples belonging to the nighttime group are printed in blue;  $D(\text{Eye})$ : decimal difference in expression related to  $MT_1$  in the eye ( $\Delta\Delta CT_m$  converted from base 2 to base 10, assuming a linear amplification efficiency of 100 %).

Analysis of the mean expression levels shows a tiny elevation in  $MT_1$  mRNA expression in the nighttime group compared to the daytime group of  $\Delta CT_m$  21.60 (Sd 0.82) vs 21.84 (Sd 0.84). See Figure 32 for a graphical representation. As a trend, this is indeed what was observed in the qualitative PCR, but the difference is minute and the standard deviations of the means are many times bigger.

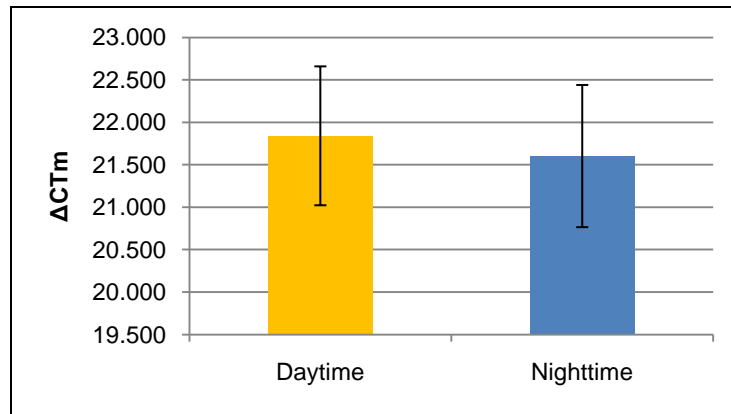


**Figure 32:** Diagram showing the mean  $\Delta CT_m$  values of the aortas from the two investigated time points. The lines on top of the bars indicate the respective standard deviations.  $\Delta CT_m$ : mean  $\Delta CT$  value based on the *ACTB*  $CT_m$  values as reference.

In summary,  $MT_1$  mRNA is expressed in the rat aorta; however, there is no significant difference in expression levels between aortas from animals sacrificed at daytime or nighttime.

### 5.3.2 Aortas from SHR and control rats

#### RT-PCR for $MT_1$ mRNA expression

The experiments with the rat aortas from different time points had already established that  $MT_1$  is present in the rat aorta, and there was no significant difference in  $MT_1$  mRNA expression found in the aorta that depends on the diurnal phase state. The remaining question was whether  $MT_1$  mRNA expression is different between hypertensive and normotensive rats. To investigate this issue, an RT-PCR was performed for  $MT_1$  mRNA expression in the SHR and control rat aortas.

As the RNA yield from these samples was very low (see Table 29), only a small amount of cDNA was available for experiments. Therefore, 200 ng cDNA (RNA equivalent) per sample or water (no cDNA) were subjected to PCR. A -RT sample (ASHR 02) was included as well. See 4.6.2 for the general protocol and 4.6.3 for experiment specific conditions.

The majority of bands in the SHR group was much stronger than the bands in the control group (see Figure 33). Amplification succeeded in all SHR samples, with a particularly strong band for the ASHR 05 sample, but failed in ACTRL 06 and ACTRL 07. These findings were confirmed by a repeat of the experiment, which yielded the same results (not shown). The variations in expression levels concur with the findings from the aortas from two different time points (see 5.3) and emphasize the possibility of interindividual differences in  $MT_1$  expression levels. This could also explain the observed difference in  $MT_1$  and  $MT_2$  mRNA expression between our experiment with various rat organs (see 5.1.2) and the experiment by Ishii et al. [26]. To further investigate this difference in mRNA expression between SHR and control rats, a qPCR was performed next.

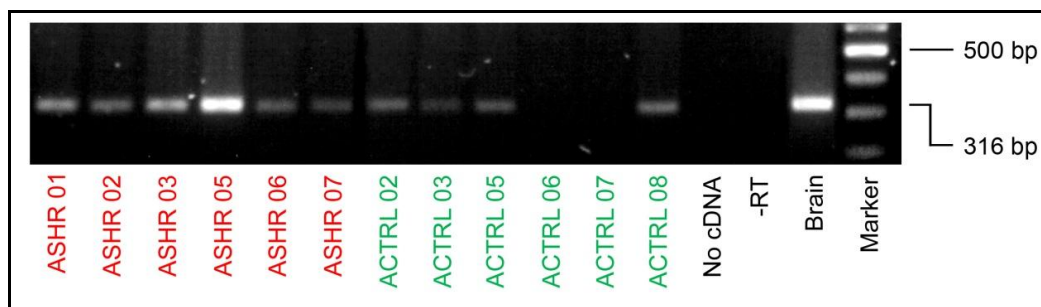


**Figure 33:** RT-PCR analysis of  $MT_1$  mRNA expression in aortas from SHR and control rats. Expected length: 316 bp.

### RT-qPCR for $M_{T1}$ mRNA expression in aortas

RT-qPCR was executed after the described method (see 4.10) using only 50 ng of cDNA (RNA equivalent), because of the very low yield of the RNA extraction already discussed.

All samples were prepared in triplicates. A positive control (brain) from the various rat aortas already investigated (5.1.2) was used as reference. Also, -RT samples were included from both the SHR (ASHR 02) and control group (ACTRL 03).

## 5 Results

**Table 31:** ACTB ( $\beta$ -actin),  $MT_1$  and  $MT_2$  mRNA expression in aortas from SHR and control rats and rat brain as positive control analyzed by RT-qPCR. Empty cells indicate failed amplification. CTm: mean CT value from three repeats; CTmSd: standard deviation for CTm;  $\Delta$ CTm: mean  $\Delta$ CT value based on the ACTB CTm values as reference;  $\Delta$ CTmSd: cumulative standard deviation for  $\Delta$ CTm; D(ACTB): decimal difference in expression related to ACTB ( $\Delta$ CTm converted from base 2 to base 10, assuming a linear amplification efficiency of 100 %);  $\Delta\Delta$ CTm: mean  $\Delta\Delta$ CT value for  $MT_1$  related to brain as positive control (difference  $\Delta$ CTm for  $MT_1$  in the aortas and  $MT_1$  in the brain);  $\Delta\Delta$ CTmSd: cumulative standard deviation for  $\Delta\Delta$ CTm; D(Brain): decimal difference in expression related to  $MT_1$  expression in the brain ( $\Delta\Delta$ CTm converted from base 2 to base 10, assuming a linear amplification efficiency of 100 %).

Sample	Target	CTm	CTmSd	$\Delta$ CTm	$\Delta$ CTmSd	D(ACTB)	$\Delta\Delta$ CTm	$\Delta\Delta$ CTmSd	D(Brain)
ACTRL02	ACTB	16.751	16.815	0.148					
ACTRL03	ACTB	16.180	16.061	0.103					
ACTRL05	ACTB	16.203	16.187	0.043					
ACTRL06	ACTB	16.271	16.112	0.152					
ACTRL07	ACTB	16.941	16.683	0.274					
ACTRL08	ACTB	16.610	16.411	0.319					
ASHR01	ACTB	17.283	17.277	0.060					
ASHR02	ACTB	16.671	16.718	0.068					
ASHR03	ACTB	17.038	16.954	0.075					
ASHR05	ACTB	17.298	16.906	0.420					
ASHR06	ACTB	17.090	17.163	0.064					
ASHR07	ACTB	16.810	16.860	0.098					
B2	ACTB	18.931	18.888	0.052					
Blind	ACTB		38.639						
-RTCTRL	ACTB	35.899	35.687	1.161					
-RTSHR	ACTB	32.776	32.862	0.076					
ACTRL 02	MT1	37.745	37.255	0.692	20.440	0.840	7.0E-07	7.302	1.456
ACTRL 03	MT1	38.611	38.611		22.549		1.6E-07	9.411	0.616
ACTRL 05	MT1	36.731	37.619	1.255	21.432	1.298	3.5E-07	8.293	1.915
ACTRL 06	MT1	39.039	39.039		22.927		1.3E-07	9.789	0.616
ACTRL 07	MT1	38.961	38.961		22.278		2.0E-07	9.140	0.616
ACTRL 08	MT1	38.179	37.371	1.143	20.959	1.463	4.9E-07	7.821	2.079
ASHR 01	MT1	36.889	37.144	0.221	19.867	0.281	1.0E-06	6.729	0.897
ASHR 02	MT1	36.835	36.496	0.331	19.778	0.399	1.1E-06	6.640	1.015
ASHR 03	MT1	36.552	37.014	0.711	20.060	0.786	9.1E-07	6.922	1.402
ASHR 05	MT1	35.862	34.589	1.473	17.682	1.893	4.8E-06	4.544	2.509
ASHR 06	MT1	38.928	38.247	1.257	21.084	1.321	4.5E-07	7.946	1.937
ASHR 07	MT1	37.540	36.944	0.600	20.084	0.698	9.0E-07	6.946	1.315
Brain	MT1	31.650	32.026	0.565	13.138	0.616	1.1E-04		
No cDNA	MT1								
-RTCTRL	MT1								
-RTSHR	MT1								

Like in the other RT-qPCR experiments (see 5.1.3 and 5.3.1), a signal for ACTB occurred even in the blind and -RT samples, although again at much higher CT values (35–38 versus 16–17 in the positive groups), which means the contamination will not affect analysis of the data. No signal was detected for  $MT_1$  in the -RT and blind samples (see Table 31).

The control samples exhibited generally higher  $\Delta$ CT values than the SHR samples. The biggest difference is evident between the aorta samples and the brain sample, where the concentration of mRNA is several orders of magnitude higher. Calculated

(see 4.10) decimal differences between  $MT_1$  expression in the eye and the samples can be seen in Figure 34. The band intensity observed in the qualitative RT-PCR correlates nicely with data from the RT-qPCR (see above).

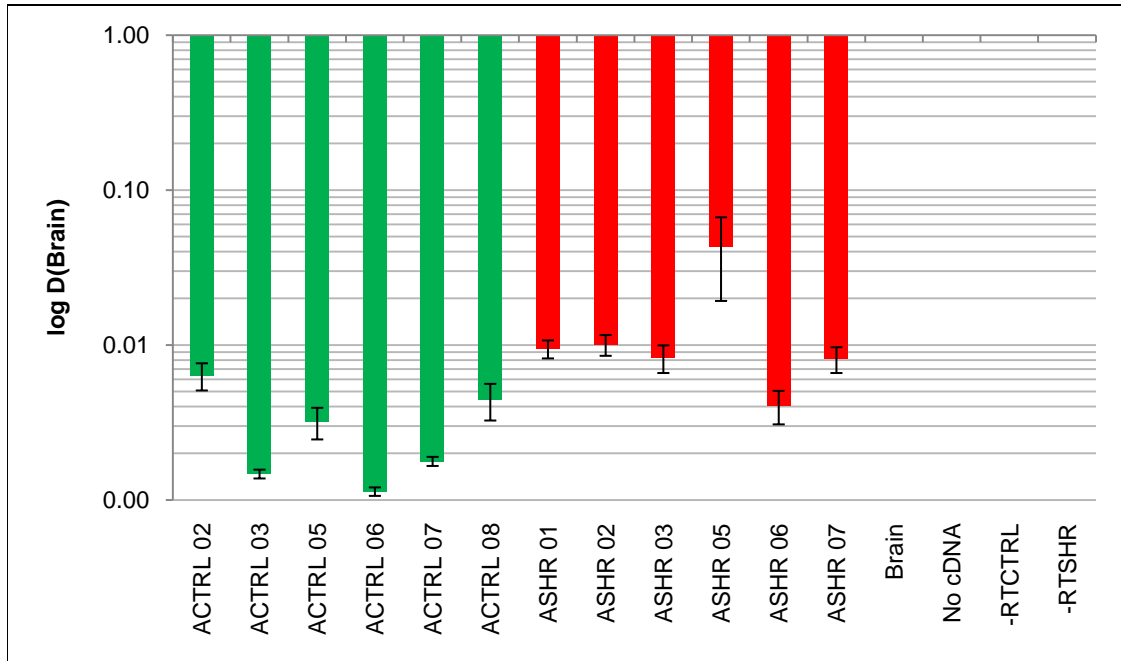


**Figure 34:** The diagram shows the logarithmic difference in  $MT_1$  mRNA expression in the aortas of SHR and control rats in relation to  $MT_1$  mRNA expression in the eye. Base  $MT_1$  expression of the eye is 1.00. The lines on the bottom ends of the bars indicate the respective standard deviations. Lower reaching bars mean less expression. Groups: bars of samples belonging to the control group printed in green, bars of samples belonging to the SHR group are printed in red;  $D(\text{Eye})$ : decimal difference in expression related to  $MT_1$  in the brain ( $\Delta\Delta CT_m$  converted from base 2 to base 10, assuming a linear amplification efficiency of 100 %).

Analysis of the mean  $MT_1$  mRNA expression levels showed a distinct elevation in  $MT_1$  mRNA expression in the SHR group compared to the control group of  $\Delta CT_m$  19.76 (Sd 1.12) vs 21.76 (Sd 0.97). A graphical representation can be seen in Figure 35. Also, the observed mean expression level and standard deviation of the control group are comparable with the observed mean expression levels and standard deviations for the aortas from two different time points (control vs nighttime vs daytime):  $\Delta CT_m$  21.76 (Sd 0.97) vs 21.60 (Sd 0.82) vs 21.84 (Sd 0.84).

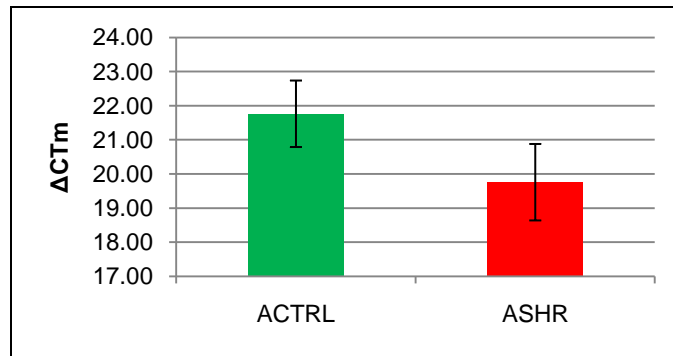


**Figure 35:** The diagram shows the mean  $\Delta CT_m$  values of the aortas from the two investigated time points. The lines on top of the bars indicate the respective standard deviations.  $\Delta CT_m$ : mean  $\Delta CT$  value based on the *ACTB*  $CT_m$  values as reference.

By calculating the  $\Delta\Delta CT$  values for the two groups and conversion to the decimal system (see 4.10), the mean difference between the SHR and control rats turned out to be about four-fold (4.01). However, the standard deviation is very high (4.19, relative standard deviation 104 %). Nevertheless, taking the standard deviation into account, the difference in expression ranges from about zero- to eight-fold. This means that the expression of mRNA in aortas of SHR is zero to eight times higher than in normotensive rats (see Figure 36). A RT-qPCR experiment with a bigger number of samples would probably show the difference in mRNA expression to a greater extent.

It should also be noted that the amplification succeeded in all of the SHR samples' replicates, but not in all replicates of the control samples (18 SHR vs 9 controls). This fact can also be attributed to the observed difference in expression levels: because the levels of mRNA in the control rats' aortas are lower than in the SHR's aortas, amplification might easily fail, since the observed  $CT$  values are already extremely high ( $CT$  36–39; see Table 31).

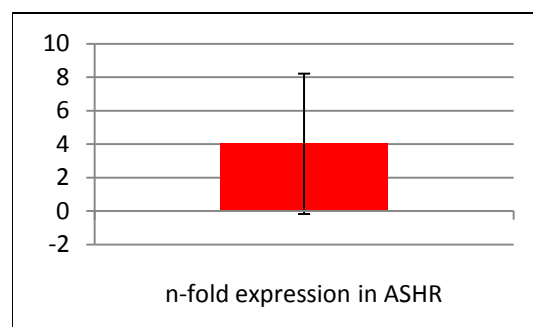


**Figure 36:** The diagram shows the  $n$ -fold expression of *MT<sub>1</sub>* mRNA in SHR aortas compared to control aortas.

In conclusion, we proved significantly higher expression of *MT<sub>1</sub>* mRNA in SHR compared to control rat aortas.

## 5.4 Expression of MT<sub>2</sub> mRNA in rat aortas

### 5.4.1 RT-PCR for MT<sub>2</sub> mRNA expression according to the established method

The first RT-PCR experiment concerning MT<sub>2</sub> mRNA expression in the aorta was performed on the aortas from two different time points (see 4.1.2.) according to the method by Ishii et al. [26] modified as described in 5.1.2. 400 ng of cDNA (RNA equivalent) per sample or water (no cDNA) were subjected to PCR. A negative sample (no cDNA), a -RT sample (A35) and a positive control (brain) were also included in the experiment. See 4.6.2 for the general protocol and 4.6.3 for experiment specific conditions.

In the positive control (brain), amplification succeeded and yielded a very strong and distinctive band at the expected length. Under close inspection, bands at the expected length of 396 bp seemed also to be present in some of the aorta samples (A32, A38 and A77). However, bands of other lengths were present too, some of them much stronger (A38) than the alleged MT<sub>2</sub> bands (see Figure 37). The experiment was repeated with similar results (not shown).

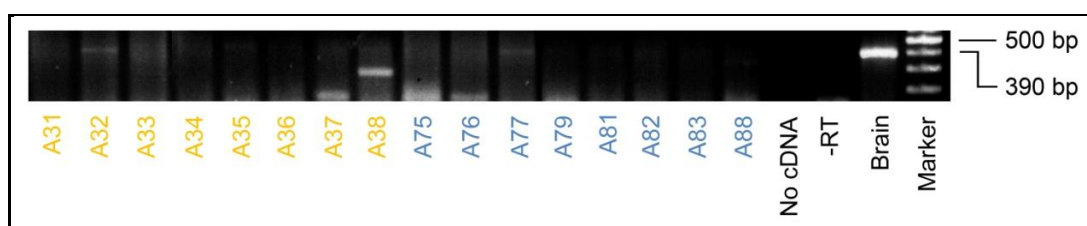


**Figure 37** : MT<sub>2</sub> mRNA expression in aortas from two different time points analyzed by RT-PCR. Expected length of the PCR product was 390 bp. Daytime group (orange): A31–A38; nighttime group (blue): A75–A88.

The bands from the brain sample were excised from the gel and processed for sequencing according to 5.4.2.

### 5.4.2 Sequencing of the MT<sub>2</sub> PCR product from the brain sample

The DNA from the gel slices was extracted and purified according to the described procedure (see 4.8). Concentration measurement of the eluated DNA by photometry (see 4.3) revealed a concentration of 5.2 ng /  $\mu$ L. 5  $\mu$ L of the eluate were analyzed using GE to determine the extracted DNA's purity. Only a singular band at the expected length of 390 bp was visible (not shown). The eluate was then sent to MWG Eurofins Operon (Ebersberg, Germany) for sequencing (see 4.9) together with aliquots containing 30 pmol of each primer (rat\_MT<sub>2</sub>\_fwd and rat\_MT<sub>2</sub>\_rev, see 4.6.3).

MT2	60	GGAGCGCCCCAAGCAGTGCACACCTTGCGCATCTATCCCGGGCTGCAGCGTCACCATGC	119
fwd	1	TAT-CCGGGCTGCAGCGTCACCATGC	25
rev	349	GGAGCGCCCCAAGCAGTGCACACCTTGCGCATCTATCCCGGGCTGCAGCGTCACCATGC	290
MT2	120	CTGACAACAGCTCCATCGCCAACTGCTGTGCGGCCAGCGGGCTGGCAGCGCGCCCTAGTT	179
fwd	26	CTGACAACAGCTCCATCGCCAACTGCTGTGCGGCCAGCGGGCTGGCAGCGCGCCCTAGTT	85
rev	289	CTGACAACAGCTCCATCGCCAACTGCTGTGCGGCCAGCGGGCTGGCAGCGCGCCCTAGTT	230
MT2	180	GGCCCGGGTCAGCGGAGGCGGAGCCCCCTGAGACTCCCCGGGCACCCTGGGTGGCTCCCA	239
fwd	86	GGCCCGGGTCAGCGGAGGCGGAGCCCCCTGAGACTCCCCGGGCACCCTGGGTGGCTCCCA	145
rev	229	GGCCCGGGTCAGCGGAGGCGGAGCCCCCTGAGACTCCCCGGGCACCCTGGGTGGCTCCCA	170
MT2	240	TGCTATCTACAGTAGTCATTGTACCACAGCTGTGGACTTCGTGGGGAACCTGCTTGTGA	299
fwd	146	TGCTATCTACAGTAGTCATTGTACCACAGCTGTGGACTTCGTGGGGAACCTGCTTGTGA	205
rev	169	TGCTATCTACAGTAGTCATTGTACCACAGCTGTGGACTTCGTGGGGAACCTGCTTGTGA	110
MT2	300	TCCTCTCGGTGCTCAGGAACCGCAAGCTGCGGAACGCAGGTAATTTATTTGTGGTGAATC	359
fwd	206	TCCTCTCGGTGCTCAGGAACCGCAAGCTGCGGAACGCAGGTAATTTATTTGTGGTGAATC	265
rev	109	TCCTCTCGGTGCTCAGGAACCGCAAGCTGCGGAACGCAGGTAATTTATTTGTGGTGAATC	50
MT2	360	TGGCCTTGGCTGACCTGGTGGTAGCCCTGTACCCTTACCCACTCATCCTTGTGGCCATTC	419
fwd	266	TGGCCTTGGCTGACCTGGTGGTAGCCCTGTACCCTTACCCACTCATCCTTGTGGCCATTC	325
rev	49	TGGCCTTGGCTGACCTGGTGGTAGCCCTGTACCCT-ACCCACTCATCCT	2
MT2	420	TCCATGACGGTTGGGTACTTGGGGAGATCCA	450
fwd	326	TCCATGACGGTTGGGTACTTGGGGAGATCCA	356

**Figure 38:** Comparison of the sequencing results from the MT<sub>2</sub> RT-PCR products of the brain sample and the published sequence for MT<sub>2</sub> mRNA ([26], RefSeq: NM\_001100641.1). Combined length of the sequencing results of both primers: 390 bp. E-values: fwd = 0.0, rev = 0.0; fwd: rat\_MT2\_fwd; rev: rat\_MT2\_rev.

Sequencing worked well and comparison with the published sequence for the rat MT<sub>2</sub> mRNA ([26], RefSeq: NM\_001100641.1) showed 99 % identity over a length of 390 bp (expected: 390 bp). This result confirmed the identity of the observed amplicons in the brain sample as MT<sub>2</sub> and proved that the PCR method by Ishii et al. (2009) worked to detect MT<sub>2</sub> mRNA.

#### 5.4.3 Search for and selection of alternative PCR protocols

Because of the unsatisfactory results with the Ishii primers with regard to MT<sub>2</sub> in the aorta (sequencing proved its efficacy for the brain sample; 5.4.2), a search in the literature for other primers for rat MT<sub>2</sub> was performed. The published sequence of MT<sub>2</sub> ([26], RefSeq: NM\_001100641.1) was used to compare the positions of the varying primer pairs. See Table 32 for the results of the search.

**Table 32:** Primer pairs for rat MT<sub>2</sub> available in the literature. The primers published in the respective papers are highlighted in the same way as the corresponding sequence in the drawing of the sequence further below. For the reverse primers, the corresponding reverse complements are denoted in brackets.



Source		Sequence	Product	Notes
Ishii et al. [26]	fwd.	5' -GGAGCGCCCCAAGCAGTG-3'	316 bp	
	rev.	5' -GGATCTCCCCAAGTACCCAACCGTCAT-3' (ATGACGGTTGGGTAAGTTGGGGAGATCC)		
Sallinen et al. [35]	fwd.	5' -ATGTTTCGCAGTGTGTTGTGGTTTT-3'	65 bp	for qPCR, equiv. to [159] and [160]
	rev.	5' -ACTGCAAGGCCAATACAGTTGA-3' (TCAACTGTATTGGCCTTCGAGT)		
Sugden et al. [34]	fwd.	5' -ATCTGTACAGTGCAGCTACC-3'	292 bp	"outer" primers of a nested PCR
	rev.	5' -TTCTCTCAGCCTTTGCCTTC-3' (GAAGGCAAAGGCTGAGAGAA)		
Sugden et al. [34]	fwd.	5' -AGCCTCATCTGGCTTCTCAC-3'	154 bp	"inner" primers of a nested PCR
	rev.	5' -TTGGAAGGAGGAAGTGGATG-3' (CATCCACTTCCCTCCTTCCAA)		
Masana et al. [36]	fwd.	5' -CCCTCTACATCAGCCTCA-3'	264 bp	
	rev.	5' -CACTGGGTCTCAGGCGTA-3' (TACGCTGAGACCCAGTG)		

```

CCTCTTGGTCCCTCCACAGCCTCTTCTTAGCACTTGTGGGCGGGAGGGGACAGCGGGAGCGCCCCAAGCAGTG
CACACCTTGCATCTATCCCGGCTGCAGCGTCACCATGCCTGACAACAGCTCCATCGCAACTGCTGTGCGGCCAG
CGGGCTGGCAGCGCCCTAGTTGGCCCGGTCAGCGGAGGCGGAGCCCCCTGAGACTCCCCGGCACCCCTGGGTGGC
TCCCATGCTATCTACAGTAGTCATTGTACCACAGCTGTGGACTTCGTGGGGAACCTGCTTGTGATCCTCTCGGTGCT
CAGGAACCGCAAGCTGCGGAACGCAAGTAATTTATTTGTGGTGAATCTGGCCTTGGCTGACCTGGTGGTAGCCCTGTA
CCCTTACCCACTCATCCTTGTGGCCATTCTCCATGACGGTTGGGTAAGTTGGGGAGATCCACTGTAAGGCCAGTGCCTT
TGTGATGGGCTGAGTGTCAATGGCTCTGTCTTCAACATCACAGCCATTGCCATCAACCGCTACTGGTGCATCTGTCA
CAGTGCAGCTACCACCGAGCCTGCAGTCAGTGGCATGCTCCCTCTACATCAGCCTCATCTGGCTTCTCACTCTGGT
GGCCTTGGTGCCAATTTCTTGTGGGTCTCTAGAATATGACCCGGAATCTATTCTGCACCTCATCCAGACAGC
CAGCACCAATACACTATGGCTGTGGTGGCATCCACTTCCCTCCTCCAAATTGCTGTGGTGTCCCTTTTGTCTACCTGCC
AATATGGATACTGGTGTCCAGGCCGAAGGAAGGCAAAGGCTGAGAGAAAGCTACGCTGAGACCCAGTGCACCTGCC
CAGTTTCTAACCCTGGTGGAGTGTGGTGGTTCGCCATATGTGGGCCCCCTCAACTGTATTGGCTTGGAGT
GGCCATCAATCCAGAGGCAATGGCTCTTCAGATCCAGAAAGGGCTTTTGTACCAGTTACTTCCCTAGCTTACTTCAA
CAGCTGCCTTAATGCTATTGTTTATGGGCTTCTGAACCAGAACTCCCGAGGGAGTACAAGAGGATCCTCTCGGCCCT
CTGGAGCACTGGGCGCTGCTTCCATGATGCTTCCAAATGCCACCTGACTGAGGATTTGCAGGGCCAGTGCACCTGC
TGCCATGGCCACCATACCTGTCCAGGAAGGTGCTCTAGCCTGCATCAGCTCGTGGACCTAGCAGCAAACCTGTGAA
ATGAGCAGAACGGAATTGCTGTCAAGTGTGTTCAATTACTTGTCTCACACTGCAGCCACAACCTGGTGAACCTCAAGTGA
CCACAGGGACAAACCTGCAGACACTCCTAATGGCAAACCTGGGCACTGGATTCCAATTGGCTGGGACAGAACTCAAGCT
GTACTCATAAGATGTCATTTTCCCTGCCACCTTGACCTGTTACTGAATGTTGCCTCTTCCCTGAAGGGCCAGGGGAAA
AAGATCTCTTGATTACCTGAGCCGAAAGATCAAATCTGCAGTGTGAAGTGAGACTTCGTTCCATATGGAAGGAGAAG
TAACCTACATCTACACTCATCGAACAGCCACTGTAACCCAGAAATCGCAGTTCTGAGAGTTCAGCAATAAGATCGAAG
TCAAGATCTCACTGACTTACGTGCACTCCCATGTCTGTGATGATACTGCTCAAATGGCCAGATGTGAAAACATCTG
TTGTATTCAAATGTTCTGATACCCTTGGCACTTAGATGAATTTCAAGTGTGGTCCATTCTTAGCATTTTGGGTAA
AATGCTGTGGGTCAAAGTGGCTGCTTGATTTCAGTCCAACAAAAGTGTGATACTCCAACCCCC

```

**Figure 39:** Sequence of rat *MT<sub>2</sub>*, showing the position of various primer pairs. Exon 1 is printed in blue, exon 2 is printed in bordeaux, exon 3 is printed in dark green. See Table 32 for highlight color mapping. The underlined portion is part of two overlapping primers (Sequence: modified after [26], NM\_001100641.1).

Except for the primers designed by Ishii et al. [26], all primer pairs are located exclusively in exon 2 (see Figure 39). This is problematic because not only reversely transcribed mRNA, but also traces of genomic DNA in the samples will be amplified in the course of the PCR. However, two primer pairs (outer and inner) used by Sugden et al. [34] were selected for further investigation of *MT<sub>2</sub>* mRNA expression, because a

nested PCR provides a method of amplifying very weak products with high specificity (see 4.6.1).

#### 5.4.4 RT-PCR for $MT_2$ mRNA expression according to the Sugden-protocol

A PCR experiment using the selected primers from Sugden et al. [34] was set up. To conserve cDNA of the aorta samples, the cDNA from the various rat organs (see 5.1.2) was used to test the new primers. 400 ng of cDNA (RNA equivalent) per sample or water (no cDNA) were subjected to PCR. A -RT sample (intestine) was included as well. See 4.6.2 for the general protocol and 4.6.3 for experiment specific conditions.

Unfortunately, all samples exhibited strong bands at the expected length of 292 bp. In addition to other bands of varying lengths appearing in many samples, the -RT sample exhibited a band of similar strength as did the rest of the samples at the expected length (Figure 40). This proved that the intra-exon primers from Sugden et al. [34] amplified traces of genomic DNA left after the RNA extraction procedure. Also, when compared with the results gained by usage of the method and primers by Ishii et al. [26] (see 5.4.1), the ubiquitous presence of very strong bands, with almost no difference between the samples, seemed rather improbable.

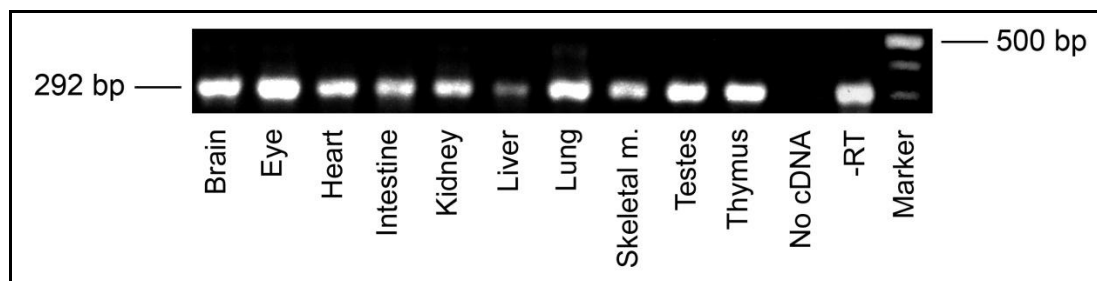


**Figure 40:**  $MT_2$  mRNA expression in various rat organs analyzed by RT-PCR according to Sugden et al. [34]. Expected length of the PCR product was 390 bp.

The nested PCR was performed nevertheless with 1  $\mu$ L PCR product from the outer PCR to test the primers for function. It produced bands of high intensity in all samples at the expected length of 154 bp (not shown).

To address the problem of genomic contamination in the extracted RNA, DNase treatment was performed according to the described method (see 4.7). DNase digestion should degrade DNA contaminations in the samples of extracted RNA, leaving the RNA intact. After the procedure was completed, the RNA was reversely transcribed following the described method (see 4.5). After DNase treatment, amplification using the intra-exon Sugden primers would be expected to happen only in

samples containing cDNA (and not genomic DNA) for MT<sub>2</sub>, thus providing evidence for MT<sub>2</sub> receptor expression in the respective samples. -RT samples of all DNase treated RNA samples were prepared as well to check if DNase treatment was successful.

The method was used on RNA samples of brain and eye from the various rat organs gained in 5.1.1., and aliquots of the aorta samples from two different time points (see 5.2) with the highest particular total amount of isolated RNA (A35, A36, A37, A81, A83 and A88).

Intactness of the cDNA after reverse transcription was checked via a PCR for  $\beta$ -actin according to the established method (see 5.1.2) and proved that the RT worked and DNase treatment did not result in RNA degradation, as correct amplification occurred in all samples (data not shown).

The following PCR experiments for MT<sub>2</sub> in the eye and liver according to the method after Sugden et al. [34] indicated, however, that some of the reaction components were contaminated, because amplification occurred also in the negative controls with no cDNA (data not shown). After a series of experiments (data not shown), the outer primers of the nested PCR were identified as the source of the contamination. Therefore, only the inner primers were used for the following PCR for MT<sub>2</sub> mRNA expression in the rat aortas.

In this experiment, six DNase treated aorta samples from the aortas of two different time points were used in a PCR experiment with the inner Sugden primers only. The experiment was immediately done with the more “valuable” aorta samples instead of the samples from the rat organs, to minimize the risk of another contamination. The cycles for this inner PCR had to be changed from 20 to 40 to account for the reduced amount of template (because of the lack of a preceding outer PCR). A positive control sample (eye), as well as -RT samples of all investigated samples were included in the reaction setup. 400 ng cDNA or water (no cDNA) were subjected to the PCR reaction. See 4.6.2 for the general protocol and 4.6.3 for experiment specific conditions.

The reaction went well and distinctive bands of the expected length of 154 bp were visible in all samples. The blind sample showed no bands, indicating that no contamination had occurred. However, all -RT controls still exhibited bands of 154 bp length as well, albeit of smaller intensity than their respective +RT counterpart (see Figure 41). Also, the bands from the aorta samples were as strong as the band from the eye sample, which seemed rather unlikely after the results for MT<sub>1</sub> (see 5.3.1).

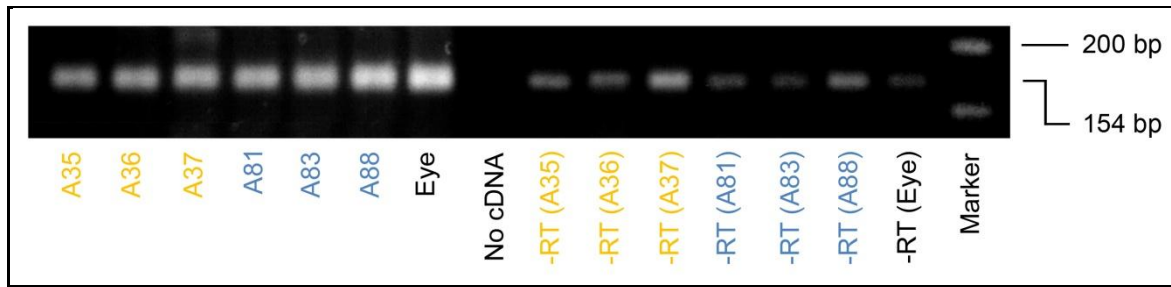


**Figure 41:**  $MT_2$  mRNA expression in rat aortas from two different time points and rat eye as positive control analyzed by RT-PCR according to Sugden et al. [34] using the protocol for the inner PCR only. Expected length of the PCR product was 154 bp. Daytime group (orange): A35–A37; nighttime group (blue): A81–A88.

These results suggest that DNase treatment does not work efficiently enough for total degradation of genomic DNA in the samples. Therefore, no further experiments were conducted using this method.

#### 5.4.5 Design of new exon spanning primers for $MT_2$

Based on the described results, new sets of exon spanning primers were designed following standard guidelines for primer design [161] using the primer design software tool of the National Center for Biotechnology Information [162]. The published sequence of  $MT_2$  ([26], RefSeq: NM\_001100641.1) was used to compare the positions of the varying primer pairs (see Figure 42). From a wide selection of possible candidates (not shown), the primer pairs MS1\_rMT2 and MS2\_rMT2 (see 4.6.3 and Table 33) were chosen and custom-synthesized by MWG Eurofins Operon (Ebersberg, Germany).

**Table 33:** Self-designed primer pairs for rat  $MT_2$  (MS1\_rMT2 and MS2\_rMT2) and the Ishii primers for comparison (rat\_MT2). MS1\_rMT2 rev. and MS2\_rMT2 rev. are identical. The primers are highlighted in the same way as the corresponding sequence in the schematic of the sequence (Figure 42). For the reverse primers, the corresponding reverse complements are denoted in brackets.

Name		Sequence	Tm [° C]	Product
rat_MT2	fwd	5' -GGAGCGCCCCAAGCAGTG-3'	65.3	390 bp
	rev	5' -GGATCTCCCAAGTACCCAACCGTCAT-3' (ATGACGGTTGGGTACTTGGGGAGATCC)	68.0	
MS1_rMT2	fwd	5' -TAGCACTTGCTGGGCGGGGA-3'	60.1	540 bp
	rev	5' -AGGCTCGGTGGTAGGTCGCA-3' (TGCGACCTACCACCGAGCCT)	59.7	
MS2_rMT2	fwd	5' -GCGCATCTATCCCGGGCTGC-3'	60.3	483 bp
	rev	5' -AGGCTCGGTGGTAGGTCGCA-3' (TGCGACCTACCACCGAGCCT)	59.6	

```

CCTCTTGGTCCCTCCACAGCCTCTTCTTAGCACTTGGTGGGGGGGGGGGGGGGACAGCGGGAGCGCCCCCAAGCAGTG
CACACCTTGGCATCTATCCCGGGCTGCAGCGTACCATGCCTGACAACAGCTCCATCGCCAACCTGCTGTGCGGCCAG
CGGGCTGGCAGCGCGCCCTAGTTGGCCCGGGTACAGCGGAGGCGGAGCCCCCTGAGACTCCCCGGGCACCCTGGGTGGC
TCCCATGCTATCTACAGTAGTCATTGTCCACACAGCTGTGGACTTCGTGGGAACCTGCTTGTGATCCTCTCGGTGCT
CAGGAACCGCAAGCTGCGGAACGCAAGTAATTTTGTGGTGAATCTGGCCTTGGCTGACCTGGTGGTAGCCCTGTA
CCCTTACCACTCATCCTTGTGGCCATTCTCCATGACGGTTGGGTAAGTGGGGAGATCCACTGTAAGGCCAGTGCCTT
TGTGATGGCCCTGAGTGTTCATTGGCTCTGTCTTCAACATCACAGCCATTGCCATCAACCGCTACTGGTGCATCTGTCA
CAGGCAGTGCAGTGGCATGCTCCCCTTACATCAGCCTCATCTGGCTTCTCACTCTGGT
GGCCTTGGTGGCCAATTTCTTTTGGGGTCTCTAGAATATGACCCGCGAATCTATCCTGCACCTTCATCCAGACAGC
CAGCACCCAATACTACTATGGCTGTGGTGGCCATCCACTTCTCTTCCAATTGCTGTGGTGTCTTTTGTACTCTGGC
AATATGGATACTGGTGTCCAGGCCGAAGGAAGGCAAGGCTGAGAGAAAGCTACGCTGAGACCCAGTGCCTGGC
CAGTTTCCTAACCATGTTTCGAGTGTGGTGGTTTCGCCATATGCTGGGCCCCCTCAACTGTATGGCCTTGCAGT
GGCCATCAATCCAGAGGCAATGGCTCTTTCAGATCCAGAAAGGGCTTTTGTACCAGTTACTTCTAGCTTACTTCAA
CAGCTGCCTTAATGCTATTGTTTATGGGCTTCTGAACCAGAACTTCCGAGGGAGTACAAGAGGATCTCTCGGCCCT
CTGGAGCACTGGGCGCTGCTTCCATGATGCTTCCAATGCCACCTGACTGAGGATTTGCAGGGCCAGTGCACCTGC
TGCCATGGCCACCATACTGTCCAGGAAGGTGCTCTTAGCCTGCATCAGCTCGTGGACCTAGCAGCAAACCTGTGAA
ATGAGCAGAACGGAATTGCTGTGAGTGTCTCAATTAAGTGTCTCAGCTGCAGCCACAACCTGGTGAAGTCAAGTGA
CCACAGGGACAAAACCTGCAGACACTCCTAATGGCAAACCTGGGCACTGGATTCCAATTGGCTGGGACAGAAGTCAAGT
GTACTCATAAGATGTCATTTTCCCTGCCACCTTGACCTGTTACTGAATGTTGCCTTCTTGAAGGGCCAGGGGAAA
AAGATCTCTTGATTACCTGAGCCGAAAGATCAAAATCTGCAGTGTGAAGTGAAGTTCGTTTCTATGGAAGGAGAAG
TAACCTACATCTACTCATCGAACAGCCACTGTAACCCAGAAATCGAGTTCAGAGTTCAGCAATAAGATCGAAG
TCAAGATCTCACTGACTTACGTGCACTCCCATGCTGTGATGATACTGCTCAAAATGGCCAGATGTGAAAACATCTG
TTGTATTCAAATGTTCTGATACCCTTGGCACTTAGATGAATTTCAAGTGTGGTTCATTTCTTAGCATTTTGGGTAA
AATGCTGTGGGTCAAAGTGGCTGCTTGAATTCAGTCCAACAAAAGTGTGATACTCCAACCC

```

**Figure 42:** Sequence of rat  $MT_2$ , showing the position of the self-designed primer pairs and the Ishii primers (see Table 33 for highlight color mapping). Exon 1 is printed in blue, exon 2 is printed in bordeaux, exon 3 is printed in dark green. (Sequence: modified after [26], NM\_001100641.1).

The mastermix recipe and temperature program for the primers' respective PCR procedures was designed according to the described method (0).

These particular two primer pairs were selected because they allow combination with the Ishii primers, if necessary, or the execution of a nested PCR, using the Ishii primers as inner primers, when using MS1\_rMT2 as outer primers. Also, because the melting temperatures of these three primer pairs are relatively similar, PCR experiments using all three primer pairs could be conducted in one batch.

#### 5.4.6 RT-PCR for $MT_2$ mRNA expression with the newly designed primers

##### Assessment of primer functionality and effectiveness

Three simultaneous PCRs were carried out on the confirmed  $MT_2$  expressing brain sample (see 5.4.2) from the various rat organs (see 4.1.1) to assess the effectiveness of the new primers by comparing their respective band intensities with those derived from the Ishii primers. The experiments were performed in one batch. All the PCRs worked and produced single, defined bands at the respective expected lengths for  $MT_2$ . The band for the MS2\_rMT2 primer was extremely weak, whereas the bands for the Ishii and MS1\_rMT2 primers were about equal in intensity (data not shown). Therefore, the primer pair MS1\_rMT2 was used for the next experiment on the aorta samples.

### **RT-PCR for MT<sub>2</sub> mRNA expression in rat aortas from two different time points**

Six samples of the aortas from two different time points (A31, A35, A36, A37, A81, A83 and A88; see 4.1.2) and the positive controls brain and eye (see 4.1.1) were investigated. 400 ng cDNA or water (no cDNA) were subjected to the PCR reaction using the self-designed primers MS1\_rMT2. See 4.6.2 for the general protocol and 4.6.3 for experiment specific conditions.

Singular bands of the expected length of 540 bp were visible in the eye and brain positive controls. In the aorta samples weaker bands at lengths of 500 bp and / or 600 bp, but not at 540 bp were observed (data not shown). The bands of both lengths from the aorta samples and the singular bands of the expected length from the eye and brain samples were excised from the gel and processed for sequencing.

### **Sequencing of alleged MT<sub>2</sub> RT-PCR products**

The excised bands were pooled for a higher DNA yield after extraction: the first pool included the bands from the aorta samples with a length of 600 bp; the second pool included the bands from the aorta samples with a length of 500 bp; the third pool included the bands with a length of 540 bp from the eye and brain positive controls.

The DNA from the gel slices was extracted and purified according to the described procedure (see 4.8). Concentration measurement of the eluated DNAs by photometry (see 4.3) revealed concentrations of 5.9 ng /  $\mu$ L (first pool), 7.0 ng /  $\mu$ L (second pool) and 8.3 ng /  $\mu$ L (third pool). 5  $\mu$ L of the eluates were analyzed using GE to determine the extracted DNA's purity. Only singular bands at the expected length for each pool were visible (not shown). The eluates were then sent to MWG Eurofins Operon (Ebersberg, Germany) for sequencing (see 4.9) together with aliquots containing 30 pmol of each primer (MS1\_rMT2\_fwd and MS1\_rMT2\_rev, see 4.6.3).

Unfortunately, sequencing worked only for pool three (brain and eye samples). Comparison with the published sequence for the rat MT<sub>2</sub> mRNA ([26], RefSeq: NM\_001100641.1) showed 100 % identity over a length of 540 bp (expected: 540 bp). This result confirmed the identity of the observed amplicons from the brain and eye sample as MT<sub>2</sub> and proves that the new method with the self-designed primers is able to amplify MT<sub>2</sub> in rat tissue correctly. However, for pools one and two (all aorta samples), sequencing failed, producing no results.

MT2	29	TTAGCACTTGCTGGGCGGGGAGGGGACAGCGGGAGCGCCCCCAAGCAGTGCACACCTTGC	88
fwd	1	CAGTGCACACCTTGC	15
rev	278	TTAGCACTTGCTGGGCGGGGAGGGGACAGCGGGAGCGCCCCCAAGCAGTGCACACCTTGC	219
MT2	89	GCATCTATCCCGGGCTGCAGCGTCACCATGCCTGACAACAGCTCCATCGCCAACTGCTGT	148
fwd	16	GCATCTATCCCGGGCTGCAGCGTCACCATGCCTGACAACAGCTCCATCGCCAACTGCTGT	75
rev	218	GCATCTATCCCGGGCTGCAGCGTCACCATGCCTGACAACAGCTCCATCGCCAACTGCTGT	159
MT2	149	GCGGCCAGCGGGCTGGCAGCGCGCCCTAGTTGGCCCGGGTCAGCGGAGGCGGAGCCCCCT	208
fwd	76	GCGGCCAGCGGGCTGGCAGCGCGCCCTAGTTGGCCCGGGTCAGCGGAGGCGGAGCCCCCT	135
rev	158	GCGGCCAGCGGGCTGGCAGCGCGCCCTAGTTGGCCCGGGTCAGCGGAGGCGGAGCCCCCT	99
MT2	209	GAGACTCCCCGGGCACCCCTGGGTGGCTCCCATGCTATCTACAGTAGTCATTGTCACCACA	268
fwd	136	GAGACTCCCCGGGCACCCCTGGGTGGCTCCCATGCTATCTACAGTAGTCATTGTCACCACA	195
rev	98	GAGACTCCCCGGGCACCCCTGGGTGGCTCCCATGCTATCTACAGTAGTCATTGTCACCACA	39
MT2	269	GCTGTGGACTTCGTGGGGAACCTGCTTGTGATCCTCTCGGTGCTCAGGAACCGCAAGCTG	328
fwd	196	GCTGTGGACTTCGTGGGGAACCTGCTTGTGATCCTCTCGGTGCTCAGGAACCGCAAGCTG	255
rev	38	GCTGTGGACTTCGTGGGGAACCTGCTTGTGATCCTCTC	1
MT2	329	CGGAACGCAGGTAATTTATTTGTGGTGAATCTGGCCTTGGCTGACCTGGTGGTAGCCCTG	388
fwd	256	CGGAACGCAGGTAATTTATTTGTGGTGAATCTGGCCTTGGCTGACCTGGTGGTAGCCCTG	315
MT2	389	TACCCTTACCCACTCATCCTTGTGGCCATTCTCCATGACGGTTGGGTACTTGGGGAGATC	448
fwd	316	TACCCTTACCCACTCATCCTTGTGGCCATTCTCCATGACGGTTGGGTACTTGGGGAGATC	375
MT2	449	CACTGTAAGGCCAGTGCCTTTGTGATGGGCCCTGAGTGTTCATTGGCTCTGTCTTCAACATC	508
fwd	376	CACTGTAAGGCCAGTGCCTTTGTGATGGGCCCTGAGTGTTCATTGGCTCTGTCTTCAACATC	435
MT2	509	ACAGCCATTGCCATCAACCGCTACTGGTGCATCTGTTCACAGTGGCACCCTACCACCGAGCC	568
fwd	436	ACAGCCATTGCCATCAACCGCTACTGGTGCATCTGTTCACAGTGGCACCCTACCACCGAGCC	495
MT2	569	T	569
fwd	496	T	496

**Figure 43:** Comparison of the sequencing results from pool three (brain and eye) and the published sequence for MT<sub>2</sub> mRNA (RefSeq NM\_001100641.1) Combined length of the sequencing results of both primers: 540 bp; E-values: fwd = 0.0, rev = 7E-150; fwd: MS1\_rMT2 fwd; rev: MS1\_rMT2 rev.

To ensure that a methodical error was not the cause for the failed sequencing of the aorta bands, the experiment was repeated. Similar results as in the experiment above were obtained after RT-PCR and sequencing of the bands from the aorta samples failed again (data not shown).

### **Nested RT-PCR for MT<sub>2</sub> mRNA expression in rat aortas from two different time points**

The previous experiments already indicated that MT<sub>2</sub> mRNA was not expressed in the rat aorta. To confirm this hypothesis, a nested PCR, using the self-designed primers as outer primers and the Ishii primers as inner primers, was performed. The nested PCR should enrich a possibly very faint MT<sub>2</sub> amplicon in the rat aorta samples and show selectively only single bands of the expected product.

Again, 400 ng cDNA (RNA equivalent) of the six samples of the aortas from two different time points (A31, A35, A36, A37, A81, A83 and A88; see 4.1.2) and the positive controls brain and eye (see 4.1.1) were subjected to the outer RT-PCR with

the self-designed primers MS1\_rMT2. See 4.6.2 for the general protocol and 4.6.3 for experiment specific conditions. The two positive controls (brain and eye) were diluted 1:5 and the eye sample was additionally diluted 1:10 to account for the low amount – if any – of  $MT_2$  mRNA expected to be present in the aorta samples. A 1:10 dilution of the brain sample was also prepared but not included in the experiment because of spillage. Analysis of the outer RT-PCR showed again bands at varying lengths and intensities in the aorta samples. In contrast to previous PCR (0), almost all aorta samples (except for A35) exhibit bands at the observed lengths of 600 and 500 bp.

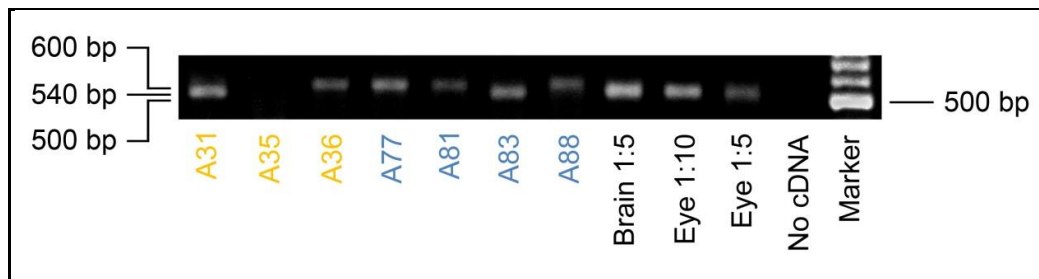


**Figure 44:**  $MT_2$  mRNA expression in rat aortas of two different time points and rat brain and eye as positive controls analyzed by RT-PCR according to the self-designed PCR protocol as outer PCR. Expected length of the PCR product was 540 bp. Daytime group (orange): A35–A37; nighttime group (blue): A81–A88.

The inner PCR was performed with 1  $\mu$ L of the PCR products of the outer PCR used as template according to the method by Ishii et al. [26] modified as described in 5.1.3. See 4.6.2 for the general protocol and 4.6.3 for experiment specific conditions. The number of cycles was reduced from 40 to 20 to accommodate the use of the protocol as an inner PCR.

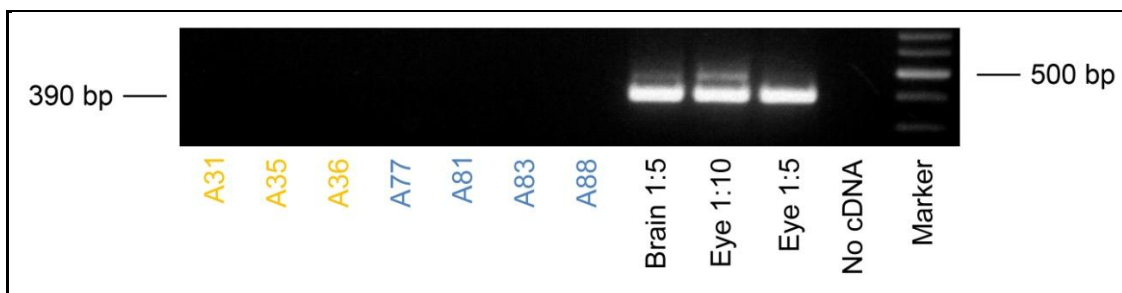


**Figure 45:**  $MT_2$  mRNA expression in rat aortas of two different time points and rat brain and eye as positive controls analyzed by RT-PCR according to the modified method by Ishii et al. [26] as inner PCR. Expected length of the PCR product was 390 bp. Daytime group (orange): A35–A37; nighttime group (blue): A81–A88.



Amplification occurred only in the three positive controls. The bands were very intense and at the expected length of 390 bp. In addition to these bands, a single low intensity band occurred at approximately 500 bp. No bands whatsoever were visible in the aorta samples. The experiment was repeated, yielding the same results (not shown).

From this experiment it was concluded that  $MT_2$  mRNA is not expressed in the rat aorta. Therefore, no further experiments (aortas from SHR and control rats, qPCR, IF) were performed for  $MT_2$ .

## **5.5 Expression analysis of $MT_1$ protein in the rat aorta by IF**

Aortas of control and SHR rats were investigated for  $MT_1$  protein expression using IF experiments. As mentioned above, because of the results from the mRNA level (no  $MT_2$  mRNA is present in the rat aorta), experiments for  $MT_2$  were not performed. For information on antibodies and blocking buffers, see the respective materials and methods sections (4.11.6).

Because of the postulated mechanism of  $MT_1$ 's influence on blood vessels, where  $MT_1$  acts through direct activation of smooth muscle cells, causing vasoconstriction [61], we first established IF localization of the smooth muscle cell marker  $\alpha$ -smooth muscle-actin (SM-actin) and the endothelial cell marker pecam-1 in single and double stainings for use in possible co-localization experiments with  $MT_1$ .

### **5.5.1 Single stainings for SM-actin and pecam-1 protein expression**

The first IF experiments were performed on frozen rat aortas from SHR and control rats (prepared by M. Benova, Department of Pathophysiology, Medical University Vienna, in 2008; see 4.1.4). The aortas were cryo-sectioned according to the described procedure (see 4.11.2).

The aorta sections were stained either for SM-actin or pecam-1 and photographed according to the described procedures (see 4.11.4 and 4.11.7). Negative samples using the secondary ABs only were prepared as well. See chapter 4.11.8, Table 18 and Table 19 for experiment parameters.

Both single stainings worked well, as shown in Figure 46: There was bright staining in the tunica media showing staining for SM-actin. Staining for pecam-1 highlighted only the endothelial cells of the tunica intima, as expected. In both cases, the negative controls showed no fluorescence, indicating that the observed stainings was due to specific binding of the primary ABs only.

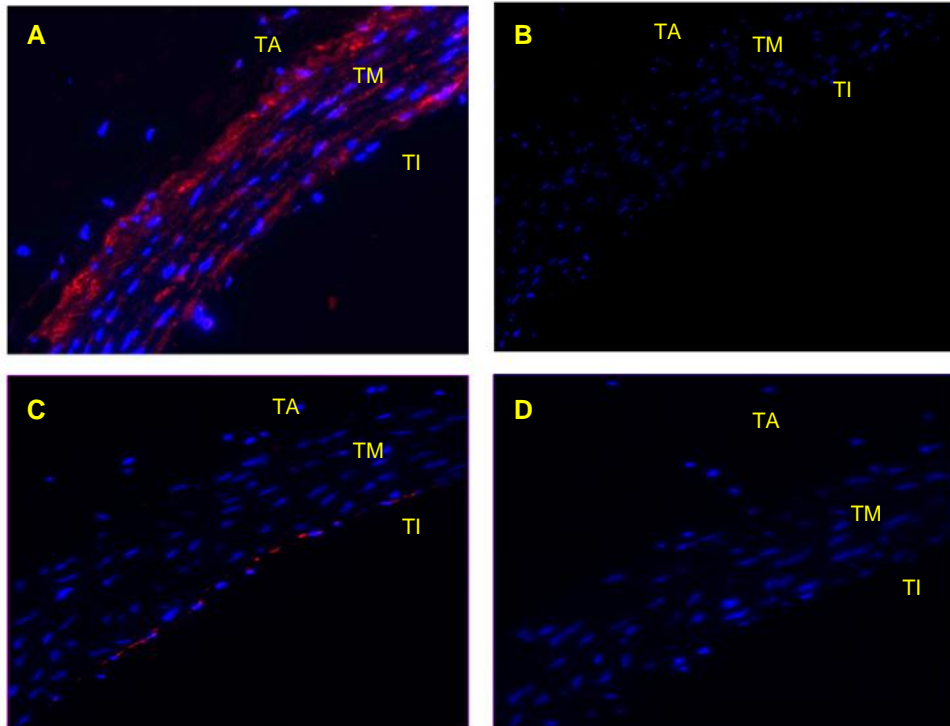


**Figure 46:** IF analysis of SM-actin and pecam-1 protein localization in rat aorta sections. A: SM-actin positive; B: SM-actin negative; C: pecam-1 positive; D: pecam-1 negative; secondary antibody: Alexa Fluor® 568; TA: tunica adventitia; TM: tunica media; TI: tunica intima.

### 5.5.2 Double staining for SM-actin + pecam-1 protein expression

Since the single stainings went well, the same antibodies and samples were used for establishment of double staining protocols.

The aorta sections were stained and photographed according to the described procedures for sequential and parallel double staining (see 4.11.4 and 4.11.7). For the sequential staining, two groups of samples were investigated: in one group the first primary AB was for SM-actin, in the other group the first primary AB was for pecam-1. Because the incubation with the primary AB was done overnight, this setup was chosen to determine if the duration of the incubation (overnight vs 1 h) with either of the two primary antibodies has an effect on the staining. In the parallel experiment, both primary ABs were applied overnight simultaneously. Because both primary antibodies are detected with secondary antibodies gained from goat, the same blocking buffer was used. See chapter 4.11.8, Table 20 for experiment parameters.

Negative samples using the secondary ABs only were prepared, as well as cross negatives, containing a primary antibody and the respective other secondary antibody to exclude false positive detections of the secondary antibodies.

All staining procedures went well, and the antibodies were selective for their respective targets (see Figure 47).

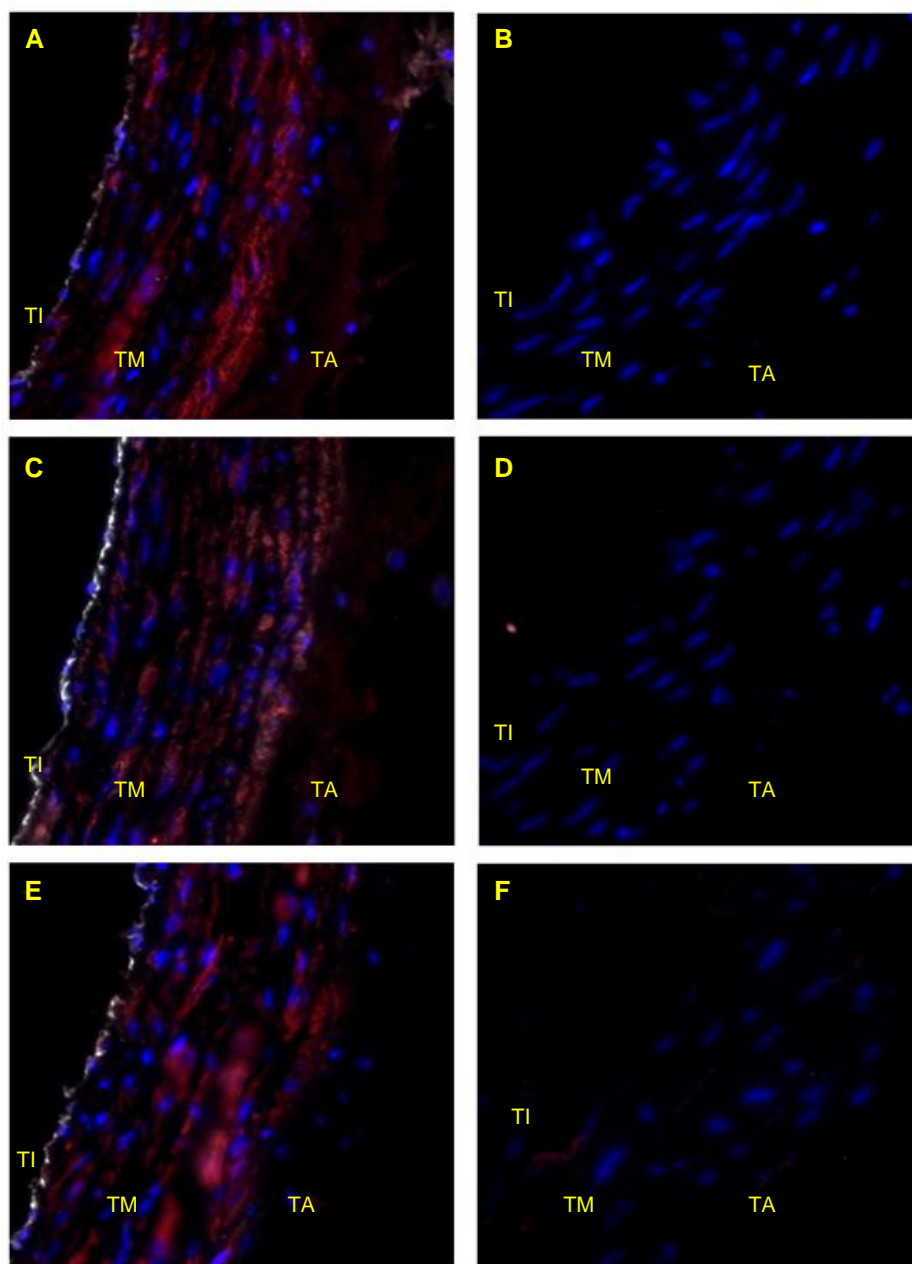


**Figure 47:** IF analysis of double stainings for SM-actin + pecam-1 protein localization in rat aorta sections. A: SM-actin overnight, pecam-1 1h; B: pecam-1 cross negative; C: SM-actin 1h, pecam-1 overnight; positive; D: SM-actin cross negative; E: parallel staining positive; F: parallel staining negative; secondary antibodies: Alexa Fluor® 647 (pecam-1) and Alexa Fluor® 568 (SM-actin) TA: tunica adventitia; TM: tunica media; TI: tunica intima.

There is a striking – yet not unexpected – difference between the three different groups: while the pecam staining was not very strong when the primary AB was only applied for 1 hour, the staining was vibrant when the section was incubated with the AB

overnight. The actin staining was strong even when the AB was only applied for 1 hour. The adventitia exhibited some background fluorescence.

The cross negatives showed that the secondary antibodies are selective for their respective targets. No staining of the “wrong” primary antibody or of the tissue in general occurs. The same was observed in the negatives (not shown).

The parallel staining procedure produced a very nicely stained section, with less staining of the adventitia than in the sequential approaches. Since both primary antibodies were applied overnight (together), the stainings of both types were very vibrant. There was little staining visible in the negative (mostly in the media).

### **5.5.3 Single stainings for MT<sub>1</sub> protein expression on cryo-sections**

The first IF experiment for MT<sub>1</sub> protein expression in the rat aorta was performed on the cryo-sectioned aortas. The aorta sections were stained for MT<sub>1</sub> using the Abbotec 25076 and SC sc-13186 antibodies and were photographed according to the described procedures (see 4.11.4 and 4.11.7). Negative samples using the secondary ABs only were prepared as well. See chapter 4.11.8, Table 21 and Table 22 for experiment parameters.

All stained sections (representatives are shown in Figure 48) showed some background fluorescence, mainly in the elastic lamellae in the tunica media. The staining was brighter with the Abbotec AB (Figure 48, panel A) than with the SC AB (Figure 48, panel C). The negative controls showed no staining. However, it has to be noted that the exposure time was very high (400 ms) for the red channel (for pecam-1 or SM-actin, a brighter and much more defined staining was captured at only 150 ms; see 5.5.1 and 5.5.2); therefore the specificity of these findings was questionable.

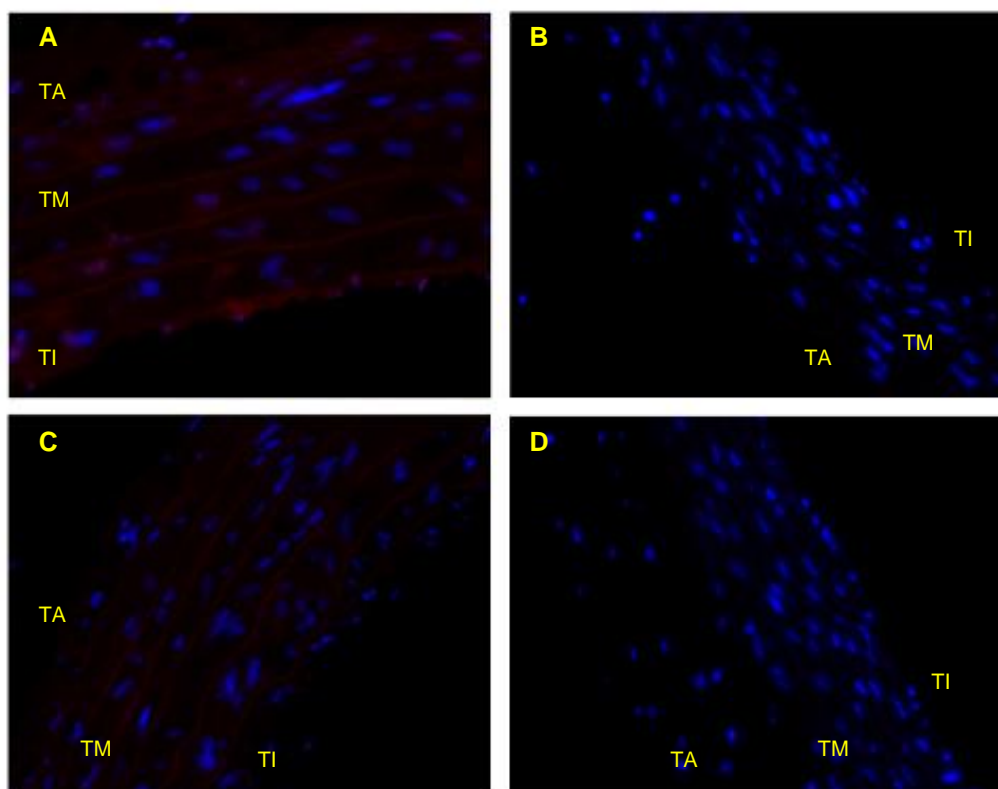


**Figure 48:** IF analysis of stainings for  $MT_1$  protein localization in rat aorta cryo-sections. A: Abbotec positive; B: Abbotec negative; C: SC positive; D: SC negative; secondary antibody: Alexa Fluor® 568; TA: tunica adventitia; TM: tunica media; TI: tunica intima.

Because the staining achieved with the SC AB was especially weak, another experiment, using a different secondary antibody and an additional higher concentration of the primary antibody, was performed. See chapter 4.11.8, Table 23 for experiment parameters.

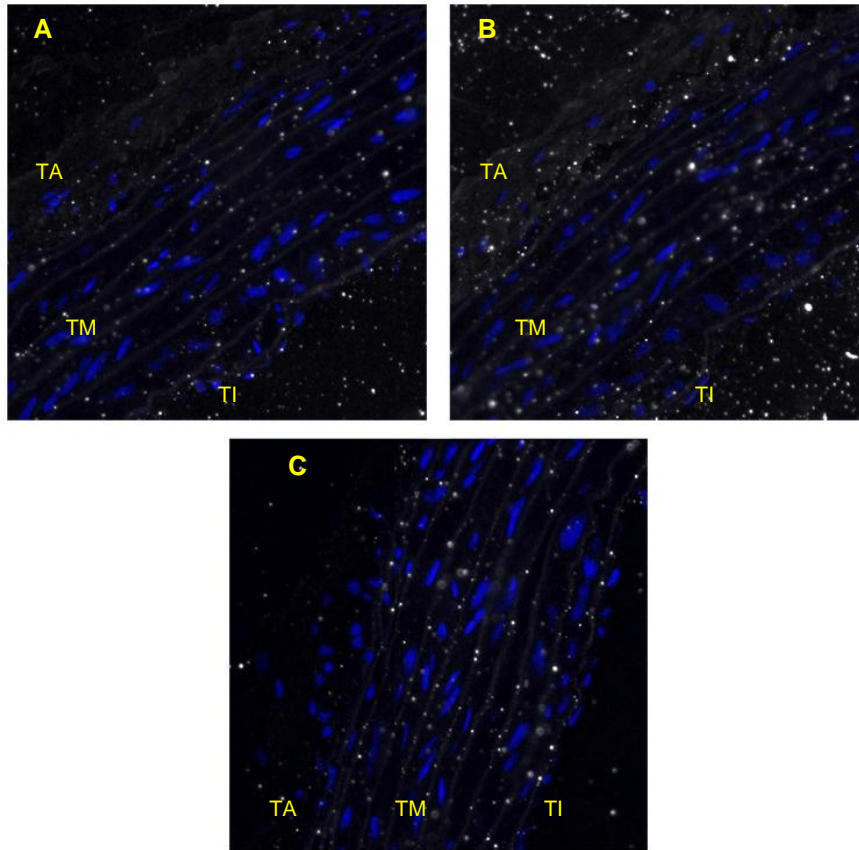


**Figure 49:** IF analysis of stainings for  $MT_1$  protein localization in rat aorta cryo-sections using the SC AB in two different concentrations and Alexa Fluor® 647 as secondary AB. A: SC 1:50; B: SC 1:20; C: SC negative; TA: tunica adventitia; TM: tunica media; TI: tunica intima.

There was some staining visible in the sections (mainly in the tunica adventitia; a representative is shown in Figure 49) and it was a little stronger in the sections stained with the 1:20 diluted antibody (Figure 49, panel B), than with the 1:50 diluted antibody (Figure 49, panel A). Grain-like noise was observed scattered over the tissue, in the positive sections as in the negative sections, but stronger in the positive sections. However, the staining of the adventitia observed in the positive sections is not present in the negative section.

#### 5.5.4 Single stainings for $MT_1$ protein expression on paraffin sections

After the unsatisfactory results from the cryo-sections, the staining for  $MT_1$  was conducted on the paraffin sections. Aorta sections prepared by H. Uhrova (Department of Pathophysiology and Allergy Research, Medical University Vienna; see 4.1.3) were used for the following experiments. Because these aortas are the same ones that were analyzed for  $MT_1$  mRNA expression in 5.3.2, it was already known that the SHR group expressed more mRNA than the control group. Therefore it seemed obvious to conduct

the experiments on the SHR aortas, because the expression (if any) of MT<sub>1</sub> protein in the cryo-sections was extremely low.

In the paraffin section group, positive controls were available: because of the results from the MT<sub>1</sub> mRNA expression experiments in various rat organs (see 5.1.2 and 5.1.3), we knew what organs contained mRNA for MT<sub>1</sub> in rats. Rats were not available at the time, therefore mice were used. All antibodies are selective for proteins from human, rat or mice origin, so the use of mouse organs was not a problem. R. Stumberger, C. Brünner-Kubath and H. Uhrova (all Department of Pathophysiology and Allergy Research, Medical University Vienna) prepared a mouse (*mus musculus*) intestine and brain. H. Uhrova did the HOPE® fixation and paraffin-embedding, as well as the sectioning of these organs.

### **Stainings using the Abbiotec anti MT<sub>1</sub> Antibody**

Sections of mouse brain and intestine were stained together with the aorta sections (SHR aortas) for MT<sub>1</sub> using the Abbiotec 25076 antibody. The aortas were stained in different concentrations of 1:50 and 1:10, while the organs were stained only 1:10. Staining and photography was done according to the described procedures (see 4.11.5 and 4.11.7). Negative samples using the secondary ABs only were prepared as well. See chapter 4.11.8, Table 24 for experiment parameters.

At 1:50 staining was visible in the aortas (a representative is shown in Figure 50) which became much more pronounced at 1:10. It seems that the antibody's target is primarily located in the adventitia and also – but to a lesser extent – in the cells of the media and intima. The negative control exhibited no staining.

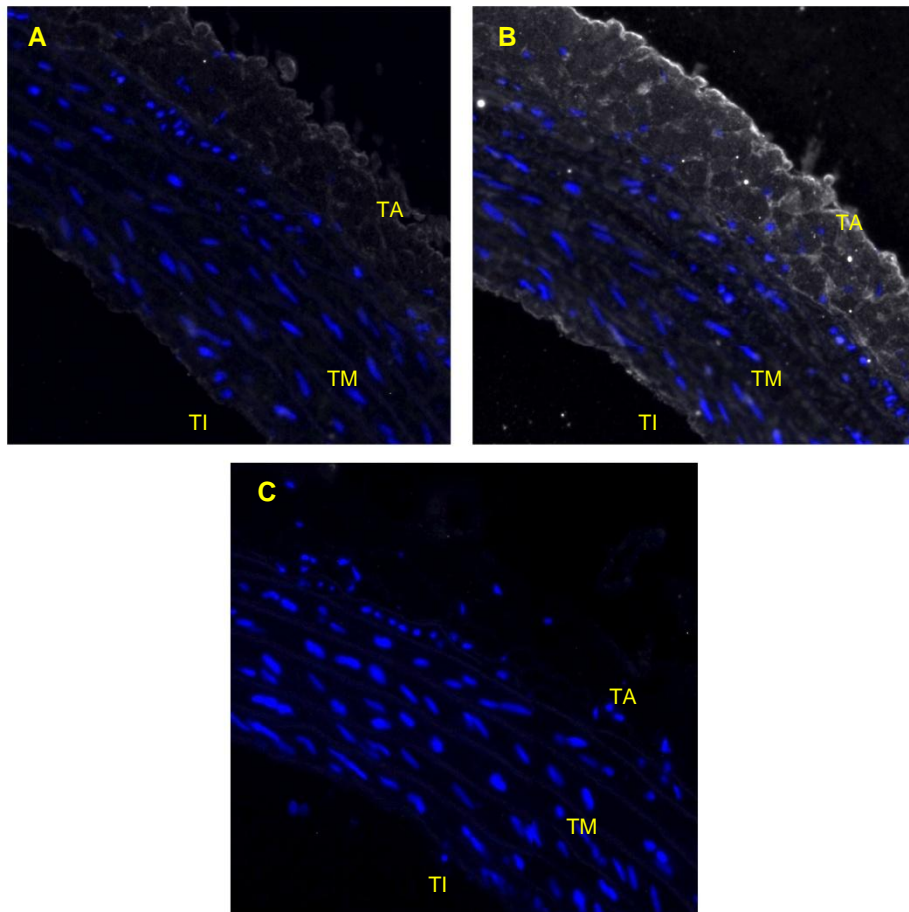


**Figure 50:** IF analysis of stainings for  $MT_1$  localization in rat aorta paraffin sections using the Abbotec AB in two different concentrations and Alexa Fluor® 647 as secondary AB. A: Abbotec 1:50; B: Abbotec 1:10; C: Abbotec negative; TA: tunica adventitia; TM: tunica media; TI: tunica intima.

In the brain, staining with the Abbotec AB produced a marked amount of tissue background fluorescence (in contrast to the negative control; Figure 51) as well as stained fibers in the brain, and nuclei and meninges of the cerebellum (Figure 52, red arrows).



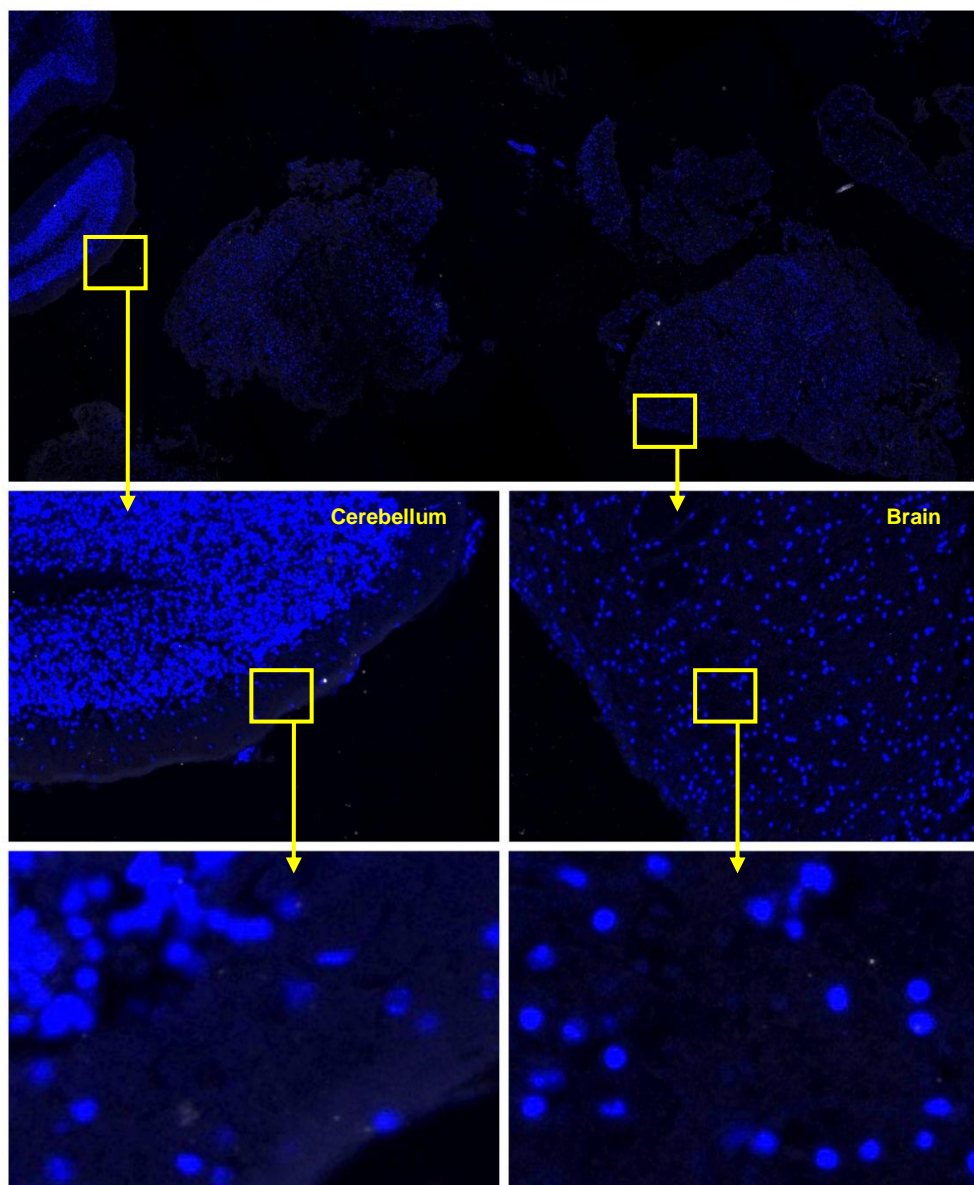


**Figure 51:** IF analysis of the negative control for MT<sub>1</sub> localization in mouse brain paraffin sections, using the Abbotec AB and Alexa Fluor® 647 as secondary AB. The framed parts are magnified. The pictures of the middle panel correspond to 200 x magnification.

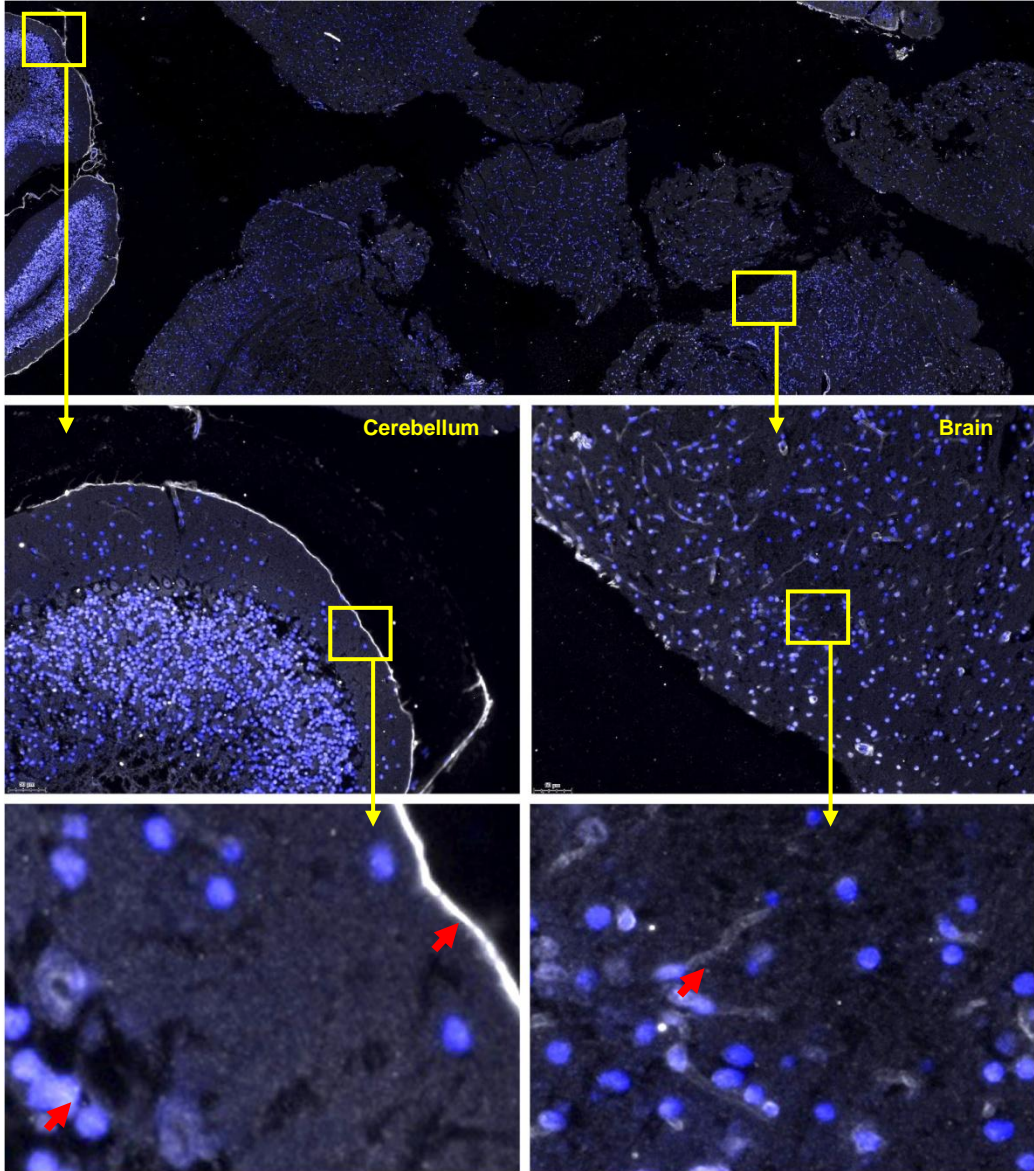


**Figure 52:** IF analysis of staining for MT<sub>1</sub> localization in mouse brain paraffin sections using the Abbotec AB and Alexa Fluor® 647 as secondary AB. The framed parts are magnified. The pictures of the middle panel correspond to 200 x magnification. Red arrows mark areas of interest (see main text).

In the staining of the intestine, the tissue showed extremely high tissue background fluorescence and again staining of the tissue borders. The negative tissue exhibited no fluorescence (see Figure 53).

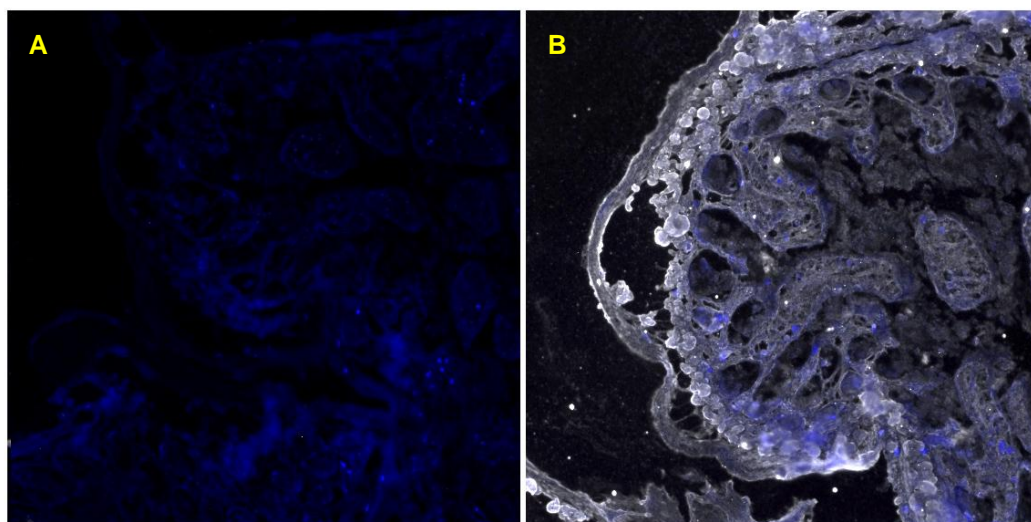


**Figure 53:** IF analysis of staining for  $MT_1$  localization in mouse intestine paraffin sections using the Abbotec AB and Alexa Fluor® 647 as secondary AB. A: Abbotec positive; B: Abbotec negative.

### Stainings using the SC anti $MT_1$ antibody

Sections of both organs were stained with the aorta sections (ASHR 02, ASHR 03 and ASHR 06) for  $MT_1$  using SC sc-13186 antibody. The aortas were stained in different concentrations of 1:50 and 1:20, while the organs were stained only 1:20. Staining and photography was done according to the described procedures (4.11.5 and 4.11.7). Negative samples using the secondary ABs only were prepared as well. See chapter 4.11.8, Table 25 for experiment parameters.

A new batch of antibody was used for this experiment, therefore concentrations of 1:50 and 1:20 (and not 1:10) were used because it was probable that the staining with the new antibody would be stronger than with the old batch.

Like with the Abbiotec AB and the cryo-sections, the (weak) staining found was mainly located in the tunica adventitia (TA). Also, there was a lot of grain-like noise visible in and around the tissue. The staining in the 1:20 (Figure 54, panel B) treated sections was a little bit stronger than in the 1:50 treated ones (Figure 54, panel A).

There was no staining visible in the negatives (Figure 54, panel C). However, some grain-like noise can still be seen scattered over the tissue (similar to the – stronger – pattern in the cryo-sections, see Figure 49).

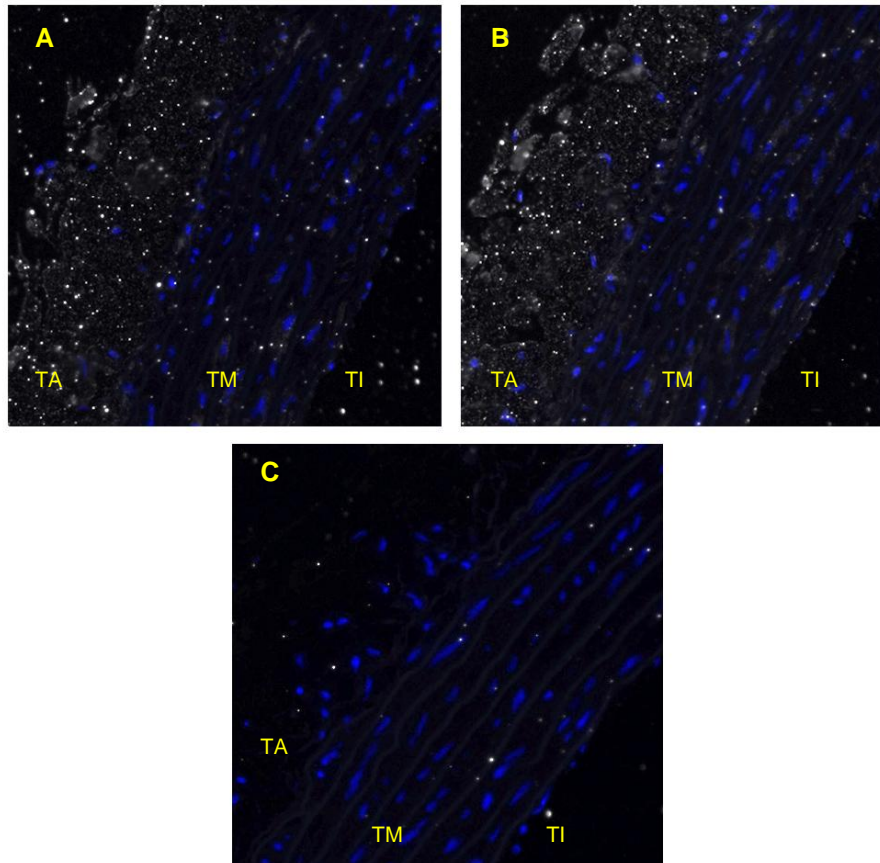


**Figure 54:** IF analysis of stainings for  $MT_1$  localization in rat aorta paraffin sections using the SC AB in two different concentrations and Alexa Fluor® 647 as secondary AB. A: SC 1:50; B: SC 1:20; C: Abbiotec negative; TA: tunica adventitia; TM: tunica media; TI: tunica intima.

A lot of background was visible in the negative control of the brain sample (outer layer of cerebellum; Figure 55).

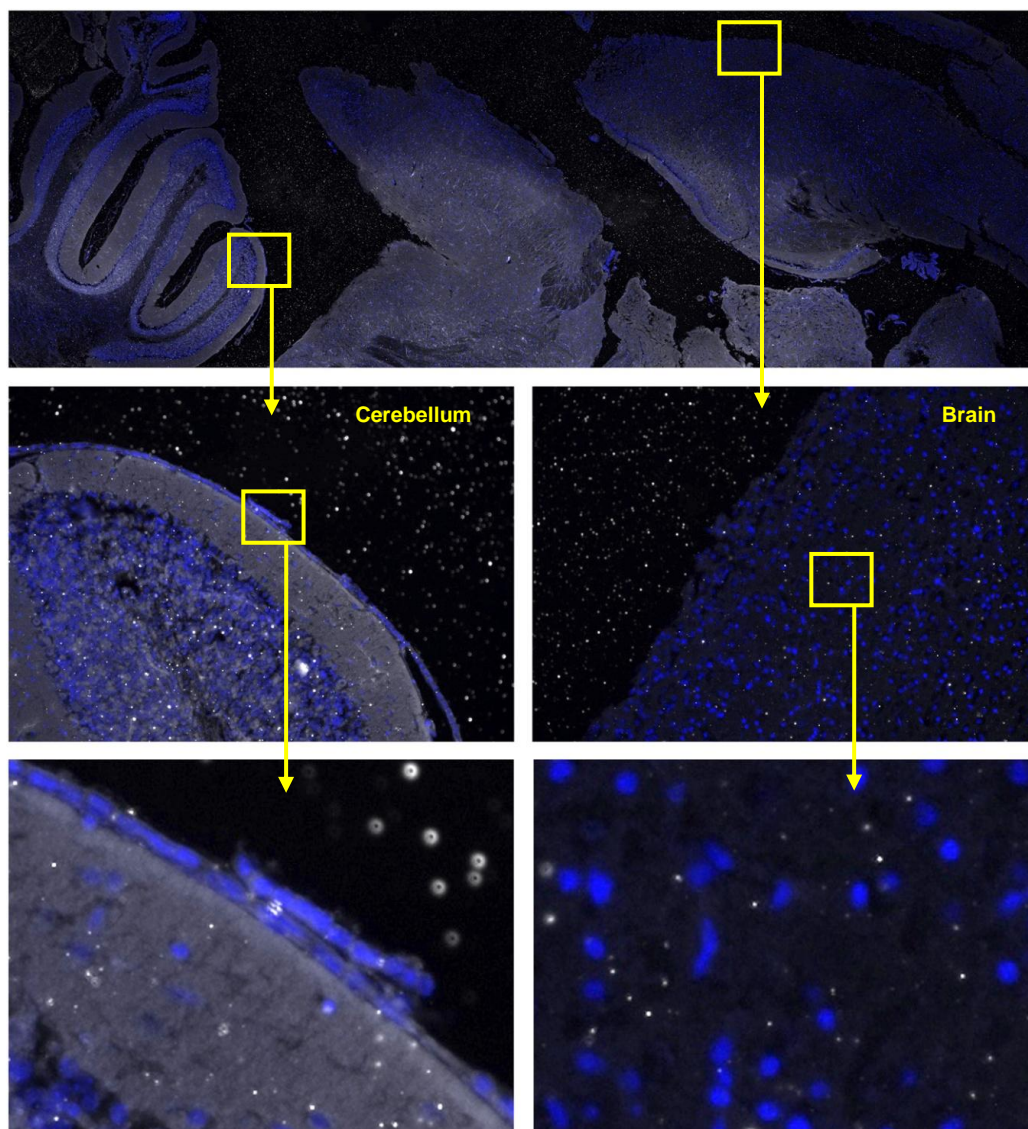


**Figure 55:** IF analysis of the negative control for MT<sub>1</sub> localization in mouse brain paraffin sections, using the SC AB and Alexa Fluor® 647 as secondary AB. The framed parts are magnified. The pictures of the middle panel correspond to 200 x magnification.

Like in the brain sample stained with the Abbotec anti MT<sub>1</sub> AB (Figure 52), fibers in the brain tissue and the meninges of the cerebellum were stained the strongest (Figure 56, red arrows). Like in the aorta samples, there was a lot of grain-like noise on and around the tissue.

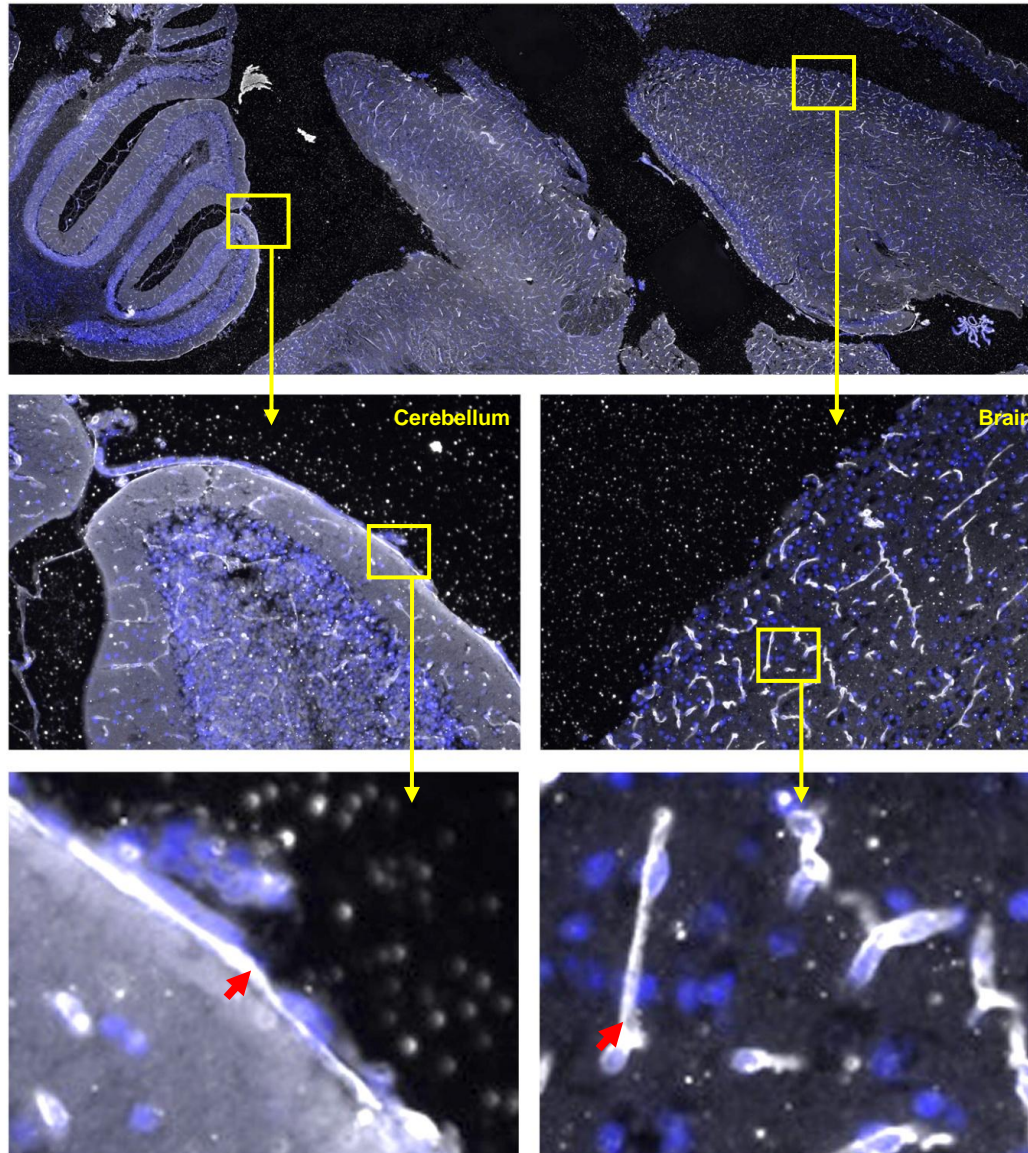


**Figure 56:** IF analysis of staining for MT<sub>1</sub> localization in mouse brain paraffin sections using the SC AB and Alexa Fluor® 647 as secondary AB. The framed parts are magnified. The pictures of the middle panel correspond to 200 x magnification. Red arrows mark areas of interest (see main text).

In contrast to the staining with the Abbotec AB (Figure 53), the stained regions of tissue (Paneth cells?) in the intestine were much more defined and restricted to specific clusters of cells (Figure 58, red arrows). There was no staining in the negative sample. There is also notably less noise than in the other negative samples (Figure 57).

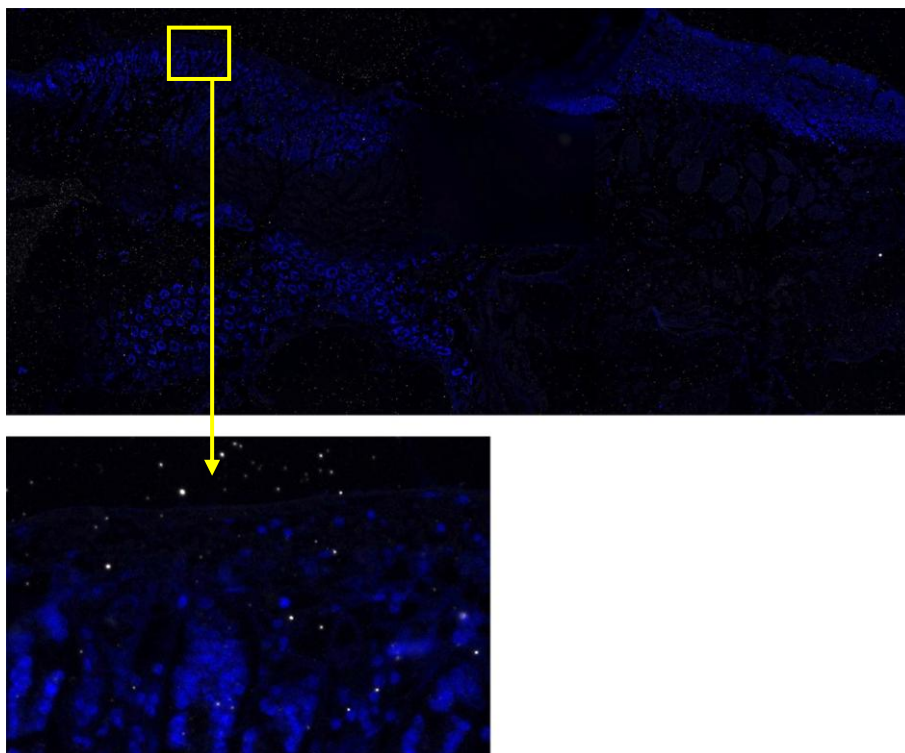


**Figure 57:** IF analysis of the negative control for  $MT_1$  localization in mouse intestine paraffin sections, using the Abbotec AB and Alexa Fluor® 647 as secondary AB. The framed parts are magnified.

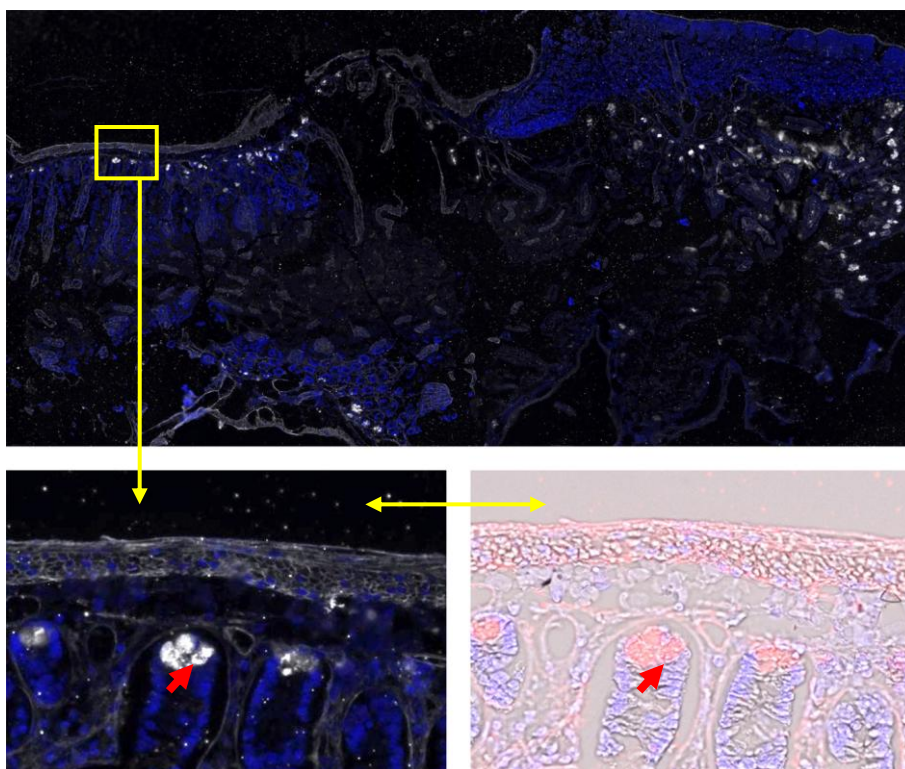


**Figure 58:** IF analysis of staining for  $MT_1$  localization in mouse brain paraffin sections using the SC AB and Alexa Fluor® 647 as secondary AB. The framed parts are magnified. The bottom right picture shows an additional overlay with the respective transmission image. Red arrows mark areas of interest (see main text).

In conclusion, we showed that specific and strong stainings for MT<sub>1</sub> protein expression with the available antibodies from SC and Abbiotec are possible (mouse brain and intestine). In contrast, the stainings observed in the aorta sections, both paraffin as well as cryo-sectioned, were very weak and did not look very specific. The best results were obtained with the Abbiotec antibody on paraffin sections, where a dilution of 1:10 produced a moderate staining for MT<sub>1</sub> in the tunica adventitia. Because of this weak expression in tissue layers other than the expected (tunica adventitia), no co-localization experiments with pecam-1 (for the tunica intima) or SM-actin (for the tunica media) were performed.



## 6 DISCUSSION

The results are discussed according to the order of the aims of the thesis.

### 1) Establishment of molecular biological methods for demonstration of MT<sub>1</sub> and MT<sub>2</sub> mRNA expression

The establishment of the methods for RNA extraction and reverse transcription worked well and provided no difficulty. RT-PCR method establishment for MT<sub>1</sub> worked without problems as well, however, for the MT<sub>1</sub> RT-PCR, the cycles had to be adjusted from 35 to 40 and the template cDNA (RNA equivalent) from 200 to 400 ng compared to the described method by Ishii et al. [26]. This could indicate worse transcription efficiency of our polymerase or reverse transcriptase.

The observed amplifications for MT<sub>1</sub> mRNA in the rat organs are not congruent with the results from Ishii et al. [26], as e.g. testes, liver and kidney, which showed the strongest expression of all organs in [26], only exhibited weak bands for MT<sub>1</sub> in our experiment. These results were confirmed by the qPCR, where the observed  $\Delta$ CT values were for the most part congruent with the band intensities from the qualitative PCR. In our experiment, the intestine, brain and eye showed the highest expression for MT<sub>1</sub>. The expression in these tissues is well established already [35]. A possible explanation of this discrepancy could be variation of expression between different rat strains, or expression dependent on the circadian phase state (at least in some tissues). However, diurnal variations in MT<sub>1</sub> expression have only been reported for humans [129] and not for the rat [108]. Of course it is also possible that the observed differences in melatonin GPCR mRNA expression are the result of interindividual variations, like the ones found for MT<sub>1</sub> mRNA expression in the aorta.

The method for MT<sub>2</sub> RT-PCR experiments had to be changed initially, since the original protocol according to [26] did not produce any results even for tissues where MT<sub>2</sub> occurrence is well established, e.g. brain or eye [6]. In contrast to Ishii et al. [26], who observed MT<sub>2</sub> mRNA expression in most of the investigated tissues (see Figure 6), RT-qPCR analysis showed that MT<sub>2</sub> mRNA was only expressed in 4 out of 10 tissues (the eye sample was not included in the RT-qPCR experiment) and at very low levels. Sallinen et al. [35] also tested various rat organs for MT<sub>2</sub> mRNA and demonstrated expression in the intestine, the liver and the heart, where no amplification was observed in our experiment. Nevertheless, the positive results from brain [26, 163], testes [26], kidney [26, 159] and thymus [159] are confirmed in the literature for the respective rat tissues. The reasons for the observed differences in expression of MT<sub>2</sub> might be the same as for MT<sub>1</sub> expression.

### **2a) Expression of MT<sub>1</sub> mRNA in the rat aorta**

In experiments performed with aortas from the two different time points, MT<sub>1</sub> mRNA expression was confirmed in the rat aorta, which is in line with the findings of other studies on the rat aorta [108] and other rat [36] and human [127, 129] blood vessels. MT<sub>1</sub> mRNA was detected in all samples, though at varying intensities. The identity of the bands was confirmed by sequencing of the PCR product. The absence of a band in one sample and the different intensities in the various samples are interesting because they indicate large interindividual differences in MT<sub>1</sub> receptor expression between the animals. RT-qPCR did indeed confirm these great interindividual differences of MT<sub>1</sub> mRNA expression at the same time of day.

### **2b) Expression of MT<sub>2</sub> mRNA in the rat aorta**

Concerning MT<sub>2</sub> mRNA, different methods were tried to find an expression of its mRNA in the aorta, since various studies reported an expression of MT<sub>2</sub> mRNA in the vascular system of humans [128] and rats alike [35-36], even if the data is – as discussed in the introduction, see 2.6.6 – conflicting.

The only method that yielded amplification of MT<sub>2</sub> in the aorta samples was the nested PCR method from Sugden et al. [34], using inter-exon primers. Unfortunately, the bands for MT<sub>2</sub> persisted even in DNase treated -RT samples and as long as the -RT samples exhibit any bands at all, the results for the normal (+RT) samples are not valid, thus indicating presence of genomic DNA. Additionally, with this method, the observed bands for MT<sub>2</sub> were much stronger than those for MT<sub>1</sub>. Even if a direct comparison is illicit, it seems rather improbable that MT<sub>2</sub> would be so readily detectable when the aorta samples exhibit only weak MT<sub>1</sub> bands, or even, in one case, none at all and MT<sub>1</sub> is usually higher expressed than MT<sub>2</sub> [24].

The results from the nested PCR using the exon spanning self-designed and Ishii primers performed on the rat aortas from two different time points then clearly proved that no mRNA for MT<sub>2</sub> is present in the rat aorta. Our results support the findings of other studies which showed no expression of MT<sub>2</sub> mRNA in rat cerebral arteries [132]. Preparation or methodical error can be excluded because amplification of MT<sub>2</sub> mRNA in the positive controls brain and eye worked and was confirmed by sequencing. Based on the absence of MT<sub>2</sub> mRNA, we did not perform a RT-qPCR or IF staining for MT<sub>2</sub> on any of the aorta samples.

### **3) Quantification of MT<sub>1</sub> mRNA expression difference in the rat aorta depending on the time of day**

Maybe as a result of those large interindividual differences, this experiment showed no significant difference in expression levels of MT<sub>1</sub> mRNA between the two time points.

Therefore, it cannot be concluded that MT<sub>1</sub> mRNA expression in the aorta is related to the time of day, or if it is, the sample size and number of time points in this experiment were far too small and too few to detect it with any significance. This confirms the results of Benova et al. [108], who did not find any difference in MT<sub>1</sub> expression in the rat aorta at the protein level and emphasizes the organ specificity of the circadian rhythms of this receptor, because in other organs, a circadian expression pattern was indeed observed [129, 136].

#### **4) Quantification of MT<sub>1</sub> mRNA expression difference in the rat aorta depending on BP**

In contrast to this result, both RT-PCR and RT-qPCR experiments showed a significant increase (about 4-fold) in MT<sub>1</sub> receptor mRNA in SHR when compared to control rats. This difference proves that there is indeed some kind of link between hypertension and melatonin GPCR expression. However, it seems to occur only in genetically predisposed hypertensive animals, since L-NAME induced hypertension did not increase MT<sub>1</sub> protein expression in the aorta [108]. Then again, even though changes in MT<sub>1</sub> expression levels were observed as a result of the genetic Alzheimer's disease [135], they were also observed as a result of artificially created ischemia [160], putting this hypothesis of genetic influence in perspective. Therefore, other additional mechanisms might account for the observed differences.

Because exogenous melatonin reduces BP in spontaneously hypertensive rats [115], and MT<sub>2</sub>, supposed to have vasodilating effects [61], seems not to be present in the aorta, the BP reducing effects of melatonin might be attributed rather to melatonin's non receptor-mediated antioxidative capability [61] or GABAergic influence on the central nervous system [109] than effects on the vasculature mediated via GPCRs.

#### **5) Localization of MT<sub>1</sub> protein in the rat aorta**

Although expression of MT<sub>1</sub> mRNA was demonstrated in this study for the rat aorta and expression of MT<sub>1</sub> protein by western blotting (Prof. M. Zeman, Comenius University of Bratislava, Slovakia; personal communication; and [108]), the location of MT<sub>1</sub> protein in the various layers of the aorta remains questionable.

The functioning of the staining procedures was confirmed by the stainings for pcam-1 and  $\alpha$ -SM-actin, which worked fine in single as well as sequential and parallel double stainings. These stainings proved that the aorta sections were still antigenic and that the endothelium was intact (positive staining with pcam-1).

When staining for MT<sub>1</sub> however, only very weak cell-associated fluorescence, but high background noise was observed. These grain-like speckles were only observed with the anti-MT<sub>1</sub> AB from SC, using Alexa Fluor® 647 as secondary AB, but not with

the primary anti-MT<sub>1</sub> AB from Abbotec using the same secondary AB, or the SC primary AB with Alexa Fluor® 568 as secondary AB. Therefore, it might be possible that this background was the result of formation of unspecific aggregates of the SC AB with the Alexa Fluor® 647 secondary antibody.

Though the combination of the SC antibody with Alexa Fluor® 568 did not result in background noise, the observed staining was also very weak. It seems likely that it is the result of unspecific adhesion of the primary AB to the tissue, rather than target specific binding. The anti-MT<sub>1</sub> Abbotec antibody generally produced stronger stainings with less background noise. With both antibodies, the staining was stronger in the tunica adventitia than in the other layers of the aorta. This was observed in paraffin sections as well as – to a lesser extent – in cryo-sections. However, this staining pattern was only seen using Alexa Fluor® 647 as secondary antibody. When used with Alexa Fluor® 568, only some extremely faint staining of the tunica media could be seen.

From the proposed vasoconstrictive function of MT<sub>1</sub>, a localization of the receptor in smooth muscle cells was expected. Surprisingly, the only staining for MT<sub>1</sub> in aortas was associated with the tunica adventitia. However, a similar situation has been reported in the literature. Immunohistochemical staining of cerebral vessels from Alzheimer patients showed MT<sub>1</sub> localization only in the adventitia, too [135]. The applied anti-human-MT<sub>1</sub> AB is described as being well characterized. Since no other studies exist that have investigated MT<sub>1</sub> localization in blood vessels, it is possible that MT<sub>1</sub> indeed is only localized in the tunica adventitia.

It has to be noted that paraffin embedding is known to mask antigens and the tissue we used for cryo-sectioning had already been frozen for more than a year. It is possible that the receptor protein, even more so since the expression is very low, had already been degraded and was therefore not detectable any more by IF methods. Furthermore, the reliability of the available antibodies remains somewhat questionable, because other studies indicate that at least a SC AB against human MT<sub>1</sub> is rather unspecific (Ramezani and Ellinger, unpublished data).

Nonetheless, we can exclude procedural error or degraded antibodies, because staining of the positive controls (mouse brain and intestine) worked nicely and produced quite interesting results. To our knowledge, no studies on the localization of MT<sub>1</sub> in the intestine have been performed, and our experiments show highly selective staining of what may be Paneth cells at the bottom of the intestinal villi. In the brain, specific staining of fibers of yet undetermined nature was shown. One might speculate that these fibers are capillaries, which would be of great interest with respect to the aims of this thesis. Both of these occurrences of MT<sub>1</sub> have to be investigated in a later work.

## 7 CONCLUSION AND OUTLOOK

The principal aim of this thesis was to prove the expression of the melatonin GPCRs MT<sub>1</sub> and MT<sub>2</sub> in the rat aorta on mRNA level, thereby helping to understand the mechanism by which melatonin contributes to BP regulation.

We confirmed MT<sub>1</sub> is indeed expressed in the rat aorta. We observed no differences in expression between samples collected at night and samples collected at day, but the sample size (eight from each group) might have been too small for a definitive conclusion. However, an about 4-fold increase in mRNA levels was observed in aortas from SHR compared to control rats, adding to the evidence of melatonin's BP regulating activity. On the other side, we proved that MT<sub>2</sub> mRNA is not expressed in the rat aorta.

Since our results from IF indicate that MT<sub>1</sub> is not expressed in the smooth muscle cells of the tunica media, and MT<sub>2</sub> was shown not to be present in the rat aorta at all, the proposed mechanism of action of melatonin's BP modulating properties [61] might have to be reviewed, even if the increase in mRNA in SHR emphasizes a role of MT<sub>1</sub> in BP regulation.

In future studies, the investigation of a difference in mRNA expression levels of MT<sub>1</sub> could be redone, using a larger population of samples and perhaps more than two time points. Additionally, we discovered very specific localization of MT<sub>1</sub> in the mouse brain and intestine, which has to be investigated further in additional studies.

## 8 LIST OF ABBREVIATIONS

$\Delta\Delta\text{CT}$	Difference between two $\Delta\text{CT}$ values
$\Delta\text{CT}$	Difference between two CT values
AANAT	Arylalkylamine-N-transferase
AB(s)	Antibody(ies)
AC	Adenylate cyclase
ACTB	$\beta$ -actin (in context of qPCR)
AGA-GE	Agarose gel electrophoresis
approx.	approximately
BP	Blood pressure
bp	Base pairs
BSA	Bovine serum albumin
C	Concentration
cAMP	Cyclic adenosine monophosphate
CCR	CC chemokine receptors
CHS	Coronary heart syndrome
CREB	cAMP-response-element-binding-protein
CT	Cycle threshold
CTRL	Control (as part of a sample's name)
DAG	Diacylglycerol
DAPI	4',6-diamidino-2-phenylindole
DNA	Deoxyribonucleic acid
DNase	Deoxyribonuclease
dNTP(s)	Deoxyribonucleotide(s)
EDTA	Ethylenediaminetetraacetic-acid
GABA	Gamma-aminobutyric-acid
GABA <sub>A</sub>	Gamma-aminobutyric-acid A receptor
GE	Gel electrophoresis
GPCR	G-protein coupled receptor
GPR50	G protein-coupled receptor 50
h	Hour(s)
HIOMT	Hydroxyindole-O-methyltransferase
IF	Immunofluorescence
L-NAME	N-nitro-L-arginine-methyl-ester
min	Minute(s)
mRNA	Messenger RNA
MT <sub>1</sub>	Melatonin receptor 1
MT <sub>2</sub>	Melatonin receptor 2

NO	Nitric oxide
NOS	Nitric oxide synthase
o/n	Overnight
PBS	Phosphate buffered saline
PCR	Polymerase chain reaction
PCR water	DNase, RNase, DNA free water
PFA	Paraformaldehyde
PKA	Protein kinase A
PKC	Protein kinase C
qPCR	Real time (quantitative) polymerase chain reaction
QR2	Quinone reductase 2
RNA	Ribonucleic acid
RNase	Ribonuclease
rRNA	ribosomal RNA
rt	Room temperature
RT	Reverse transcription
RT-PCR	Reverse transcription polymerase chain reaction
RT-qPCR	Reverse transcription real time (quantitative) polymerase chain reaction
s	Second(s)
SC	Santa Cruz
SCN	Suprachiasmatic nucleus
Sd	Standard deviation
SHR	Spontaneously hypertensive rats
TAE	Tris-acetic-acid-EDTA buffer
Taq	Thermus aquaticus
TF	TissueFAXS, TissueGnostics GmbH
UV	Ultraviolet
Vol.	Volume
vs	Versus

## 9 REFERENCES

1. Ganguly, S., Coon, S.L., and Klein, D.C., *Control of melatonin synthesis in the mammalian pineal gland: the critical role of serotonin acetylation*. Cell Tissue Res, 2002. **309**(1): p. 127-37.
2. Klein, D.C., *Circadian rhythms in indole metabolism in the rat pineal gland.*, in *The neurosciences: third study program*, F.G. Schmitt and F.G. Warden, Editors. 1974, MIT Press: Cambridge, MA. p. 509-516.
3. Reghunandanan, V. and Reghunandanan, R., *Neurotransmitters of the suprachiasmatic nuclei*. J Circadian Rhythms, 2006. **4**: p. 2.
4. Hamada, T., Ootomi, M., Horikawa, K., Niki, T., Wakamatu, H., and Ishida, N., *The expression of the melatonin synthesis enzyme: arylalkylamine N-acetyltransferase in the suprachiasmatic nucleus of rat brain*. Biochem Biophys Res Commun, 1999. **258**(3): p. 772-7.
5. Finocchiaro, L.M., Nahmod, V.E., and Launay, J.M., *Melatonin biosynthesis and metabolism in peripheral blood mononuclear leucocytes*. Biochem J, 1991. **280 ( Pt 3)**: p. 727-31.
6. Pandi-Perumal, S.R., Srinivasan, V., Maestroni, G.J., Cardinali, D.P., Poeggeler, B., and Hardeland, R., *Melatonin: Nature's most versatile biological signal?* FEBS J, 2006. **273**(13): p. 2813-38.
7. Tan, D.X., Manchester, L.C., Hardeland, R., Lopez-Burillo, S., Mayo, J.C., Sainz, R.M., and Reiter, R.J., *Melatonin: a hormone, a tissue factor, an autocoid, a paracoid, and an antioxidant vitamin*. J Pineal Res, 2003. **34**(1): p. 75-8.
8. Lerner, A.B., Case, J.D., Takahashi, Y., Lee, T.H., and Mori, W., *Isolation of melatonin, a pineal factor that lightens melanocytes*. J Am Soc, 1958. **80**.
9. Arnao, M.B. and Hernandez-Ruiz, J., *The physiological function of melatonin in plants*. Plant Signal Behav, 2006. **1**(3): p. 89-95.
10. Jang, S.S., Kim, W.D., and Park, W.Y., *Melatonin exerts differential actions on X-ray radiation-induced apoptosis in normal mice splenocytes and Jurkat leukemia cells*. J Pineal Res, 2009. **47**(2): p. 147-55.
11. Zawilska, J.B., Skene, D.J., and Arendt, J., *Physiology and pharmacology of melatonin in relation to biological rhythms*. Pharmacol Rep, 2009. **61**(3): p. 383-410.
12. Wideman, C.H. and Murphy, H.M., *Constant light induces alterations in melatonin levels, food intake, feed efficiency, visceral adiposity, and circadian rhythms in rats*. Nutr Neurosci, 2009. **12**(5): p. 233-40.



13. Odaci, E. and Kaplan, S., *Chapter 16: Melatonin and nerve regeneration*. Int Rev Neurobiol, 2009. **87**: p. 317-35.
14. Klein, D.C., *Arylalkylamine N-acetyltransferase: "the Timezyme"*. J Biol Chem, 2007. **282**(7): p. 4233-7.
15. Hastings, M.H., Maywood, E.S., and Reddy, A.B., *Two decades of circadian time*. J Neuroendocrinol, 2008. **20**(6): p. 812-9.
16. Aggelopoulos, N.C. and Meissl, H., *Responses of neurones of the rat suprachiasmatic nucleus to retinal illumination under photopic and scotopic conditions*. J Physiol, 2000. **523 Pt 1**: p. 211-22.
17. Ceinos, R.M., Chansard, M., Revel, F., Calgari, C., Miguez, J.M., and Simonneaux, V., *Analysis of adrenergic regulation of melatonin synthesis in Siberian hamster pineal emphasizes the role of HIOMT*. Neurosignals, 2004. **13**(6): p. 308-17.
18. Sugden, A.L., Sugden, D., and Klein, D.C., *Essential role of calcium influx in the adrenergic regulation of cAMP and cGMP in rat pinealocytes*. J Biol Chem, 1986. **261**(25): p. 11608-12.
19. Baler, R., Covington, S., and Klein, D.C., *The rat arylalkylamine N-acetyltransferase gene promoter. cAMP activation via a cAMP-responsive element-CCAAT complex*. J Biol Chem, 1997. **272**(11): p. 6979-85.
20. Ganguly, S., Gastel, J.A., Weller, J.L., Schwartz, C., Jaffe, H., Namboodiri, M.A., Coon, S.L., Hickman, A.B., Rollag, M., Obsil, T., Beauverger, P., Ferry, G., Boutin, J.A., and Klein, D.C., *Role of a pineal cAMP-operated arylalkylamine N-acetyltransferase/14-3-3-binding switch in melatonin synthesis*. Proc Natl Acad Sci U S A, 2001. **98**(14): p. 8083-8.
21. Ma, X., Idle, J.R., Krausz, K.W., and Gonzalez, F.J., *Metabolism of melatonin by human cytochromes p450*. Drug Metab Dispos, 2005. **33**(4): p. 489-94.
22. Ebisawa, T., Karne, S., Lerner, M.R., and Reppert, S.M., *Expression cloning of a high-affinity melatonin receptor from Xenopus dermal melanophores*. Proc Natl Acad Sci U S A, 1994. **91**(13): p. 6133-7.
23. Strosberg, A.D. and Nahmias, C., *G-protein-coupled receptor signalling through protein networks*. Biochem Soc Trans, 2007. **35**(Pt 1): p. 23-7.
24. Jockers, R., Maurice, P., Boutin, J.A., and Delagrange, P., *Melatonin receptors, heterodimerization, signal transduction and binding sites: what's new?* Br J Pharmacol, 2008. **154**(6): p. 1182-95.
25. Reppert, S.M., Weaver, D.R., and Ebisawa, T., *Cloning and characterization of a mammalian melatonin receptor that mediates reproductive and circadian responses*. Neuron, 1994. **13**(5): p. 1177-85.

26. Ishii, H., Tanaka, N., Kobayashi, M., Kato, M., and Sakuma, Y., *Gene structures, biochemical characterization and distribution of rat melatonin receptors*. J Physiol Sci, 2009. **59**(1): p. 37-47.
27. Hardeland, R., *Melatonin: signaling mechanisms of a pleiotropic agent*. Biofactors, 2009. **35**(2): p. 183-92.
28. Reppert, S.M., Godson, C., Mahle, C.D., Weaver, D.R., Slaugenhaupt, S.A., and Gusella, J.F., *Molecular characterization of a second melatonin receptor expressed in human retina and brain: the Mel1b melatonin receptor*. Proc Natl Acad Sci U S A, 1995. **92**(19): p. 8734-8.
29. Kato, K., Hirai, K., Nishiyama, K., Uchikawa, O., Fukatsu, K., Ohkawa, S., Kawamata, Y., Hinuma, S., and Miyamoto, M., *Neurochemical properties of ramelteon (TAK-375), a selective MT1/MT2 receptor agonist*. Neuropharmacology, 2005. **48**(2): p. 301-10.
30. Dubocovich, M.L., *Luzindole (N-0774): a novel melatonin receptor antagonist*. J Pharmacol Exp Ther, 1988. **246**(3): p. 902-10.
31. Dubocovich, M.L., Masana, M.I., Iacob, S., and Sauri, D.M., *Melatonin receptor antagonists that differentiate between the human Mel1a and Mel1b recombinant subtypes are used to assess the pharmacological profile of the rabbit retina ML1 presynaptic heteroreceptor*. Naunyn Schmiedebergs Arch Pharmacol, 1997. **355**(3): p. 365-75.
32. Tsotinis, A., Vlachou, M., Papahatjis, D.P., Calogeropoulou, T., Nikas, S.P., Garratt, P.J., Piccio, V., Vonhoff, S., Davidson, K., Teh, M.T., and Sugden, D., *Mapping the melatonin receptor. 7. Subtype selective ligands based on beta-substituted N-acyl-5-methoxytryptamines and beta-substituted N-acyl-5-methoxy-1-methyltryptamines*. J Med Chem, 2006. **49**(12): p. 3509-19.
33. Pandi-Perumal, S.R., Trakht, I., Srinivasan, V., Spence, D.W., Maestroni, G.J., Zisapel, N., and Cardinali, D.P., *Physiological effects of melatonin: role of melatonin receptors and signal transduction pathways*. Prog Neurobiol, 2008. **85**(3): p. 335-53.
34. Sugden, D., McArthur, A.J., Ajpru, S., Duniec, K., and Piggins, H.D., *Expression of mt(1) melatonin receptor subtype mRNA in the entrained rat suprachiasmatic nucleus: a quantitative RT-PCR study across the diurnal cycle*. Brain Res Mol Brain Res, 1999. **72**(2): p. 176-82.
35. Sallinen, P., Saarela, S., Ilves, M., Vakkuri, O., and Leppaluoto, J., *The expression of MT1 and MT2 melatonin receptor mRNA in several rat tissues*. Life Sci, 2005. **76**(10): p. 1123-34.

36. Masana, M.I., Doolen, S., Ersahin, C., Al-Ghoul, W.M., Duckles, S.P., Dubocovich, M.L., and Krause, D.N., *MT(2) melatonin receptors are present and functional in rat caudal artery*. J Pharmacol Exp Ther, 2002. **302**(3): p. 1295-302.
37. Dubocovich, M.L. and Markowska, M., *Functional MT1 and MT2 melatonin receptors in mammals*. Endocrine, 2005. **27**(2): p. 101-10.
38. Reppert, S.M., Weaver, D.R., and Godson, C., *Melatonin receptors step into the light: cloning and classification of subtypes*. Trends Pharmacol Sci, 1996. **17**(3): p. 100-2.
39. Sethi, S., Adams, W., Pollock, J., and Witt-Enderby, P.A., *C-terminal domains within human MT1 and MT2 melatonin receptors are involved in internalization processes*. J Pineal Res, 2008. **45**(2): p. 212-8.
40. Barrett, P., Conway, S., and Morgan, P.J., *Digging deep—structure-function relationships in the melatonin receptor family*. J Pineal Res, 2003. **35**(4): p. 221-30.
41. Silva, C.L., Tamura, E.K., Macedo, S.M., Cecon, E., Bueno-Alves, L., Farsky, S.H., Ferreira, Z.S., and Markus, R.P., *Melatonin inhibits nitric oxide production by microvascular endothelial cells in vivo and in vitro*. Br J Pharmacol, 2007. **151**(2): p. 195-205.
42. Tamura, E.K., Cecon, E., Monteiro, A.W., Silva, C.L., and Markus, R.P., *Melatonin inhibits LPS-induced NO production in rat endothelial cells*. J Pineal Res, 2009. **46**(3): p. 268-74.
43. Ayoub, M.A., Levoye, A., Delagrange, P., and Jockers, R., *Preferential formation of MT1/MT2 melatonin receptor heterodimers with distinct ligand interaction properties compared with MT2 homodimers*. Mol Pharmacol, 2004. **66**(2): p. 312-21.
44. Reppert, S.M., Weaver, D.R., Ebisawa, T., Mahle, C.D., and Kolakowski, L.F., Jr., *Cloning of a melatonin-related receptor from human pituitary*. FEBS Lett, 1996. **386**(2-3): p. 219-24.
45. Levoye, A., Dam, J., Ayoub, M.A., Guillaume, J.L., Couturier, C., Delagrange, P., and Jockers, R., *The orphan GPR50 receptor specifically inhibits MT1 melatonin receptor function through heterodimerization*. EMBO J, 2006. **25**(13): p. 3012-23.
46. Duncan, M.J., Takahashi, J.S., and Dubocovich, M.L., *2-[125I]iodomelatonin binding sites in hamster brain membranes: pharmacological characteristics and regional distribution*. Endocrinology, 1988. **122**(5): p. 1825-33.

47. Molinari, E.J., North, P.C., and Dubocovich, M.L., *2-[125I]iodo-5-methoxycarbonylamino-N-acetyltryptamine: a selective radioligand for the characterization of melatonin ML2 binding sites*. Eur J Pharmacol, 1996. **301**(1-3): p. 159-68.
48. Nosjean, O., Ferro, M., Coge, F., Beauverger, P., Henlin, J.M., Lefoulon, F., Fauchere, J.L., Delagrangé, P., Canet, E., and Boutin, J.A., *Identification of the melatonin-binding site MT3 as the quinone reductase 2*. J Biol Chem, 2000. **275**(40): p. 31311-7.
49. Calamini, B., Santarsiero, B.D., Boutin, J.A., and Mesecar, A.D., *Kinetic, thermodynamic and X-ray structural insights into the interaction of melatonin and analogues with quinone reductase 2*. Biochem J, 2008. **413**(1): p. 81-91.
50. Chomarat, P., Coge, F., Guenin, S.P., Mailliet, F., Vella, F., Mallet, C., Giraudet, S., Nagel, N., Leonce, S., Ferry, G., Delagrangé, P., and Boutin, J.A., *Cellular knock-down of quinone reductase 2: a laborious road to successful inhibition by RNA interference*. Biochimie, 2007. **89**(10): p. 1264-75.
51. Benitez-King, G., Huerto-Delgadillo, L., and Anton-Tay, F., *Binding of 3H-melatonin to calmodulin*. Life Sci, 1993. **53**(3): p. 201-7.
52. Bazwinsky-Wutschke, I., Muhlbauer, E., Wolgast, S., and Peschke, E., *Transcripts of calcium/calmodulin-dependent kinases are changed after forskolin- or IBMX-induced insulin secretion due to melatonin treatment of rat insulinoma beta-cells (INS-1)*. Horm Metab Res, 2009. **41**(11): p. 805-13.
53. Macias, M., Escames, G., Leon, J., Coto, A., Sbihi, Y., Osuna, A., and Acuna-Castroviejo, D., *Calreticulin-melatonin. An unexpected relationship*. Eur J Biochem, 2003. **270**(5): p. 832-40.
54. Andrabi, S.A., Sayeed, I., Siemen, D., Wolf, G., and Horn, T.F., *Direct inhibition of the mitochondrial permeability transition pore: a possible mechanism responsible for anti-apoptotic effects of melatonin*. FASEB J, 2004. **18**(7): p. 869-71.
55. Poeggeler, B., Thuermann, S., Dose, A., Schoenke, M., Burkhardt, S., and Hardeland, R., *Melatonin's unique radical scavenging properties - roles of its functional substituents as revealed by a comparison with its structural analogs*. J Pineal Res, 2002. **33**(1): p. 20-30.
56. Lartaud, I., Faure, S., Tabellion, A., Resende, A.C., Nadaud, S., Bagrel, D., Capdeville-Atkinson, C., and Atkinson, J., *Melatonin counteracts the loss of agonist-evoked contraction of aortic rings induced by incubation*. Fundam Clin Pharmacol, 2007. **21**(3): p. 273-9.

57. Lee, Y.M., Chen, H.R., Hsiao, G., Sheu, J.R., Wang, J.J., and Yen, M.H., *Protective effects of melatonin on myocardial ischemia/reperfusion injury in vivo*. J Pineal Res, 2002. **33**(2): p. 72-80.
58. Ceyran, H., Narin, F., Narin, N., Akgun, H., Ceyran, A.B., Ozturk, F., and Akcali, Y., *The effect of high dose melatonin on cardiac ischemia- reperfusion Injury*. Yonsei Med J, 2008. **49**(5): p. 735-41.
59. Quiroz, Y., Ferrebuz, A., Romero, F., Vaziri, N.D., and Rodriguez-Iturbe, B., *Melatonin ameliorates oxidative stress, inflammation, proteinuria, and progression of renal damage in rats with renal mass reduction*. Am J Physiol Renal Physiol, 2008. **294**(2): p. F336-44.
60. Sonmez, M.F., Narin, F., and Balcioglu, E., *Melatonin and vitamin C attenuates alcohol-induced oxidative stress in aorta*. Basic Clin Pharmacol Toxicol, 2009. **105**(6): p. 410-5.
61. Paulis, L. and Simko, F., *Blood pressure modulation and cardiovascular protection by melatonin: potential mechanisms behind*. Physiol Res, 2007. **56**(6): p. 671-84.
62. Tan, D.X., Manchester, L.C., Terron, M.P., Flores, L.J., and Reiter, R.J., *One molecule, many derivatives: a never-ending interaction of melatonin with reactive oxygen and nitrogen species?* J Pineal Res, 2007. **42**(1): p. 28-42.
63. Reiter, R.J., Paredes, S.D., Manchester, L.C., and Tan, D.X., *Reducing oxidative/nitrosative stress: a newly-discovered genre for melatonin*. Crit Rev Biochem Mol Biol, 2009. **44**(4): p. 175-200.
64. Arendt, J. and Rajaratnam, S.M., *Melatonin and its agonists: an update*. Br J Psychiatry, 2008. **193**(4): p. 267-9.
65. Bjorvatn, B., Stangenes, K., Oyane, N., Forberg, K., Lowden, A., Holsten, F., and Akerstedt, T., *Randomized placebo-controlled field study of the effects of bright light and melatonin in adaptation to night work*. Scand J Work Environ Health, 2007. **33**(3): p. 204-14.
66. Brzezinski, A., Vangel, M.G., Wurtman, R.J., Norrie, G., Zhdanova, I., Ben-Shushan, A., and Ford, I., *Effects of exogenous melatonin on sleep: a meta-analysis*. Sleep Med Rev, 2005. **9**(1): p. 41-50.
67. Wright, B., Sims, D., Smart, S., Alwazeer, A., Alderson-Day, B., Allgar, V., Whitton, C., Tomlinson, H., Bennett, S., Jardine, J., McCaffrey, N., Leyland, C., Jakeman, C., and Miles, J., *Melatonin Versus Placebo in Children with Autism Spectrum Conditions and Severe Sleep Problems Not Amenable to Behaviour Management Strategies: A Randomised Controlled Crossover Trial*. J Autism Dev Disord, 2010. **ahead of print**.

68. Korkmaz, A., Kunak, Z.I., Paredes, S.D., Yaren, H., Tan, D.X., and Reiter, R.J., *The use of melatonin to combat mustard toxicity. REVIEW.* Neuro Endocrinol Lett, 2008. **29**(5): p. 614-9.
69. Lin, A.M., Feng, S.F., Chao, P.L., and Yang, C.H., *Melatonin inhibits arsenite-induced peripheral neurotoxicity.* J Pineal Res, 2009. **46**(1): p. 64-70.
70. Nava, M., Romero, F., Quiroz, Y., Parra, G., Bonet, L., and Rodriguez-Iturbe, B., *Melatonin attenuates acute renal failure and oxidative stress induced by mercuric chloride in rats.* Am J Physiol Renal Physiol, 2000. **279**(5): p. F910-8.
71. Rao, M.V., Purohit, A., and Patel, T., *Melatonin protection on mercury-exerted brain toxicity in the rat.* Drug Chem Toxicol, 2010. **33**(2): p. 209-16.
72. Xu, S.C., He, M.D., Zhong, M., Zhang, Y.W., Wang, Y., Yang, L., Yang, J., Yu, Z.P., and Zhou, Z., *Melatonin protects against Nickel-induced neurotoxicity in vitro by reducing oxidative stress and maintaining mitochondrial function.* J Pineal Res, 2010. **ahead of print**.
73. Aranda, M., Albendea, C.D., Lostale, F., Lopez-Pingarron, L., Fuentes-Broto, L., Martinez-Ballarín, E., Reiter, R.J., Perez-Castejon, M.C., and Garcia, J.J., *In vivo hepatic oxidative stress because of carbon tetrachloride toxicity: protection by melatonin and pinoline.* J Pineal Res, 2010.
74. Othman, A.I., El-Missiry, M.A., Amer, M.A., and Arafa, M., *Melatonin controls oxidative stress and modulates iron, ferritin, and transferrin levels in adriamycin treated rats.* Life Sci, 2008. **83**(15-16): p. 563-8.
75. Sahna, E., Parlakpınar, H., Ozer, M.K., Ozturk, F., Ozugurlu, F., and Acet, A., *Melatonin protects against myocardial doxorubicin toxicity in rats: role of physiological concentrations.* J Pineal Res, 2003. **35**(4): p. 257-61.
76. Rezzani, R., Rodella, L.F., Bonomini, F., Tengattini, S., Bianchi, R., and Reiter, R.J., *Beneficial effects of melatonin in protecting against cyclosporine A-induced cardiotoxicity are receptor mediated.* J Pineal Res, 2006. **41**(3): p. 288-95.
77. Fan, L.L., Sun, G.P., Wei, W., Wang, Z.G., Ge, L., Fu, W.Z., and Wang, H., *Melatonin and Doxorubicin synergistically induce cell apoptosis in human hepatoma cell lines.* World J Gastroenterol, 2010. **16**(12): p. 1473-81.
78. Lundmark, P.O., Pandi-Perumal, S.R., Srinivasan, V., Cardinali, D.P., and Rosenstein, R.E., *Melatonin in the eye: implications for glaucoma.* Exp Eye Res, 2007. **84**(6): p. 1021-30.
79. Belforte, N.A., Moreno, M.C., de Zavalía, N., Sande, P.H., Chianelli, M.S., Keller Sarmiento, M.I., and Rosenstein, R.E., *Melatonin: a novel neuroprotectant for the treatment of glaucoma.* J Pineal Res, 2010. **48**(4): p. 353-64.

- 
80. Mor, M., Rivara, S., Pala, D., Bedini, A., Spadoni, G., and Tarzia, G., *Recent advances in the development of melatonin MT(1) and MT(2) receptor agonists*. Expert Opin Ther Pat, 2010. **ahead of print**.
81. Bourin, M. and Prica, C., *Melatonin receptor agonist agomelatine: a new drug for treating unipolar depression*. Curr Pharm Des, 2009. **15**(14): p. 1675-82.
82. Pandi-Perumal, S.R., Srinivasan, V., Spence, D.W., Moscovitch, A., Hardeland, R., Brown, G.M., and Cardinali, D.P., *Ramelteon: a review of its therapeutic potential in sleep disorders*. Adv Ther, 2009. **26**(6): p. 613-26.
83. Rajaratnam, S.M., Polymeropoulos, M.H., Fisher, D.M., Roth, T., Scott, C., Birznieks, G., and Klerman, E.B., *Melatonin agonist tasimelteon (VEC-162) for transient insomnia after sleep-time shift: two randomised controlled multicentre trials*. Lancet, 2009. **373**(9662): p. 482-91.
84. Dominguez-Rodriguez, A., Abreu-Gonzalez, P., Garcia, M.J., Sanchez, J., Marrero, F., and de Armas-Trujillo, D., *Decreased nocturnal melatonin levels during acute myocardial infarction*. J Pineal Res, 2002. **33**(4): p. 248-52.
85. Brugger, P., Marktl, W., and Herold, M., *Impaired nocturnal secretion of melatonin in coronary heart disease*. Lancet, 1995. **345**(8962): p. 1408.
86. Yaprak, M., Altun, A., Vardar, A., Aktoz, M., Ciftci, S., and Ozbay, G., *Decreased nocturnal synthesis of melatonin in patients with coronary artery disease*. Int J Cardiol, 2003. **89**(1): p. 103-7.
87. Altun, A., Yaprak, M., Aktoz, M., Vardar, A., Betul, U.A., and Ozbay, G., *Impaired nocturnal synthesis of melatonin in patients with cardiac syndrome X*. Neurosci Lett, 2002. **327**(2): p. 143-5.
88. Sung, J.H., Cho, E.H., Kim, M.O., and Koh, P.O., *Identification of proteins differentially expressed by melatonin treatment in cerebral ischemic injury--a proteomics approach*. J Pineal Res, 2009. **46**(3): p. 300-6.
89. Dominguez-Rodriguez, A., Abreu-Gonzalez, P., Garcia-Gonzalez, M.J., Kaski, J.C., Reiter, R.J., and Jimenez-Sosa, A., *A unicenter, randomized, double-blind, parallel-group, placebo-controlled study of Melatonin as an Adjunct in patients with acute myocaRdial Infarction undergoing primary Angioplasty The Melatonin Adjunct in the acute myocaRdial Infarction treated with Angioplasty (MARIA) trial: study design and rationale*. Contemp Clin Trials, 2007. **28**(4): p. 532-9.
90. clinicaltrials.gov. *The Melatonin Adjunct in the Acute myocaRdial Infarction Treated With Angioplasty (MARIA)*. 2008 [cited 2009 11/02]; Available from: <http://clinicaltrials.gov/ct2/show/NCT00640094>.

91. Tengattini, S., Reiter, R.J., Tan, D.X., Terron, M.P., Rodella, L.F., and Rezzani, R., *Cardiovascular diseases: protective effects of melatonin*. J Pineal Res, 2008. **44**(1): p. 16-25.
92. Dominguez-Rodriguez, A., Abreu-Gonzalez, P., and Reiter, R.J., *Clinical aspects of melatonin in the acute coronary syndrome*. Curr Vasc Pharmacol, 2009. **7**(3): p. 367-73.
93. Gaehtgens, P., *Das Kreislaufsystem*, in *Lehrbuch der Physiologie*, R. Klinke and S. Silbernagl, Editors. 1996, Georg Thieme Verlag: Stuttgart. p. 142–146.
94. Mutschler, E., Schaible, H.-G., and Vaupel, P., *Regulation des Blutkreislaufs*, in *Anatomie Physiologie Pathophysiologie des Menschen*. 2007, Wissenschaftliche Verlagsgesellschaft mbH: Stuttgart. p. 270–277.
95. Carretero, O.A. and Oparil, S., *Essential hypertension. Part I: definition and etiology*. Circulation, 2000. **101**(3): p. 329-35.
96. Bivin, W.S., Crawford, M.P., and Brewer, N.R., *Morphophysiology*, in *The laboratory rat*, H.J. Baker, R.J. Lindsey, and S.H. Weisbroth, Editors. 1979, Academic Press: New York. p. 86–88.
97. Slomianka, L. *Blue Histology - Vascular System*. 2009 [cited 2010 06/13]; Available from:  
<http://www.lab.anhb.uwa.edu.au/mb140/CorePages/Vascular/Vascular.htm>.
98. Mutschler, E., Schaible, H.-G., and Vaupel, P., *Anatomie des Gefäßsystems*, in *Anatomie, Physiologie Pathophysiologie des Menschen*. 2007, Wissenschaftliche Verlagsgesellschaft mbH: Stuttgart. p. 242–243.
99. Histology. Histology of the Blood Vessels [cited 2010 06/13/10]; Available from:  
<http://www.courseweb.uottawa.ca/medicine-histology/english/Cardiovascular/histologybloodvessels.htm>.
100. Yoon, Y., Song, J., Hong, S.H., and Kim, J.Q., *Plasma nitric oxide concentrations and nitric oxide synthase gene polymorphisms in coronary artery disease*. Clin Chem, 2000. **46**(10): p. 1626-30.
101. McCance, K.L., *Structure and Function of the Cardiovascular and Lymphatic Systems*, in *Understanding pathophysiology*, S.E. Huether and K.L. McCance, Editors. 2004, Mosby: St. Louis. p. 626–630.
102. Zanoboni, A., Forni, A., Zanoboni-Muciaccia, W., and Zanussi, C., *Effect of pinealectomy on arterial blood pressure and food and water intake in the rat*. J Endocrinol Invest, 1978. **1**(2): p. 125-30.
103. Windle, R.J., Luckman, S.M., Stoughton, R.P., and Forsling, M.L., *The effect of pinealectomy on osmotically stimulated vasopressin and oxytocin release and*



- Fos protein production within the hypothalamus of the rat.* J Neuroendocrinol, 1996. **8**(10): p. 747-53.
104. Zeman, M., Dulkova, K., Bada, V., and Herichova, I., *Plasma melatonin concentrations in hypertensive patients with the dipping and non-dipping blood pressure profile.* Life Sci, 2005. **76**(16): p. 1795-803.
105. Escames, G., Khaldy, H., Leon, J., Gonzalez, L., and Acuna-Castroviejo, D., *Changes in iNOS activity, oxidative stress and melatonin levels in hypertensive patients treated with lacidipine.* J Hypertens, 2004. **22**(3): p. 629-35.
106. Reyes-Toso, C.F., Linares, L.M., Ricci, C.R., Obaya-Naredo, D., Pinto, J.E., Rodriguez, R.R., and Cardinali, D.P., *Melatonin restores endothelium-dependent relaxation in aortic rings of pancreatectomized rats.* J Pineal Res, 2005. **39**(4): p. 386-91.
107. Reyes-Toso, C.F., Obaya-Naredo, D., Ricci, C.R., Planells, F.M., Pinto, J.E., Linares, L.M., and Cardinali, D.P., *Effect of melatonin on vascular responses in aortic rings of aging rats.* Exp Gerontol, 2007. **42**(4): p. 337-42.
108. Benova, M., Herichova, I., Stebelova, K., Paulis, L., Krajcirovicova, K., Simko, F., and Zeman, M., *Effect of L-NAME-induced hypertension on melatonin receptors and melatonin levels in the pineal gland and the peripheral organs of rats.* Hypertens Res, 2009. **32**(4): p. 242-7.
109. Li, H.L., Kang, Y.M., Yu, L., Xu, H.Y., and Zhao, H., *Melatonin reduces blood pressure in rats with stress-induced hypertension via GABAA receptors.* Clin Exp Pharmacol Physiol, 2009. **36**(4): p. 436-40.
110. Xia, C.M., Shao, C.H., Xin, L., Wang, Y.R., Ding, C.N., Wang, J., Shen, L.L., Li, L., Cao, Y.X., and Zhu, D.N., *Effects of melatonin on blood pressure in stress-induced hypertension in rats.* Clin Exp Pharmacol Physiol, 2008. **35**(10): p. 1258-64.
111. Ersahin, M., Sehirli, O., Toklu, H.Z., Suleymanoglu, S., Emekli-Alturfan, E., Yarat, A., Tatlidede, E., Yegen, B.C., and Sener, G., *Melatonin improves cardiovascular function and ameliorates renal, cardiac and cerebral damage in rats with renovascular hypertension.* J Pineal Res, 2009. **47**(1): p. 97-106.
112. Simko, F., Pechanova, O., Pelouch, V., Krajcirovicova, K., Mullerova, M., Bednarova, K., Adamcova, M., and Paulis, L., *Effect of melatonin, captopril, spironolactone and simvastatin on blood pressure and left ventricular remodelling in spontaneously hypertensive rats.* J Hypertens Suppl, 2009. **27**(6): p. S5-10.

113. Safar, M., Chamiot-Clerc, P., Dagher, G., and Renaud, J.F., *Pulse pressure, endothelium function, and arterial stiffness in spontaneously hypertensive rats*. Hypertension, 2001. **38**(6): p. 1416-21.
114. Rezzani, R., Porteri, E., De Ciuceis, C., Bonomini, F., Rodella, L.F., Paiardi, S., Boari, G.E., Platto, C., Pilu, A., Avanzi, D., Rizzoni, D., and Agabiti Rosei, E., *Effects of melatonin and Pycnogenol on small artery structure and function in spontaneously hypertensive rats*. Hypertension, 2010. **55**(6): p. 1373-80.
115. Nava, M., Quiroz, Y., Vaziri, N., and Rodriguez-Iturbe, B., *Melatonin reduces renal interstitial inflammation and improves hypertension in spontaneously hypertensive rats*. Am J Physiol Renal Physiol, 2003. **284**(3): p. F447-54.
116. Girouard, H., Chulak, C., Lejossec, M., Lamontagne, D., and de Champlain, J., *Vasorelaxant effects of the chronic treatment with melatonin on mesenteric artery and aorta of spontaneously hypertensive rats*. J Hypertens, 2001. **19**(8): p. 1369-77.
117. Okamoto, K. and Aoki, K., *Development of a strain of spontaneously hypertensive rats*. Jpn Circ J, 1963. **27**: p. 282-93.
118. Conrad, C.H., Brooks, W.W., Hayes, J.A., Sen, S., Robinson, K.G., and Bing, O.H., *Myocardial fibrosis and stiffness with hypertrophy and heart failure in the spontaneously hypertensive rat*. Circulation, 1995. **91**(1): p. 161-70.
119. Hallback, M. and Weiss, L., *Mechanisms of spontaneous hypertension in rats*. Med Clin North Am, 1977. **61**(3): p. 593-609.
120. Arangino, S., Cagnacci, A., Angiolucci, M., Vacca, A.M., Longu, G., Volpe, A., and Melis, G.B., *Effects of melatonin on vascular reactivity, catecholamine levels, and blood pressure in healthy men*. Am J Cardiol, 1999. **83**(9): p. 1417-9.
121. Cagnacci, A., Arangino, S., Angiolucci, M., Maschio, E., and Melis, G.B., *Influences of melatonin administration on the circulation of women*. Am J Physiol, 1998. **274**(2 Pt 2): p. R335-8.
122. Nishiyama, K., Yasue, H., Moriyama, Y., Tsunoda, R., Ogawa, H., Yoshimura, M., and Kugiyama, K., *Acute effects of melatonin administration on cardiovascular autonomic regulation in healthy men*. Am Heart J, 2001. **141**(5): p. E9.
123. Cagnacci, A., Cannoletta, M., Renzi, A., Baldassari, F., Arangino, S., and Volpe, A., *Prolonged melatonin administration decreases nocturnal blood pressure in women*. Am J Hypertens, 2005. **18**(12 Pt 1): p. 1614-8.

124. Scheer, F.A., Van Montfrans, G.A., van Someren, E.J., Mairuhu, G., and Buijs, R.M., *Daily nighttime melatonin reduces blood pressure in male patients with essential hypertension*. *Hypertension*, 2004. **43**(2): p. 192-7.
125. Rechcinski, T., Trzos, E., Wierzbowska-Drabik, K., Krzeminska-Pakula, M., and Kurpesa, M., *Melatonin for nondippers with coronary artery disease: assessment of blood pressure profile and heart rate variability*. *Hypertens Res*, 2010. **33**(1): p. 56-61.
126. Pechanova, O. and Simko, F., *Chronic antioxidant therapy fails to ameliorate hypertension: potential mechanisms behind*. *J Hypertens Suppl*, 2009. **27**(6): p. S32-6.
127. Ekmekcioglu, C., Haslmayer, P., Philipp, C., Mehrabi, M.R., Glogar, H.D., Grimm, M., Leibetseder, V.J., Thalhammer, T., and Marktl, W., *Expression of the MT1 melatonin receptor subtype in human coronary arteries*. *J Recept Signal Transduct Res*, 2001. **21**(1): p. 85-91.
128. Ekmekcioglu, C., Thalhammer, T., Humpeler, S., Mehrabi, M.R., Glogar, H.D., Holzenbein, T., Markovic, O., Leibetseder, V.J., Strauss-Blasche, G., and Marktl, W., *The melatonin receptor subtype MT2 is present in the human cardiovascular system*. *J Pineal Res*, 2003. **35**(1): p. 40-4.
129. Ekmekcioglu, C., Haslmayer, P., Philipp, C., Mehrabi, M.R., Glogar, H.D., Grimm, M., Thalhammer, T., and Marktl, W., *24h variation in the expression of the mt1 melatonin receptor subtype in coronary arteries derived from patients with coronary heart disease*. *Chronobiol Int*, 2001. **18**(6): p. 973-85.
130. Viswanathan, M., Scalbert, E., Delagrangé, P., Guardiola-Lemaitre, B., and Saavedra, J.M., *Melatonin receptors mediate contraction of a rat cerebral artery*. *Neuroreport*, 1997. **8**(18): p. 3847-9.
131. Regrigny, O., Delagrangé, P., Scalbert, E., Lartaud-Idjouadiene, I., Atkinson, J., and Chillon, J.M., *Effects of melatonin on rat pial arteriolar diameter in vivo*. *Br J Pharmacol*, 1999. **127**(7): p. 1666-70.
132. Chucharoen, P., Chetsawang, B., Srikiatkachorn, A., and Govitrapong, P., *Melatonin receptor expression in rat cerebral artery*. *Neurosci Lett*, 2003. **341**(3): p. 259-61.
133. Doolen, S., Krause, D.N., Dubocovich, M.L., and Duckles, S.P., *Melatonin mediates two distinct responses in vascular smooth muscle*. *Eur J Pharmacol*, 1998. **345**(1): p. 67-9.
134. Vandeputte, C., Giummelly, P., Atkinson, J., Delagrangé, P., Scalbert, E., and Capdeville-Atkinson, C., *Melatonin potentiates NE-induced vasoconstriction*

- without augmenting cytosolic calcium concentration.* Am J Physiol Heart Circ Physiol, 2001. **280**(1): p. H420-5.
135. Savaskan, E., Olivieri, G., Brydon, L., Jockers, R., Krauchi, K., Wirz-Justice, A., and Muller-Spahn, F., *Cerebrovascular melatonin MT1-receptor alterations in patients with Alzheimer's disease.* Neurosci Lett, 2001. **308**(1): p. 9-12.
136. Richter, H.G., Torres-Farfan, C., Garcia-Sesnich, J., Abarzua-Catalan, L., Henriquez, M.G., Alvarez-Felmer, M., Gaete, F., Rehren, G.E., and Seron-Ferre, M., *Rhythmic expression of functional MT1 melatonin receptors in the rat adrenal gland.* Endocrinology, 2008. **149**(3): p. 995-1003.
137. Takeda, N. and Maemura, K., *Circadian clock and vascular disease.* Hypertens Res, 2010.
138. Pang, C.S., Xi, S.C., Brown, G.M., Pang, S.F., and Shiu, S.Y., *2[125I]iodomelatonin binding and interaction with beta-adrenergic signaling in chick heart/coronary artery physiology.* J Pineal Res, 2002. **32**(4): p. 243-52.
139. Peqlab. *peqGOLD TriFast - Optimierte Guanidinisothiocyanat/Phenol-Methode für die gleichzeitige Extraktion von RNA, DNA und Proteinen.* [cited 2010 06/21]; Available from: [http://www.peqlab.de/wcms/de/pdf/30-2010\\_m.pdf](http://www.peqlab.de/wcms/de/pdf/30-2010_m.pdf).
140. Applied Biosystems. *User Bulletin #2 ABI PRISM 7700 Sequence Detection System - Relative Quantitation of Gene Expression, 4303859B.* 2001 [cited 2010 06/21]; Available from: [http://www3.appliedbiosystems.com/cms/groups/mcb\\_support/documents/generalddocuments/cms\\_040980.pdf](http://www3.appliedbiosystems.com/cms/groups/mcb_support/documents/generalddocuments/cms_040980.pdf).
141. Bartlett, J.M. and Stirling, D., *A short history of the polymerase chain reaction.* Methods Mol Biol, 2003. **226**: p. 3-6.
142. Applied Biosystems. *High-Capacity cDNA Reverse Transcription Kits For 200 and 1000 Reactions Protocol, 4375575 Rev. C.* 2006 [cited 2010 06/21]; Available from: [http://www3.appliedbiosystems.com/cms/groups/mcb\\_support/documents/generalddocuments/cms\\_042557.pdf](http://www3.appliedbiosystems.com/cms/groups/mcb_support/documents/generalddocuments/cms_042557.pdf).
143. Fermentas. - *Products - All - PCR, qPCR, RT-PCR & dNTPs - Standard PCR - Taq DNA Polymerase (recombinant).* Additional protocols - components of the reaction mixture 2010 [cited 2010 06/21]; Available from: <http://www.fermentas.com/en/products/all/pcr-qpcr-rt-pcr/standard-pcr/ep040-taq-dna-recomb>.
144. Institute for Viral Pathogenesis. *Nested PCR for Detection of HHV-6, EBV, and HTLV-2 - IVP.* 2005 [cited 2010 06/07]; Available from: [http://www.ivpresearch.org/nested\\_pcr.htm](http://www.ivpresearch.org/nested_pcr.htm).

145. Invitrogen. *Deoxyribonuclease I, Amplification Grade 18068-015*. [cited 2010 06/21]; Available from:  
<http://tools.invitrogen.com/content/sfs/manuals/18068015.pdf>.
146. Qiagen, *QIAquick® Spin Handbook*. 2008.
147. NCBI. *Nucleotide BLAST: Search nucleotide databases using a nucleotide query*. 2010 [cited 2010 06/21]; Available from:  
<http://www.ncbi.nlm.nih.gov/blast/Blast.cgi?PAGE=Nucleotides&PROGRAM=blastn>.
148. Zhang, Z., Schwartz, S., Wagner, L., and Miller, W., *A greedy algorithm for aligning DNA sequences*. *J Comput Biol*, 2000. **7**(1-2): p. 203-14.
149. Applied Biosystems. *Introduction to Gene Expression Getting Started Guide, 4454239 Rev A*. 2010 [cited 2010 06/21]; Available from:  
[http://www3.appliedbiosystems.com/cms/groups/mcb\\_support/documents/generalddocuments/cms\\_083618.pdf](http://www3.appliedbiosystems.com/cms/groups/mcb_support/documents/generalddocuments/cms_083618.pdf).
150. Applied Biosystems. *TaqMan® Gene Expression Master Mix Protocol, 4371135 Rev. B*. 2007 [cited 2010 06/21]; Available from:  
[http://www3.appliedbiosystems.com/cms/groups/mcb\\_support/documents/generalddocuments/cms\\_039284.pdf](http://www3.appliedbiosystems.com/cms/groups/mcb_support/documents/generalddocuments/cms_039284.pdf).
151. Applied Biosystems. *Applied Biosystems StepOne™ and StepOnePlus™ Real-Time PCR Systems. Relative Standard Curve and Comparative CT Experiments, 4376785 Rev. E*. 2008 [cited 2010 06/21]; Available from:  
[http://www3.appliedbiosystems.com/cms/groups/mcb\\_support/documents/generalddocuments/cms\\_046736.pdf](http://www3.appliedbiosystems.com/cms/groups/mcb_support/documents/generalddocuments/cms_046736.pdf).
152. Santa Cruz Biotechnology. *MEL-1A-R (R-18): sc-13186*. [cited 2010 06/21]; Available from: <http://datasheets.scbt.com/sc-13186.pdf>.
153. Santa Cruz Biotechnology. *PECAM-1 (M-20): sc-1506*. [cited 2010 06/21]; Available from: <http://datasheets.scbt.com/sc-1506.pdf>.
154. Abbiotec. *TR-1A Antibody | Abbiotec™*. 2008 [cited 2010 06/21]; Available from: <http://abbiotec.com/antibodies/mtr-1a-antibody>.
155. Sigma-Aldrich, I. *Monoclonal Anti-α Smooth Muscle Actin – Product information*. [cited 2010 06/21]; Available from:  
<http://www.sigmaaldrich.com/etc/medialib/docs/Sigma/Datasheet/6/a2547dat.P ar.0001.File.tmp/a2547dat.pdf>.
156. Invitrogen Molecular Probes. *Labeled Donkey Anti-Goat IgG Antibodies*. 2006 [cited 2010 06/21]; Available from:  
<http://probes.invitrogen.com/media/pis/mp11055.pdf>.

157. Invitrogen Molecular Probes. *Labeled Goat Anti-Mouse IgM Antibodies*. 2009 [cited 2010 06/21]; Available from:  
<http://probes.invitrogen.com/media/pis/mp21042.pdf>.
158. Invitrogen Molecular Probes. *Goat Anti-Rabbit IgG Antibodies*. 2009 [cited 2010 06/21]; Available from:  
<http://probes.invitrogen.com/media/pis/mp02764.pdf>.
159. Sanchez-Hidalgo, M., Guerrero Montavez, J.M., Carrascosa-Salmoral Mdel, P., Naranjo Gutierrez Mdel, C., Lardone, P.J., and de la Lastra Romero, C.A., *Decreased MT1 and MT2 melatonin receptor expression in extrapineal tissues of the rat during physiological aging*. J Pineal Res, 2009. **46**(1): p. 29-35.
160. Sallinen, P., Manttari, S., Leskinen, H., Ilves, M., Vakkuri, O., Ruskoaho, H., and Saarela, S., *The effect of myocardial infarction on the synthesis, concentration and receptor expression of endogenous melatonin*. J Pineal Res, 2007. **42**(3): p. 254-60.
161. Premier Biosoft. *Primer Design Guide for PCR :: Learn Designing Primers for PCR*. 2010 [cited 2010 06/21]; Available from:  
[http://www.premierbiosoft.com/tech\\_notes/PCR\\_Primer\\_Design.html](http://www.premierbiosoft.com/tech_notes/PCR_Primer_Design.html).
162. NCBI. *Primer design tool*. 2010 [cited 2010 06/21]; Available from:  
<http://www.ncbi.nlm.nih.gov/tools/primer-blast/>.
163. Musshoff, U., Riewenherm, D., Berger, E., Fauteck, J.D., and Speckmann, E.J., *Melatonin receptors in rat hippocampus: molecular and functional investigations*. Hippocampus, 2002. **12**(2): p. 165-73.

## 10 CURRICULUM VITAE

### Personal details

Name	Martin Wolfgang Schepelmann
Date and place of birth	November 10 <sup>th</sup> , 1983; Vienna
Nationality	Austria

### Education and career

1990–1994	Elementary school (Maria Regina, 1190 Vienna)
1994 – 2002	Secondary school (Döblinger Gymnasium, 1190 Vienna)
05/2002	Graduation (Matura)
2003–2004	Training as paramedic (graduation with honors) in the context of the Austrian compulsory community service (Austrian Red Cross)
2004–2010	Study of Pharmacy at the University of Vienna, Austria
06/2007	Leading a workshop for microscopic plant anatomy in two tenth and one ninth grade biology classes at a secondary school (Billrothgymnasium, 1190 Vienna)

### Awards

04/1998	1 <sup>st</sup> place at the Austrian finals of CyberSchool98 (students develop IT-projects; <a href="http://www.cyberschool.at">www.cyberschool.at</a> )
05/2001	1 <sup>st</sup> place at the Austrian finals of Business@School (students develop business plans; initiated by the Boston Consulting Group; <a href="http://www.business-at-school.de">www.business-at-school.de</a> )
06/2001	3 <sup>rd</sup> place at the Austrian-German finals of Business@School (see above) in Munich, Germany
01/2008	Merit scholarship of the University of Vienna (StudFG WS2008) for excellent academic achievements in the year 2007

### Special skills

Languages	German (native language), English (fluent)
IT	Microsoft Office (Word, Excel, Powerpoint) Adobe Photoshop, Adobe Premiere, system assembling and maintenance, operating systems (DOS, Windows 3.11, 95, 98, ME, NT, 2000, XP, Vista, 7), basic network administration ECDL (European Computer Driving License; acquired at the Austrian Computer Society)
Driving license	B

### Hobbies

Movies, reading, IT, classical music, microscopy, history